Co-funded by
the European Union

Ref. Ares(2026)6477014 - 26/06/2026

BRISK II

Impact mapping of spilt oil and HNS

Deliverable D3.3

This document is developed within the BRISK II project to describe the risk of oil and HNS impact in the Baltic Sea and submitted by the Core Project team on 30.06.2026.

BRISK II, Long-term risk analysis for oil and hazardous and noxious substances (HNS) pollution from shipping accidents to the marine environment in the Baltic Sea, is a project co-funded by the EU. Views and opinions expressed are, however, those of the author(s) only and do not necessarily reflect those of the European Union or DG ECHO. Neither the European Union nor the granting authority can be held responsible for them.

This document is authored by the BRISK II Core Project Team:

Susanna Relander, HELCOM Secretariat
Anna Kiiski, Merikotka
Emilia Luoma, Merikotka
Motahareh Hosseini, Merikotka
Torben Holmgaard Iversen, Royal Danish Navy Command
Heli Haapasaari, Finnish Border Guard
Peter Eliasson, Swedish Coastguard
Thomas Larsson, Swedish Coastguard
Albrecht Lentz, COWI

CONTENTS

1	Introduction	4
1.1	Background	4
1.2	Scope	4
2	Preparation for the modelling	6
2.1	Meteorological scenarios	6
2.2	Subdivision into meteorological areas	6
2.3	Subdivision into hydrographical areas	12
2.4	Modelling of the ice cover	17
2.5	Definition of the simulation periods	18
2.6	Adjustment of the bunker model	27
3	Modelling of spreading and fate of oil	29
3.1	Description of applied model system	29
3.2	Model simulations	30
3.3	Model results	31
4	Modelling of spreading of HNS	46
4.1	Evaporating HNS	46
4.2	Floating HNS	46
4.3	Soluble HNS	46

4.4	Sinking HNS	49
5	Modelling of emergency response	50
5.1	Response modelling	50
5.2	Applied response capacity for each sub-region	50
5.3	Viscosity	55
5.4	Substance-specific reduction factors	56
5.5	Visibility	56
5.6	Darkness	57
5.7	Wave height	60
6	Risk of oil and HNS impact	62
6.1	Introduction	62
6.2	Oil and floating HNS	62
6.3	Oil and floating HNS	63
6.4	Soluble HNS	70
6.5	Sinking HNS	74
7	Abbreviations	75
8	References	76

APPENDICES

Appendix A	PEC/PNEC model results	78
Appendix B	Documentation for dilution calculations of soluble chemicals (PEC/PNEC)	80
Appendix C	Response capacity in the Baltic Sea	94

1 Introduction

1.1 Background

This data report is part of the long-term risk analysis for oil and hazardous and noxious substances (HNS) pollution from shipping accidents to the marine environment in the Baltic Sea, in short BRISK II. The BRISK II project comprises the following deliverables on the analyses:

1 Deliverables under work package 1 include project management related reports (e.g. progress reports).

2 Work package 2: Basic analysis
- 2.1 Method note
- 2.2 Data collection note
- 2.3 Traffic analysis
- 2.4 Cargo analysis
- 2.5 Accident and spill model
- 2.6 Probability of oil and HNS release

3 Work package 3: Future damage analysis
- 3.1 Traffic scenarios
- 3.2 Selection of risk reduction scenarios
- **3.3 Impact mapping of spilt oil and HNS (this report)**
- 3.4 Mapping of environmental vulnerability
- 3.5 Mapping of environmental damage due to oil
- 3.6 Mapping of environmental damage due to HNS

1.2 Scope

The present report deals with the fate and containment of spilt oil and hazardous and noxious substances (HNS) and their impact. The likelihood of oil and HNS release is described in deliverable D2.6 Probability of oil and HNS release (BRISK II, Prob. of release, 2026). Impact is about where and in which quantities released substances end up after spreading, decay and response.

The report describes both the methodology and the resulting risk of spill impact for existing situation (reference year 2024) and the two prognosis scenarios for 2036 (2036-1 and 2036-2).

It is important to highlight that BRISK II is update of BRISK I. This means that the newest data on traffic, cargo, fixed objects, prevention and response measures are taken into account whereas the basic methodology is maintained unchanged in most parts compared to BRISK I. Changes to the methodology are only made when mandated by a change in the real world, such as the appearance of new substances.

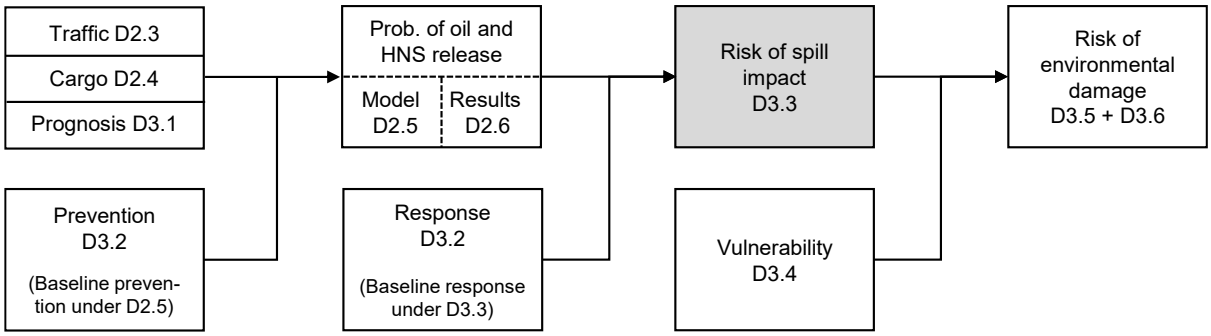

Figure 1-1 *Causal chain of the BRISK II model and corresponding deliverables numbers (The present report is highlighted with grey background)*

The accident and spill model report is divided into the following chapters:

Chapter 2: Preparation for the modelling
Chapter 3: Modelling of spreading and fate of oil
Chapter 4: Modelling of spreading of
Chapter 5: Modelling of emergency response
Chapter 6: Risk of oil and HNS impact

2 Preparation for the modelling

This chapter describes the necessary sub-division of the project area into smaller units for meteorological and hydrographical data preparation. The chapter further describes how the occurrence of ice is applied in the modelling. Finally, the chapter describes the appointment of locations for oil spill and outlines the methodology for selecting the simulation periods for the oil spill scenarios that is modelled with the detailed model.

2.1 Meteorological scenarios

The relevant meteorological scenarios have been identified and discussed in the Method note (BRISK II, Method note, 2025). They comprise the following events occurring in the open sea:

- Four wind directions
- Three wind speed classes
- Ice and no ice on the sea surface

2.2 Subdivision into meteorological areas

The project area has been divided into a number of meteorological units within which the wind conditions are assumed to be uniform. The physical scale of the meteorological areas depends on the availability of data as well as on the shape and size of oceanographic units (such as a bay or open water area).

The Admiralty Pilot publications for the Baltic Sea (Baltic Pilot, 2009) are highly valuable for the selection of meteorological areas. These publications contain seasonal wind roses at selected locations which are based on many years of wind data. The wind roses show the statistical distribution of wind speed and directions. For the present project wind roses from different locations and seasons have been compared and it has been assessed to which degree they show the same statistical features.

Examples of wind roses from the Baltic Pilots are seen in Figure 2-1 to Figure 2-3. For the Danish waters (Figure 2-1) it is seen that there is a difference between the wind conditions in the northern part (Kattegat) and the southern parts covering the straits and entrance to the Baltic Sea. This difference persists for other seasons as well.

For the southern and central Baltic Sea (Figure 2-2) it is seen that the southern most part have a larger contribution from westerly winds as compared with the central part of the Baltic Sea. For other seasons there are similar differences which clearly distinguish the southern and the central part of the Baltic Sea wind characteristics.

For the northern Baltic Sea (Figure 2-3) there is a tendency towards the wind characteristics of the Gulf of Finland being different from those of the Gulf of Bothnia. This is also the case for other seasons although the wind roses for the northern most part are based on limited data.

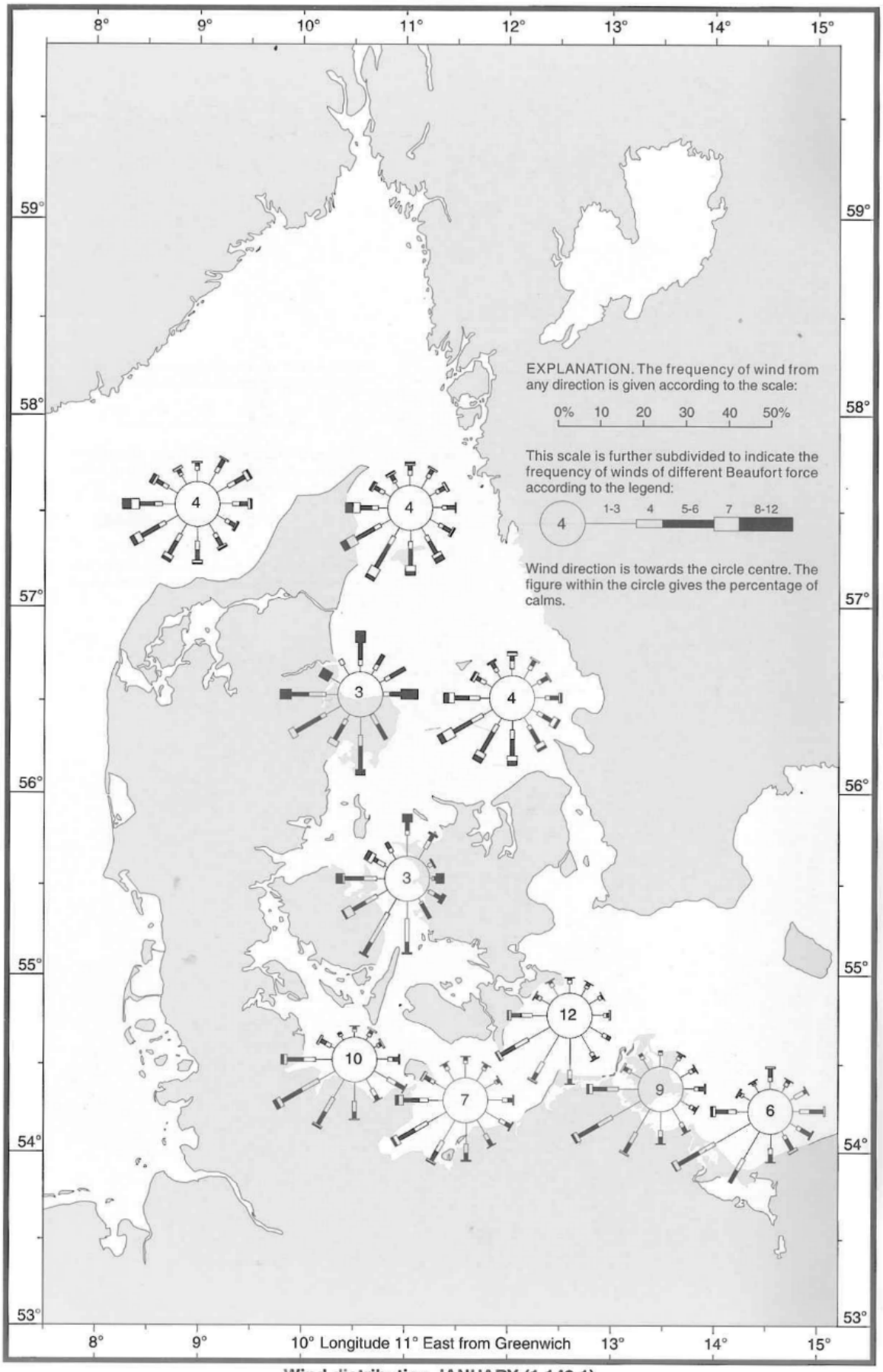

Wind distribution JANUARY (1.149.1)

Figure 2-1 Wind distribution January in the straits of Denmark, from Admiralty Sailing Directions, Baltic Pilot Volume I (NP18).

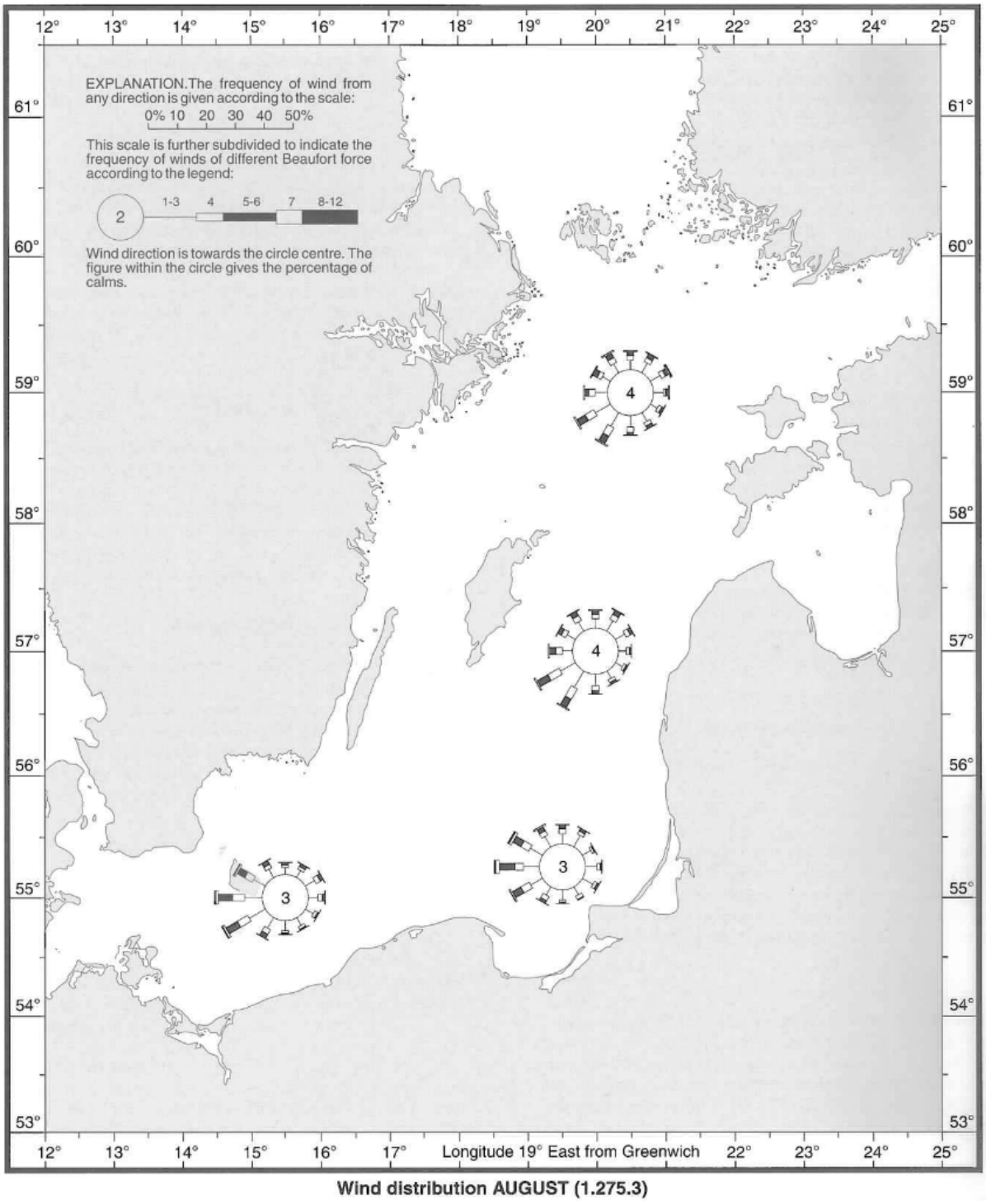

Figure 2-2 Wind distribution August in the southern Baltic Sea, from Admiralty Sailing Directions, Baltic Pilot Volume II (NP19).

Wind distribution OCTOBER (1.210.4)

Figure 2-3 Wind distribution October in the northern Baltic Sea. From Admiralty Sailing Directions, Baltic Pilot Volume III (NP20).

For the selection of meteorological areas, a general judgement has been made of the features that change the meteorological conditions. This judgement is based on experience from marine projects throughout the globe. As an example, the Gulf of Finland can be mentioned. The Gulf is aligned almost west-southwest corresponding with the direction of the predominant wind direction in autumn. Given the shape and almost constant width of the Gulf, there are no immediate reasons to sub-divide the Gulf into smaller meteorological areas, as wind conditions are likely to be uniform throughout the area.

By combining the information from the Baltic Pilots and the general experience, a map of meteorological areas has been made. This map is seen in Figure 2-4.

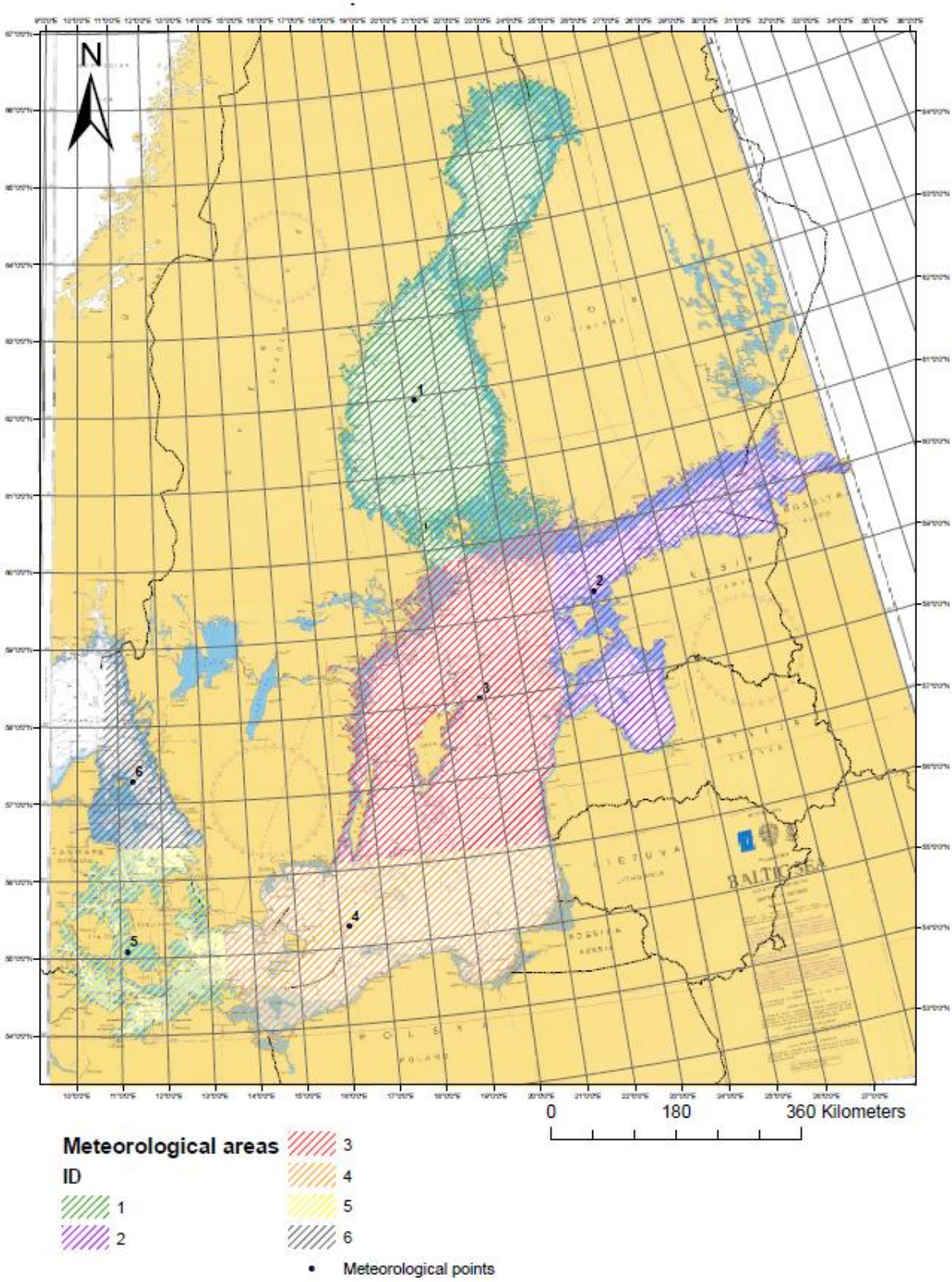

Figure 2-4 *Six meteorological areas selected for the Baltic Sea*

It is seen from the map that altogether six meteorological areas are defined within the project area. The table below shows the coverage of the six areas and provides coordinates of the representative location.

(NOTE: The six meteorological areas in Figure 2-4 are not identical with the six sub-regions in Figure 5-1 as they serve different purposes. The meteorological areas are about wind conditions whereas the sub-regions are about presentation of results).

Table 2-1: Coverage of meteorological areas and coordinates of representative location.

Meteorological area	Area coverage	Coordinates of representative location
1	Bothnia Bay including Åland Islands	19.667° E, 62.600° N
2	Gulf of Finland, Gulf of Riga	25.333° E, 59.800° N
3	Central Baltic Proper	20.000° E, 58.400° N
4	Southern Baltic Proper	16.667° E, 55.400° N
5	Entrances to the Baltic Sea	11.000° E, 54.600° N
6	Kattegat	11.667° E, 57.200° N

2.3 Subdivision into hydrographical areas

The project area has been divided into a number of hydrographical areas. A hydrographical area is defined as a smaller unit of the water area in which the hydrographical conditions can be assumed to be uniform. Thus, oil spilt anywhere in a hydrographical area will, in principle, traverse the same direction and speed until it reaches the boundary of the area. In the next area, it will presume a new direction and speed. Therefore, a every oil spill is modelled across an array of the hydrographical areas. The selection of the hydrographical areas is made on basis of experience and knowledge of the hydrographical conditions within the Baltic Sea. Further the selection is made so that the hydrographical areas fit within the borders of the meteorological areas.

First, each larger oceanographic unit (e.g. the Gulf of Bothnia) is inspected with regards to the hydrographical conditions under ice-free conditions. This leads to a division of the area into hydrographical units which under ice-free conditions have different hydrographical characteristics.

During the winter season part of the Baltic Sea is covered with ice. In ice-covered areas, the hydrographical conditions are significantly different from periods when the areas are ice-free. Therefore, the larger oceanographic units are analysed for the occurrence of ice, and a subdivision into ice covered areas are subsequently made. For this purpose, ice charts published by the Swedish Meteorological and Hydrological Institute (SMHI) have been applied. For the BRISK I project (BRISK I, Spreading, 2012), the annual ice reports from SMHI for a series of years were inspected, and among other years it was found that 2005 was a typical year in terms of ice coverage taking the Baltic Sea as a whole. Two dates during 2005 were selected, on which basis it has been evaluated which areas have occurrence of ice. The ice cover maps from these dates which represent ice the cover 1) initially in the ice period on 15 February and 2) at the maximum extent of the ice cover on 15 March, are seen in Figure 2-5 and Figure 2-6.

The data from 2005 were compared to more recent ice data from SHMI collected as part of the BRISK II data collection process. As an example, the relatively harsh winter 2024 showed a larger ice cover than in 2005 both on 15 February and 15 March. On the other hand, the winter of 2023 – which is considered “normal” by SHMI – show a smaller ice cover. Thus, it is concluded that the ice extent in 2005 continues to be a good representation of the situation also today.

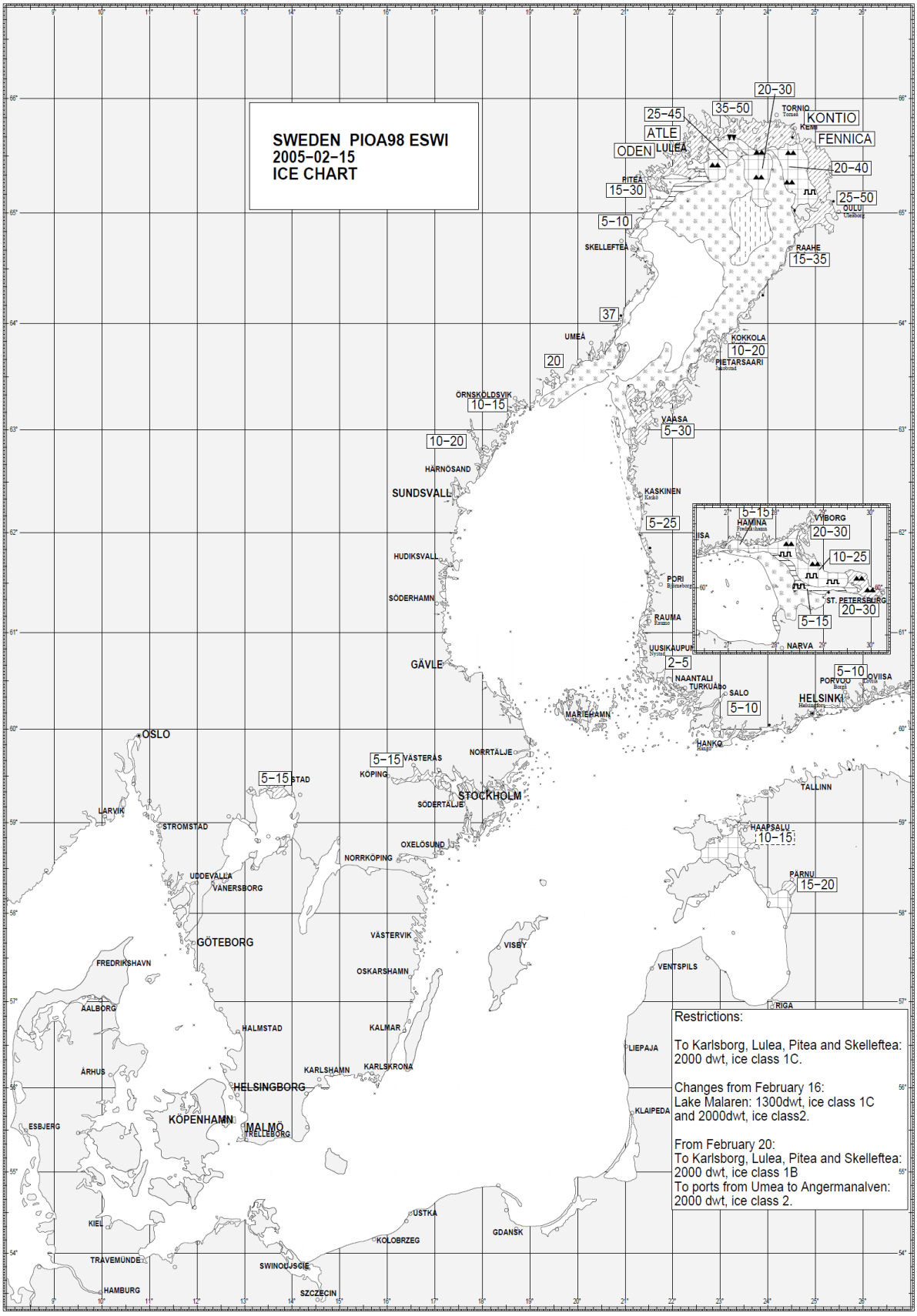

Figure 2-5: Ice cover in the year 2005 representing the ice cover initially in the ice period, 15 of February.

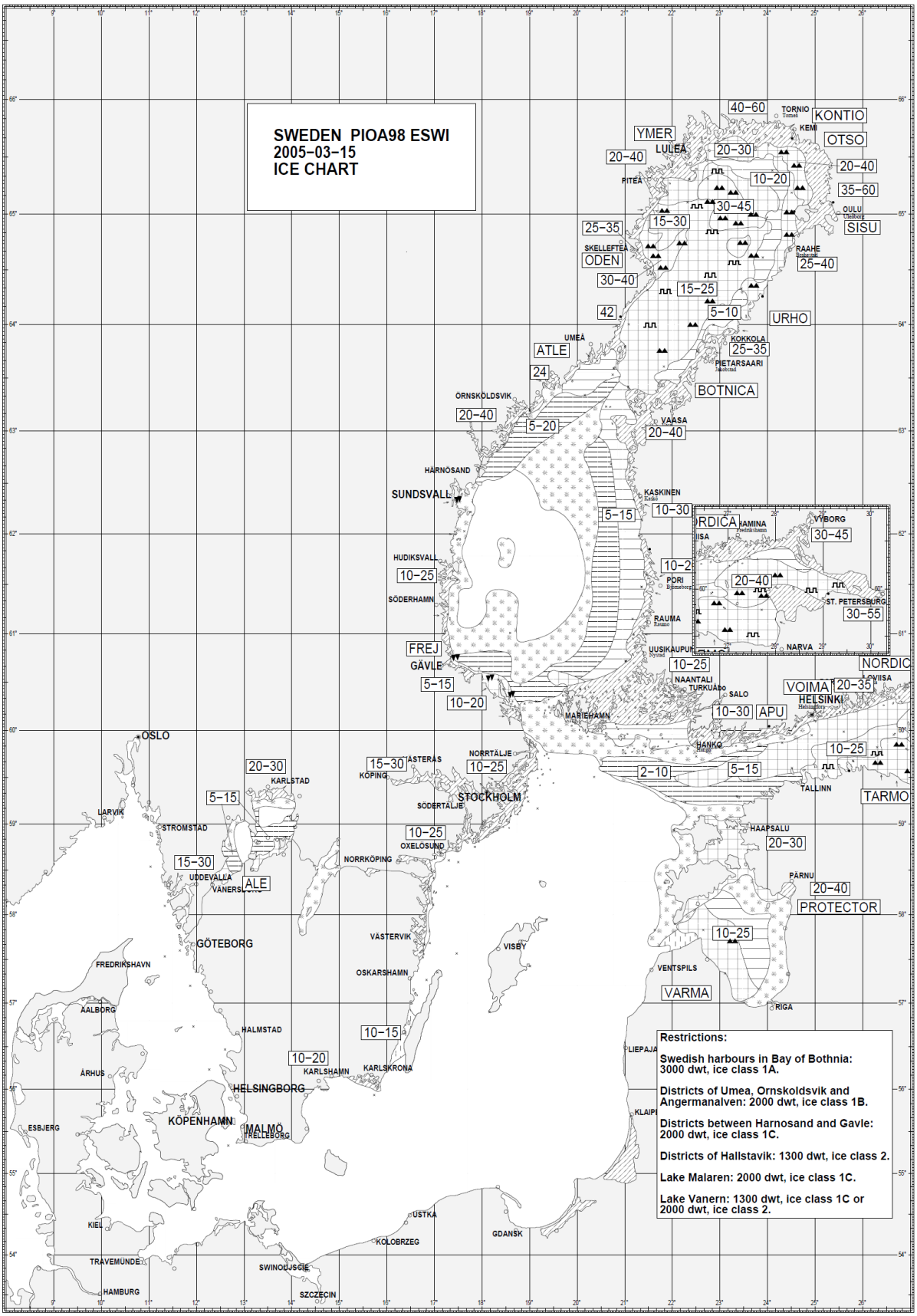

Figure 2-6: Ice cover in the year 2005 representing the maximum extent of the ice cover in the ice period, 15 of March.

The map with the hydrographical areas without ice is then compared with the map of ice-covered areas. The union of the two maps lead to a set of hydrographical areas, of which some have periods which are ice-covered.

In total 22 hydrographical areas result from this analysis. The hydrographical areas are shown in Figure 2-7.

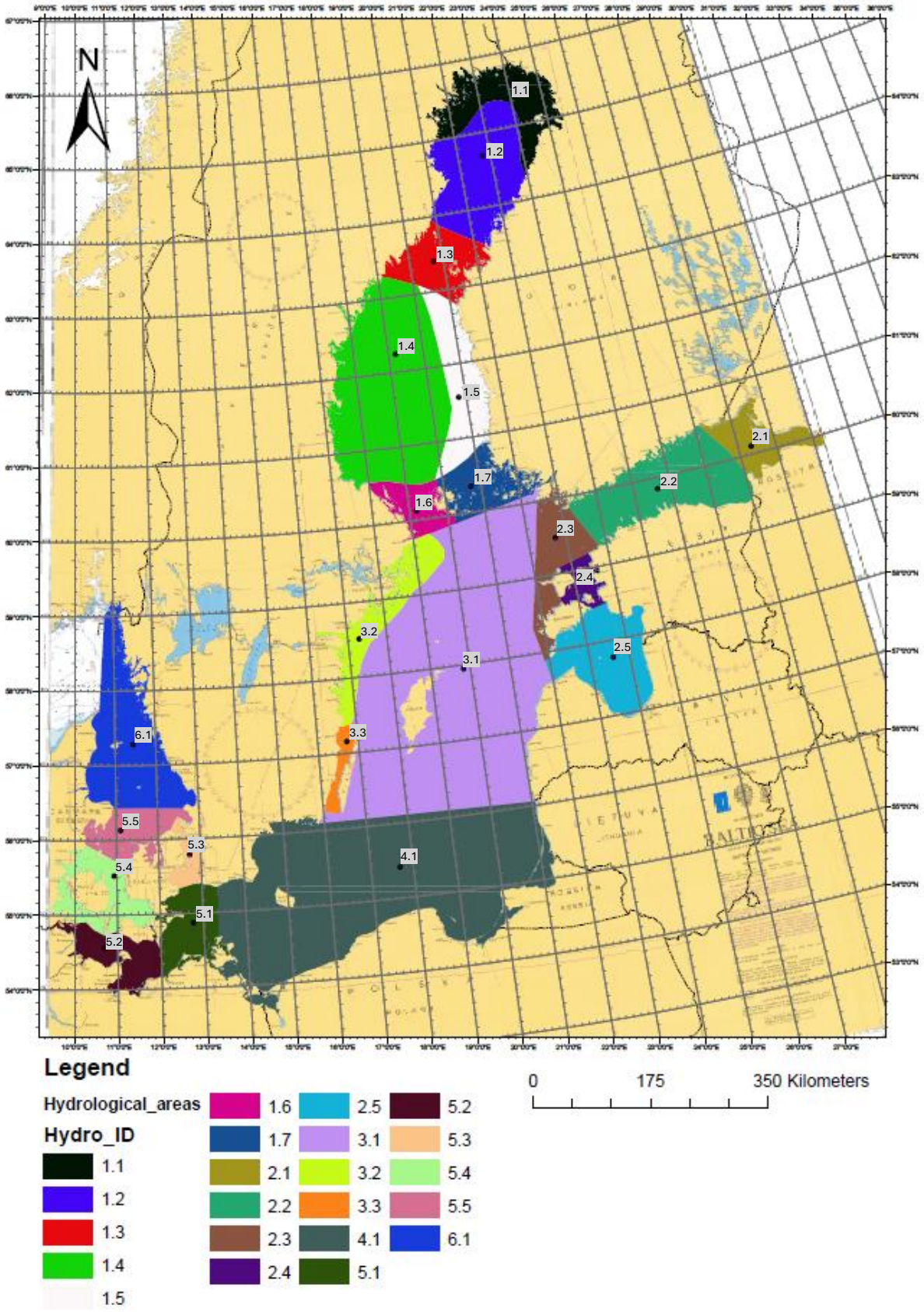

Figure 2-7: Hydrographical areas of the Baltic Sea

The table below show the numbered hydrographical areas, their coverage, ice conditions and the coordinates of the representative location. Note that these are defined as sub-divisions of the six meteorological areas introduced in Figure 2-4, hence the naming 1.1, 1.2 etc.

Table 2-2 Hydrographical areas, their coverage, ice conditions and locations

Hydrographical area	Area coverage	Ice conditions	Coordinates of representing location
1.1	Northernmost Gulf of Bothnia	Ice/No Ice	24.101°E , 65.544 N
1.2	Northern Gulf of Bothnia	Ice/No Ice	22.761° E, 64.692° N
1.3	Central Gulf of Bothnia	Ice/No Ice	20.722° E, 63.406° N
1.4	Western Gulf of Bothnia	No ice	19.212° E, 62.245° N
1.5	Eastern Gulf of Bothnia	Ice/No Ice	20.794° E, 61.544° N
1.6	Western Åland Sea	Ice/No Ice	19.186°E, 60.128° N
1.7	Eastern Åland Sea	Ice/No Ice	20.733° E, 60.349° N
2.1	Eastern Gulf of Finland	Ice/No Ice	28.347° E, 60.109° N
2.2	Central Gulf of Finland	Ice/No Ice	25.636° E, 59.855° N
2.3	Western Gulf of Finland	No ice	22.711° E, 59.483° N
2.4	Väinameri Strait	Ice/No Ice	23.269° E, 58.874° N
2.5	Gulf of Riga, Irbe Strait	Ice/No Ice	23.589° E, 57.772° N
3.1	Central Baltic Proper	No ice	19.826° E, 57.948° N
3.2	Swedish east coast	Ice/No Ice	17.291° E, 58.512° N
3.3	Kalmar Sound	No ice	16.725° E, 57.161° N
4.1	Southern Baltic Proper	No ice	17.687° E, 55.418° N
5.1	Kadetrenden	No ice	12.771° E, 54.872° N
5.2	Fehmarn Belt	No ice	10.695° E, 54.562° N
5.3	The Sound (Øresund)	No ice	12.740° E, 55.788° N
5.4	Belt Sea	No ice	10.937° E, 55.526° N
5.5	Southern Kattegat	No ice	11.107° E, 56.135° N
6.1	Northern Kattegat	No ice	11.448° E, 57.281° N

2.4 Modelling of the ice cover

In the event of an oil spill in ice covered waters, the drift velocity of the oil as well as the spreading of the oil will be drastically reduced. There are numerous ways in which oil can interact with the ice dependent on the state of the ice (ice pack, broken ice etc.) and the type of oil. Buoyant oil under ice will migrate at the underside of the ice sheet. Here, the oil will collect in pockets or stopped by keels or ridges of the uneven ice surface. The oil will typically move upwards through the freezing and thawing process, and collect in leads between ice sheets, from where it is able to evaporate. Oil in broken ice will tend to move

with the speed of the drifting ice, whereas oil under packed ice may move with the speed of the current under the ice. Details of the behaviour of oil in ice are presented in (OCC, 1998).

Due to the above-mentioned behaviour of oil in ice, and since part of the Baltic Sea may be covered by ice, it is necessary to include the effect of ice cover in the oil spill modelling. Thus, for hydrographical areas where ice is present in periods of the year, oil spill modelling is made both for the periods with ice and periods without ice. For hydrographical areas which on average are not covered with ice, simulations are carried out for ice-free conditions only.

The actual effect on drift velocity and drift direction in case of an oil spill in ice covered waters is implicitly modelled by the applied model system which has an ice module included. Thus, the various types of interaction between oil and ice do not need a separate parameterisation. A detailed description of the modelling of ice in the applied model is given in (SMHI, 1998).

However, as mentioned above, model simulations are made for situations both with and without ice. The ice cover does not appear at the same time in all hydrographical areas in the Baltic Sea. Typically, ice formation starts in the northernmost part of Gulf of Bothnia and then expands southwards. Thus, for the selection of a representative period for modelling oil spill under various wind classes in the ice-covered period (January-March), it is necessary to obtain information of the ice coverage with time in the various hydrographical areas.

This information can not immediately be retrieved from the applied model system. Therefore, the selection of periods with ice cover needs to be obtained by other means. For this purpose, ice cover maps produced by SMHI have been applied. These maps are available on the web site of SMHI on a daily basis as well as in annual publications.

The maps of ice cover which were used for BRISK I are from the following dates: 01.01.2009, 15.01.2009, 01.02.2009, 04.02.2009, 07.02.2009, 11.02.2009, 15.02.2009, 01.03.2009, 15.03.2009, 31.03.2009. The larger coverage in time during the first half of February has been chosen since the ice cover typically develops rapidly during this period. This conclusion has been made by inspecting a number of years of ice coverage on the SMHI ice cover pages. The same ice maps are applied for the BRISK II project.

2.5 Definition of the simulation periods

The simulation periods for the oil spill scenarios are found by statistical analysis of the time series of wind data. Time series of wind speed and direction covering the entire model year from the BRISK I project (July 2008-June 2009) were extracted from the hydrodynamic model at each of the meteorological locations, cf. Table 2-1. The statistical analysis of the data results in a set of representative simulation periods of three days length which are specific for each of the hydrographical areas defined in Figure 2-7.

Since the model simulations is representing three wind classes and four wind directions, altogether 12 combinations exist for combined wind-direction classes, see table below. Hence a simulation period is found for each combined wind speed-direction class.

Table 2-3 Wind speed and direction classes and their intervals

Wind speed class	Wind direction class	Combined wind speed-wind direction class	Wind speed intervals [m/s]	Wind direction intervals [°]
1	1	1	V ≤ 5	0 - 90
1	2	2	V ≤ 5	90 – 180
1	3	3	V ≤ 5	180 - 270
1	4	4	V ≤ 5	270 - 360
2	1	5	5 < V ≤ 11	0 - 90
2	2	6	5 < V ≤ 11	90 - 180
2	3	7	5 < V ≤ 11	180 - 270
2	4	8	5 < V ≤ 11	270 - 360
3	1	9	V > 11	0 - 90
3	2	10	V > 11	90 - 180
3	3	11	V > 11	180 - 270
3	4	12	V > 11	270 - 360

For each hydrographical area, the time series from July 2008 to June 2009 was analysed based on hourly averages. The year has 8,760 hours and each hour is the start of a three-day (72-hour) time series. For each of the 12 wind speed-direction classes, the three-day time series with the best match was identified. This was done by calculating a score between 0 and 1. A score of 1 means all values of speed and direction (hourly intervals) in a 3 day period fall within a single wind speed-direction class. The time series with the highest score is used for the model. For BRISK II, the same meteorological data is used, as it has been verified that climate change has not had any discernible effect on the meteorological data at question.

2.5.1 Simulation periods for hydrographical areas without ice cover

For all of the hydrographical areas which on average is not covered by ice the entire model year (01.07.2008 to 30.06.2009) is analysed. Table 2-4 to Table 2-9 show the result of the analysis in terms of assigned simulation period for the hydrographical areas without ice cover.

Table 2-4: Simulation start time for wind speed-direction classes. Hydrographical area 1.4.

Hydrographical area	Simulation start date and time for each wind speed-direction class		Score
1.4	1	12-09-2008 12:00:00	0.96
	2	15-09-2008 19:00:00	0.68
	3	25-06-2009 04:00:00	0.70
	4	22-12-2008 01:00:00	0.39
	5	03-07-2008 11:00:00	0.90
	6	18-01-2009 03:00:00	0.70
	7	02-02-2009 12:00:00	0.75
	8	27-12-2008 11:00:00	1.00
	9	22-11-2008 07:00:00	0.68
	10	20-02-2009 00:00:00	0.44
	11	23-10-2008 11:00:00	0.90
	12	30-12-2008 12:00:00	0.48

Table 2-5: Simulation start time for wind speed-direction classes. Hydrographical area 2.3.

Hydrographical area	Simulation start date and time for each wind speed-direction class		Score
2.3	1	21-06-2009 22:00:00	0.82
	2	16-09-2008 22:00:00	0.72
	3	19-05-2009 00:00:00	0.51
	4	26-01-2009 13:00:00	0.82
	5	12-09-2008 12:00:00	1.00
	6	20-02-2009 02:00:00	1.00
	7	02-09-2008 20:00:00	0.96
	8	01-01-2009 13:00:00	0.94
	9	08-09-2008 21:00:00	0.66
	10	02-08-2008 04:00:00	0.21
	11	10-01-2009 14:00:00	1.00
	12	14-11-2008 08:00:00	0.23

Table 2-6: Simulation start time for wind speed-direction classes. Hydrographical area 3.1-3.3.

Hydrographical area	Simulation start date and time for each wind speed-direction class		Score
3.1, 3.3	1	23-07-2008 12:00:00	0.80
	2	01-02-2009 09:00:00	0.49
	3	09-04-2009 04:00:00	0.66
	4	26-01-2009 22:00:00	0.52
	5	10-09-2008 17:00:00	1.00
	6	13-12-2008 14:00:00	1.00
	7	02-10-2008 04:00:00	1.00
	8	11-05-2009 00:00:00	1.00
	9	14-08-2008 10:00:00	0.25
	10	21-01-2009 15:00:00	0.31
	11	10-01-2009 18:00:00	1.00
	12	20-12-2008 21:00:00	0.51

Table 2-7: Simulation start time for wind speed-direction classes. Hydrographical area 4.1.

Hydrographical area	Simulation start date and time for each wind speed-direction class		Score
4.1	1	27-07-2008 10:00:00	0.85
	2	30-07-2008 06:00:00	0.51
	3	06-09-2008 02:00:00	0.70
	4	27-01-2009 00:00:00	0.68
	5	12-09-2008 23:00:00	1.00
	6	25-04-2009 05:00:00	0.90
	7	15-07-2008 09:00:00	0.89
	8	23-11-2008 07:00:00	0.72
	9	23-06-2009 12:00:00	0.58
	10	31-01-2009 12:00:00	0.39
	11	30-09-2008 11:00:00	0.97
	12	20-12-2008 15:00:00	0.59

Table 2-8: Simulation start time for wind speed-direction classes. Hydrographical area 5.1-5.5.

Hydrographical area	Simulation start date and time for each wind speed-direction class		Score
5.1-5.5	1	16-09-2008 13:00:00	0.82
	2	27-01-2009 18:00:00	0.85
	3	06-09-2008 15:00:00	0.41
	4	14-08-2008 19:00:00	0.49
	5	13-09-2008 10:00:00	1.01
	6	29-07-2008 16:00:00	0.94
	7	19-08-2008 11:00:00	1.00
	8	13-06-2009 16:00:00	0.87
	9	14-04-2009 02:00:00	0.31
	10	31-01-2009 06:00:00	0.55
	11	09-11-2008 09:00:00	0.54
	12	10-06-2009 16:00:00	0.68

Table 2-9: Simulation start time for wind speed-direction classes. Hydrographical area 6.1.

Hydrographical area	Simulation start date and time for each wind speed-direction class		Score
6.1	1	27-12-2008 07:00:00	0.55
	2	01-11-2008 08:00:00	0.93
	3	01-04-2009 22:00:00	0.51
	4	25-07-2008 14:00:00	0.56
	5	24-06-2009 10:00:00	0.70
	6	06-11-2008 04:00:00	1.00
	7	10-10-2008 21:00:00	0.93
	8	11-06-2009 15:00:00	0.79
	9	21-03-2009 08:00:00	0.11
	10	16-01-2009 00:00:00	0.77
	11	23-10-2008 10:00:00	0.75
	12	15-11-2008 23:00:00	0.48

2.5.2 Simulation periods for hydrographical areas with ice cover

The simulation periods for the hydrographical areas which in periods have ice cover are treated in a special manner. The simulation periods for the months without ice, i.e. April to December, are found in the same manner as described in 2.5.1, with the only difference being the shorter time series in the analysis.

For the simulation periods in the months with ice (January-March) an additional score, namely an ice score is introduced. The ice score is the percentage ice cover in a particular hydrographical area at a particular time. The model does not take the effect of differing ice cover thickness into account. As described in section 2.4 a number of ice cover maps have been used to determine the ice cover at different times for each of the hydrographical areas. The results of the ice cover are seen in table below.

Table 2-10: Estimated ice cover percentages for hydrographical areas throughout the months with ice cover.

	Season: winter with ice							**Season: spring with ice**		
Hyd.area	**jan-01**	**jan-15**	**feb-01**	**feb-04**	**feb-07**	**feb-11**	**feb-15**	**mar-01**	**mar-15**	**mar-31**
1.1	10	25	75	90	100	100	100	100	100	100
1.2	2	5	5	10	20	70	100	100	95	90
1.3	2	5	20	60	90	100	100	100	90	80
1.5	0	10	10	10	10	15	20	25	25	25
1.6	0	0	2	2	2	5	5	10	10	10
1.7	0	5	2	5	5	10	10	40	40	30
2.1	10	10	60	75	90	90	100	100	70	30
2.2	0	2	5	5	10	15	15	25	20	15
2.4	5	15	30	30	90	95	100	100	100	40
2.5	5	5	5	5	10	10	10	15	15	2
3.2	0	5	10	10	10	15	15	20	25	15

For each hour in the period January to March an ice cover percentage is found by linear interpolation between the estimated values, see Figure 2-1 which shows hydrographical area 1.3 as an example.

The wind speed-direction score is hereafter multiplied by the ice score to obtain a combined score. Seeking the maximum of the combined score over 3 day moving averages in the period January to March gives the simulation starting time for ice covered areas.

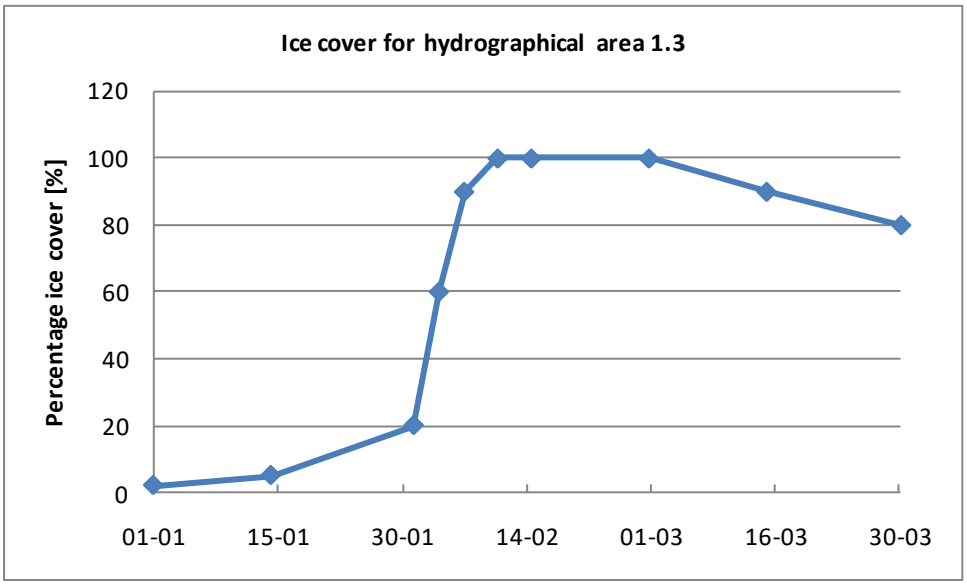

Figure 2-8: Estimated time development of ice cover percentage for hydrographical area 1.3.

The figure below shows an example of calculation of the combined score. The example shows the original wind speed-direction score together with the ice score and the combined score for hydrographical area 1.3 using wind speed-direction class 7.

It is seen from the figure that the maximum score for wind speed-direction is drastically reduced when the ice score is considered. Thus, the peak of the combined score is changed to a different date.

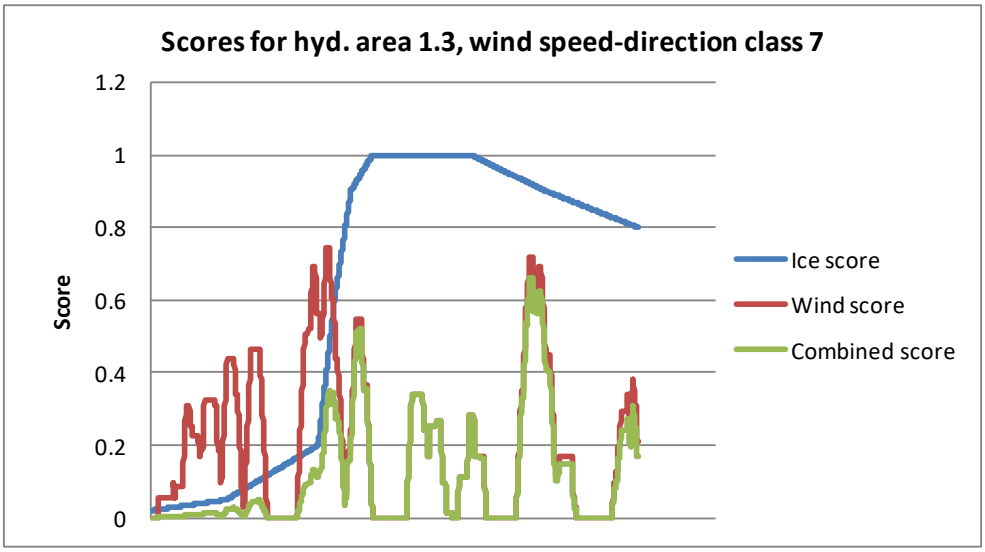

Figure 2-9: Example of scores for hydrographical area 1.3 during the ice-covered period January to March.

The derived simulation start times for the hydrographical areas with ice cover is seen in the Table 2-11 below. The table show also the combined score of wind speed-direction and ice score. The simulation start times are applied for the period with ice cover.

Table 2-11 Simulation start times and score values for hydrographical areas with ice.

W.sp-dir class	Score Hyd. 1.1	Max date Hyd. 1.1	Score Hyd. 1.2	Start date Hyd. 1.2	Score Hyd. 1.3	Start date Hyd. 1.3	Score Hyd. 1.5	Start date Hyd. 1.5	Score Hyd. 1.6	Start date Hyd. 1.6	Score Hyd. 1.7	Start date Hyd. 1.7
1	0.55	15-02-2009 03:00	0.55	15-02-2009 03:00	0.55	15-02-2009 03:00	0.11	16-02-2009 06:00	0.04	23-03-2009 11:00	0.15	23-03-2009 11:00
2	0.35	28-01-2009 00:00	0.32	04-03-2009 19:00	0.32	04-03-2009 19:00	0.08	04-03-2009 19:00	0.03	04-03-2009 19:00	0.13	04-03-2009 19:00
3	0.63	10-02-2009 04:00	0.44	10-02-2009 23:00	0.63	10-02-2009 23:00	0.10	10-02-2009 23:00	0.04	14-03-2009 07:00	0.15	14-03-2009 07:00
4	0.24	10-02-2009 16:00	0.21	22-03-2009 05:00	0.24	10-02-2009 23:00	0.06	22-03-2009 05:00	0.02	22-03-2009 05:00	0.08	22-03-2009 05:00
5	0.70	08-03-2009 21:00	0.68	08-03-2009 21:00	0.66	08-03-2009 21:00	0.18	08-03-2009 21:00	0.07	08-03-2009 21:00	0.28	08-03-2009 21:00
6	0.66	06-03-2009 15:00	0.65	06-03-2009 15:00	0.64	06-03-2009 15:00	0.17	06-03-2009 15:00	0.07	06-03-2009 15:00	0.26	06-03-2009 15:00
7	0.72	11-03-2009 23:00	0.69	11-03-2009 23:00	0.66	11-03-2009 23:00	0.18	11-03-2009 23:00	0.07	11-03-2009 23:00	0.29	11-03-2009 23:00
8	0.52	24-02-2009 15:00	0.52	24-02-2009 15:00	0.52	24-02-2009 15:00	0.13	18-03-2009 18:00	0.05	18-03-2009 18:00	0.20	18-03-2009 18:00
9	0.06	16-03-2009 03:00	0.05	16-03-2009 03:00	0.05	16-03-2009 03:00	0.01	16-03-2009 03:00	0.01	16-03-2009 03:00	0.02	16-03-2009 03:00
10	0.44	19-02-2009 23:00	0.44	19-02-2009 23:00	0.44	19-02-2009 23:00	0.10	21-02-2009 16:00	0.03	21-02-2009 16:00	0.11	21-02-2009 16:00
11	0.25	27-02-2009 21:00	0.25	27-02-2009 21:00	0.25	27-02-2009 21:00	0.06	28-02-2009 23:00	0.03	28-02-2009 23:00	0.10	28-02-2009 23:00
12	0.15	15-03-2009 06:00	0.15	15-03-2009 06:00	0.14	15-03-2009 06:00	0.04	15-03-2009 06:00	0.02	15-03-2009 06:00	0.06	15-03-2009 06:00

W.sp-dir class	Score Hyd. 2.1	Max date Hyd. 2.1	Score Hyd. 2.2	Start date Hyd. 2.2	Score Hyd. 2.4	Start date Hyd. 2.4	Score Hyd. 2.5	Start date Hyd. 2.5	Score Hyd. 3.2	Start date Hyd. 3.2
1	0.28	15-03-2009 11:00	0.08	15-03-2009 11:00	0.4	15-03-2009 11:00	0.06	15-03-2009 11:00	0.09	09-03-2009 09:00
2	0.53	10-03-2009 11:00	0.14	10-03-2009 11:00	0.66	10-03-2009 11:00	0.10	10-03-2009 11:00	0.05	01-02-2009 08:00
3	0.45	01-03-2009 12:00	0.11	01-03-2009 12:00	0.45	01-03-2009 12:00	0.07	01-03-2009 12:00	0.04	14-03-2009 23:00
4	0.37	26-01-2009 19:00	0.06	27-02-2009 12:00	0.25	26-02-2009 20:00	0.04	26-01-2009 12:00	0.05	24-02-2009 02:00
5	0.95	12-02-2009 06:00	0.15	11-02-2009 13:00	0.98	12-02-2009 06:00	0.10	11-02-2009 13:00	0.16	16-02-2009 07:00
6	1.01	20-02-2009 01:00	0.19	20-02-2009 11:00	1.01	20-02-2009 01:00	0.12	20-02-2009 11:00	0.19	04-03-2009 07:00
7	0.56	23-02-2009 20:00	0.12	24-02-2009 06:00	0.56	23-02-2009 20:00	0.08	24-02-2009 06:00	0.13	14-03-2009 05:00
8	0.54	26-02-2009 08:00	0.13	27-02-2009 18:00	0.54	26-02-2009 08:00	0.08	27-02-2009 18:00	0.11	27-02-2009 00:00
9	0.03	24-01-2009 06:00	0.00	24-01-2009 06:00	0.02	24-01-2009 06:00	0.00	21-01-2009 15:00	0.05	16-03-2009 18:00
10	0.03	24-01-2009 07:00	0.01	25-03-2009 07:00	0.04	25-03-2009 07:00	0.00	21-01-2009 18:00	0.04	22-02-2009 11:00
11	0.10	10-01-2009 13:00	0.04	28-03-2009 15:00	0.14	17-03-2009 18:00	0.05	10-01-2009 13:00	0.04	29-03-2009 00:00
12	0.01	01-01-2009 00:00	0.00	06-01-2009 21:00	0.01	06-01-2009 21:00	0.01	01-01-2009 00:00	0.1	15-03-2009 19:00

In the period of the year with no ice (April to December) the above hydrographical areas are assigned a different simulation period than during the period with ice cover.

These periods are shown in Table 2-12 to Table 2-14 below.

Table 2-12: Simulation start time for wind speed-direction classes. Hydrographical area 1.1, 1.2, 1.3,1.5, 1.6, 1.7. Period without ice.

Hydrographical area	Simulation start date and time for each wind speed-direction class		Score
1.1, 1.2, 1.3, 1.5, 1.6, 1.7	1	12-09-2008 12:00:00	0.96
	2	15-09-2008 19:00:00	0.68
	3	25-06-2009 04:00:00	0.70
	4	22-12-2008 01:00:00	0.39
	5	03-07-2008 11:00:00	0.90
	6	12-12-2008 23:00:00	0.61
	7	25-10-2008 12:00:00	0.73
	8	27-12-2008 11:00:00	1.00
	9	22-11-2008 07:00:00	0.68
	10	29-09-2008 03:00:00	0.32
	11	23-10-2008 11:00:00	0.90
	12	20-12-2008 17:00:00	0.46

Table 2-13: Simulation start time for wind speed-direction classes. Hydrographical area 2.1,2.2, 2.4,2.5. Period without ice.

Hydrographical area	Simulation start date and time for each wind speed-direction class		Score
2.1, 2.2, 2.4, 2.5	1	21-06-2009 22:00:00	0.82
	2	16-09-2008 22:00:00	0.72
	3	19-05-2009 00:00:00	0.51
	4	01-07-2008 05:00:00	0.63
	5	12-09-2008 12:00:00	1.01
	6	10-12-2008 04:00:00	0.90
	7	02-09-2008 20:00:00	0.96
	8	27-12-2008 07:00:00	0.86
	9	08-09-2008 21:00:00	0.66
	10	02-08-2008 04:00:00	0.21
	11	24-10-2008 03:00:00	0.92
	12	14-11-2008 08:00:00	0.23

Table 2-14: Simulation start time for wind speed-direction classes. Hydrographical area 3.2. Period without ice.

Hydrographical area	Simulation start date and time for each wind speed-direction class		Score
3.2	1	21-06-2009 22:00:00	0.82
	2	16-09-2008 22:00:00	0.72
	3	19-05-2009 00:00:00	0.51
	4	01-07-2008 05:00:00	0.63
	5	12-09-2008 12:00:00	1.00
	6	10-12-2008 04:00:00	0.90
	7	02-09-2008 20:00:00	0.96
	8	27-12-2008 07:00:00	0.86
	9	08-09-2008 21:00:00	0.66
	10	02-08-2008 04:00:00	0.21
	11	24-10-2008 03:00:00	0.92
	12	14-11-2008 08:00:00	0.23

2.6 Adjustment of the bunker model

In D2.4 Cargo analysis (BRISK II, Cargo analysis, 2025), the contribution of different oil types to the average bunker content in the Baltic Sea was estimated based on a survey conducted as part of the IMAROS 2 project. The resulting bunker distribution is shown in the second-last column of Table 2-15.

As the share of ultra low-sulphur fuel oil (ULSFO) must be expected to change due to changes in regulations, a revised estimate has been made based on the professional judgement of the authors of this report. It is shown in the last column of the table.

Table 2-15 Data and estimates on bunkering and bunker tank content

Substance	**Cargo group (representative substance)**	**Bunker content according to deliverable D2.4**	**Revised estimate of the bunker content**
HSFO	20 (IFO 380)	30 %	15 %
VLSFO	23 (VLSFO)	44 %	44 %
ULSFO	24 (ULSFO)	4 %	11 %
Marine gasoil	21 (Diesel)	22 %	30 %
Total		100 %	100 %

3 Modelling of spreading and fate of oil

The model system Seatrack Web has been applied for the oil spill modelling. Part of the following description stem from the Technical Documentation for Seatrack Web (SMHI, 2008a, b).

3.1 Description of applied model system

The Seatrack Web system consists of three main parts: Forcing in the form of forecasted flow and wind fields, an oil drift model and a graphical user interface.

The area covered by the Seatrack Web system is the Baltic Sea, the sounds between Sweden and Denmark, the Kattegat and the Skagerrak, and out to about longitude 3° east in the North Sea.

The forcing fields are provided by the weather model HIRLAM and the ocean model HIROMB. These are run operationally and form the basis for weather and ocean forecasts at SMHI. For longer forecasts forcing fields from the European Centre for Medium-Range Weather Forecasts replace those from HIRLAM. A number of relevant forcing variables are calculated by these models, but as yet not all are used by Seatrack Web. Some are still estimated internally.

The oil drift model PADM has been jointly developed by the Swedish Meteorological and Hydrological Institute (SMHI) and the former Danish Maritime Safety Administration (DAMSA, in the meantime succeeded by Danish Defence's Centre for Operative Oceanography, FCOO). It is executed whenever a Seatrack Web user requests a simulation via the SHMI or FCOO homepages.

The model is set up with a graphical user interface which has been developed at SMHI and is based on open-source GIS-server technology, i.e. the user interacts with geo-referenced data in a map.

3.1.1 Theoretical background

The oil drift model PADM is a Lagrangian particle spreading model. This means that the substance or object being simulated is represented as a cloud of particles. Each particle is "tracked", i.e. its trajectory is calculated based on time- and space-varying flow fields.

A fundamental assumption is that the particles do not influence the flow field, i.e. a particle does not have any effect on the flow in which it is located. Furthermore, in PADM particles are assumed not to interact directly with each other. However, some processes, such as dispersion and horizontal gravity-induced spreading, do depend on the global properties of the cloud of particles.

For example, whether a particle should be dispersed or not may depend on how many of the other particles in the cloud have already been dispersed. So, a single particle does not interact directly with a nearby particle but is affected by the global properties of the particle cloud it is part of. Particles are affected by boundaries such as the coastline, the bottom or the surface, e.g., particles may stick to a boundary or slip along it.

Each particle has a set of properties. Most important of these is of course its position. However, a particle can have a variety of additional properties depending on what substance or object it represents, e.g. mass, volume, size, chemical properties, density, etc. These can be constants or vary with time, location, temperature, etc.

Further details of the model system are given in (SMHI, 2008), including description of ice, numerical methods etc.

3.1.2 Input parameters

The Seatrack Web model has a number of possible input parameters of which not all are required for an oil spill simulation. The input parameters that vary among the oil spill simulations for the present project are

- Start and end time of the simulation
- Coordinates of outlet point
- Amount of oil

Additional parameters are necessary, but all of these are assumed the same for all of the simulations carried out. These parameters are

- Outlet type (set to point outlet)
- Calculation type (set to oil, specific)
- Substance (set to intermediate fuel oil)
- State of oil (fresh)
- Depth (set to 0, meaning spill is at the surface)
- Instantaneous spill is assumed

3.2 Model simulations

3.2.1 Preparation of input data

Seatrack Web is set up with a graphical user interface for single oil spill simulation. This means that all model parameters have to be entered manually. This is not practical for the number of simulations that need to be carried out in the present project, partly due to the risk of typing errors.

Hence, DAMSA was engaged in setting up a facility for batch execution of the model runs during the BRISK I project. COWI created a software program was automatically generating all the input data files. The input data were transferred to DAMSA who carried out all of the oil spill simulations on a designated server. As meteorology has not changed, the Seatrack Web results from BRISK I are reused by the BRISK II project.

3.2.2 Sensitivity to oil type

Initially, the intention was to simulate different oil types. A few sensitivity simulations showed that the result of the drift of the oil was not very dependent on the oil types that were relevant to simulate for the project.

The figure below shows an example of three oil spill simulations in which only the oil type varies. The types of oil simulated are diesel, light oil, and heavy oil.

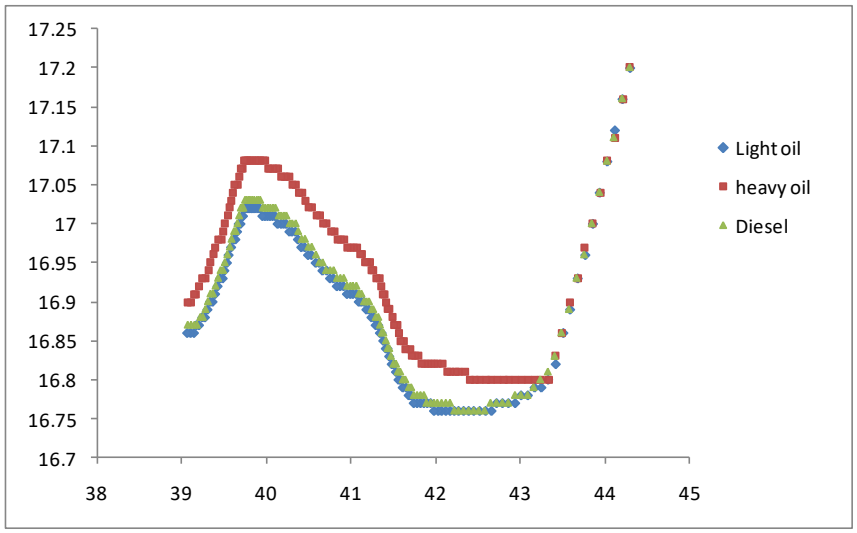

Figure 3-1: Test example of simulated path of three oil spills (centre of mass) with the only difference being the oil type. (x-axis = latitude, y-axis = longitude)

The conclusion from the test example was that the oil spill simulations under the given set of forcing functions did not produce a significantly different end position of the oil slick. On this basis it was decided to use only a single oil type, namely intermediate oil.

3.3 Model results

3.3.1 Example of detailed model results

Each oil spill is simulated for a three-day period. During this period the oil slick is subject to the wind, current and wave conditions prevailing during the simulation period. The results consist of a result file showing the position of the centre of mass of the oil slick on each time step. This result is useful for determining the drift velocity and direction of the oil spill.

Apart from this result, the model system provides two additional result files which describe the position of each particle as well as the state of the oil in detail (viscosity, density, evaporation, percentage of oil at the surface etc.). These results are not necessary for determination of the drift velocity and direction for the present purpose.

Some examples of the movement of oil spills are seen in Figure 3-2 to Figure 3-4. The figures show the position of the centre of mass of the oil spill for each hour during the 3-day simulation. The arrows indicate the direction of movement of the oil spills.

Figure 3-2 and Figure 3-3 show the route of the oil spill when the wind is primarily from one direction. In such circumstances the direction of the oil spill follows the direction of the wind (or the current for conveyance areas).

During some of the model simulations the direction of the wind changed during the 3-day simulation period. An example of this is seen in Figure 3-4.

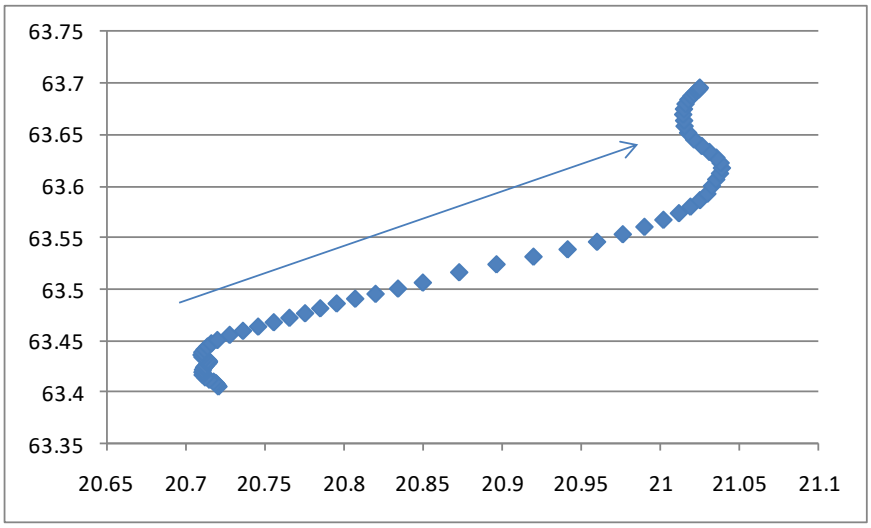

Figure 3-2 Example of simulated oil spill in hydrographical area 1.3 during south-westerly winds (x-axis = longitude, y-axis = latitude)

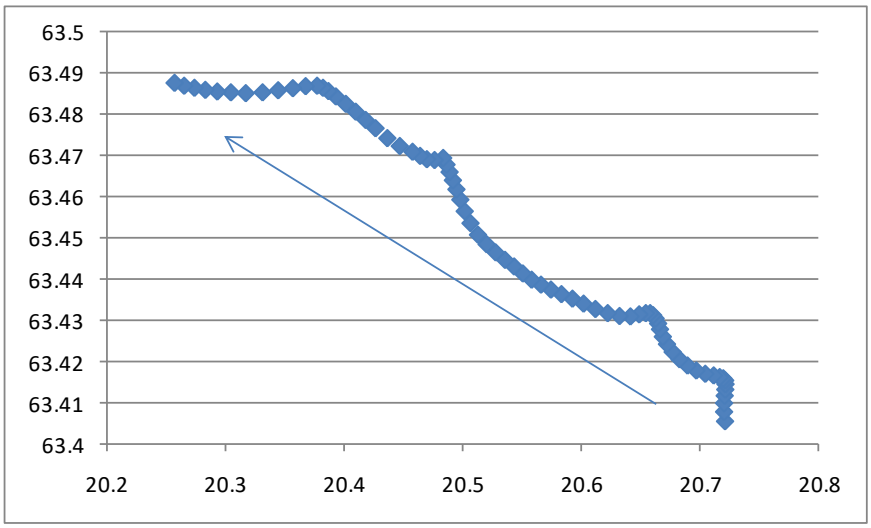

Figure 3-3 Example of simulated oil spill in hydrographical area 1.3 during south-easterly winds (x-axis = longitude, y-axis = latitude)

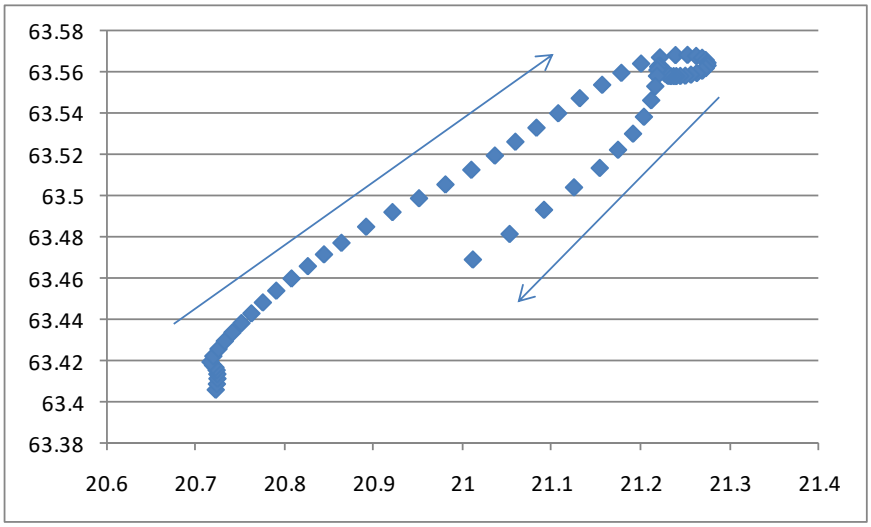

Figure 3-4: Example of simulated oil spill in hydrographical area 1.3 during south-westerly winds, followed by north-easterly winds (x-axis = longitude, y-axis = latitude)

3.3.2 Processing of drift velocity and direction

The main usage of the results from the oil spill simulations is to derive drift velocity and drift direction for each of the hydrographical areas. Based on experience, the drift velocity of the oil slick is a linear function of the wind velocity in open waters. Likewise, the drift direction in open waters of an oil slick is a linear function of the wind direction.

A practical manner to determine the drift velocity and direction is to use the start and end point coordinates of the oil spill and use this as a basis for calculation of the drift velocity over the three-day period. This approach is valid for most of the simulation results.

However, in the situation shown in Figure 3-4 this approach leads to a too small drift velocity. The oil spills have been analysed for this type of behaviour, and the drift results have been discarded in such cases.

By analysis of the model results it is found that the drift velocity is either a linear function of the wind velocity or a constant value. A constant value appears to be a better representation in water bodies which primarily serves as a conveyance of flow, such as the straits at the entrance to the Baltic Sea, the Kalmar Sound in Sweden and others.

The following general expressions are therefore derived:

$$V_{\text{drift}} = V_{\text{coef}} \cdot V_{\text{wind}} \quad \text{for open waters} \tag{3.1}$$

$$V_{\text{drift}} = V_{\text{const}} \quad \text{for waters with flow conveyance} \tag{3.2}$$

Similar expressions are derived for hydrographical areas with ice coverage.

The drift direction is generally found to vary linearly with the wind direction according to

$$\text{direction}_{\text{drift}} = D_{\text{coef}} \cdot \text{direction}_{\text{wind}} + D_{K1} \tag{3.3}$$

which also applies for ice covered areas.

However, for certain hydrographical areas a dependency of the wind direction could not be found, and a constant value is applied instead:

$$\text{direction}_{\text{drift}} = D_{K2} \qquad \text{for } 0° < \text{wind direction} < 180° \tag{3.4}$$

$$\text{direction}_{\text{drift}} = D_{K3} \qquad \text{for } 180° < \text{wind direction} < 360° \tag{3.5}$$

A similar expression is applied for ice covered hydrographical areas.

An example of the relation between drift velocity and wind velocity is seen in Figure 3-5.

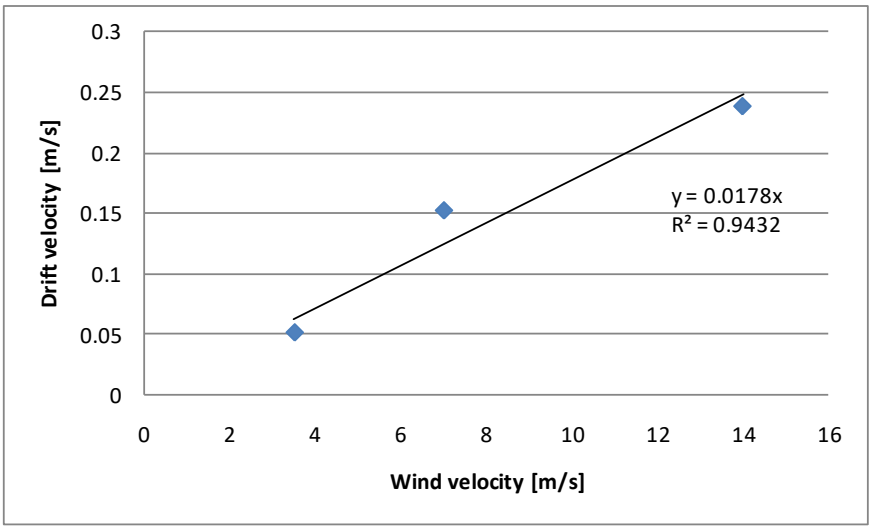

Figure 3-5: Relation between drift velocity and wind velocity in hydrographical area 4.1 (Southern Baltic Sea).

The results reveal that the drift velocity is less than 2% of the wind velocity. This is in close agreement with the general drift velocity of oil due to wind action which is 2%.

The result seen in Figure 3-5 is made on basis of average values for each of four wind directions. Individual results for each wind direction are seen in Figure 3-6.

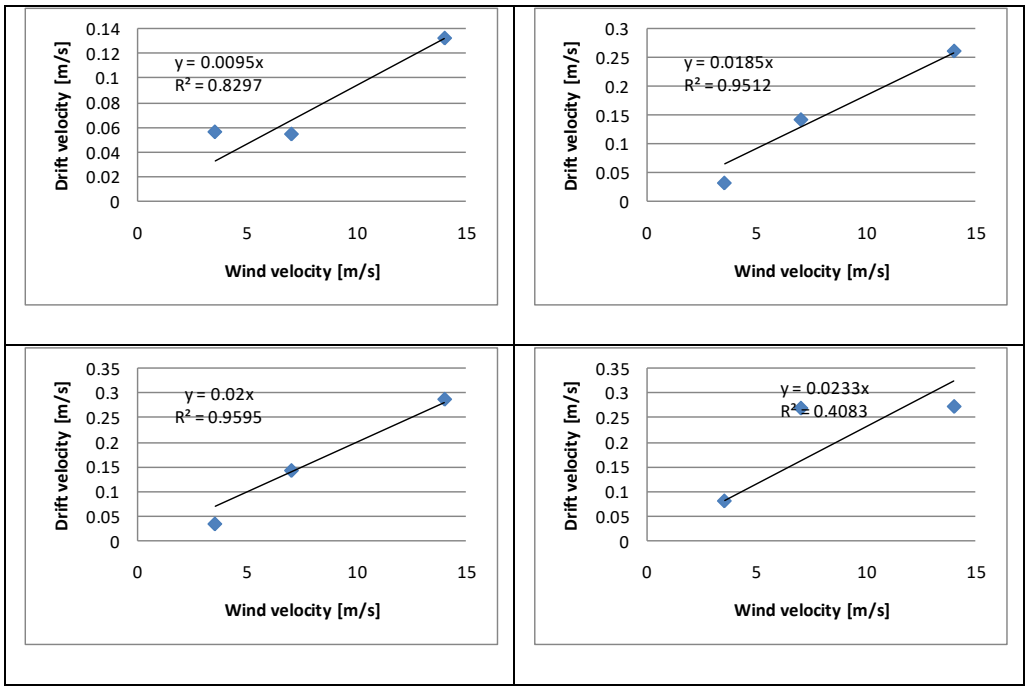

Figure 3-6 *Relation between drift velocity and wind velocity for each of the four wind direction quadrants. Hydrographical area 4.1. Wind directions: Top left: NE, Top right: SE, Bottom left: SW, Bottom right: NW*

An example from a water body which primarily acts as a conveyance for flow (The Sound, all wind directions) is seen in Figure 3-7.

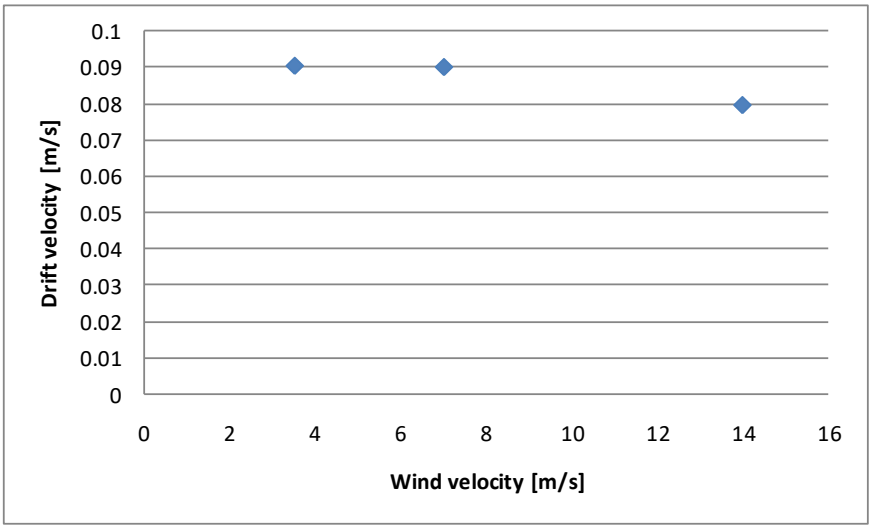

Figure 3-7 *Relation between drift velocity and wind velocity for hydrographical area 5.3 (The Sound), all directions*

It is seen from the figure above that the drift velocity is independent of the wind velocity. A constant average drift velocity of 0.087 m/s is found. The individual results for each of the four wind directions is seen in Figure 3-8.

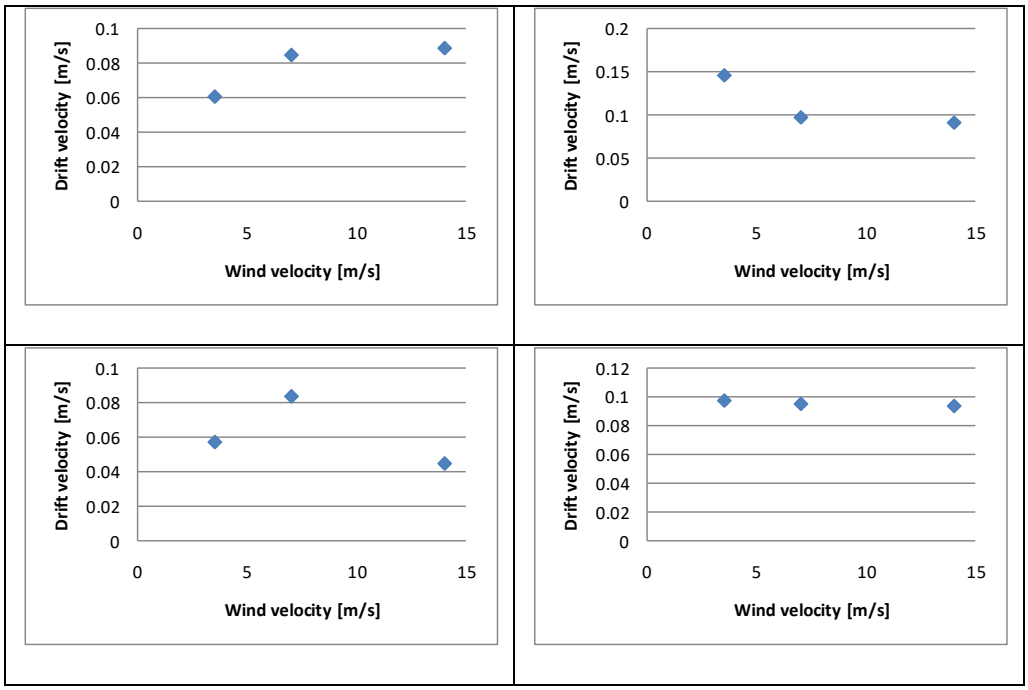

Figure 3-8: *Relation between drift velocity and wind velocity for each of the four wind direction quadrants. Hydrographical area 5.3. Wind directions: Top left: NE, Top right: SE, Bottom left: SW, Bottom right: NW*

It is seen from Figure 3-8 that none of the four wind direction quadrants shows a particular good relationship with the wind velocity.

Each of the 22 hydrographical areas have been analysed carefully in order to derive wind speed and direction factors and constants. The results are seen in Table 3-1.

Table 3-1 Results of drift velocity and drift direction from the oil spill modelling.

Hyd. area	V_coef	V_coef_ice	V_const	V_const_ice	D_coef	D_coef_ice	D_K1	D_K1_ice	D_K2	D_K2_ice	D_K3	D_K3_ice
	no ice	with ice	no ice	with ice	no ice	with ice	no ice	with ice	no ice	with ice	no ice	with ice
1.1	0.021	0.001	0	0	0.903	0.822	188.91	150.92	0	0	0	0
1.2	0.020	0.008	0	0	1.193	1.079	135.6	150.64	0	0	0	0
1.3	0	0	0.150	0.079	1.169	0.710	143.54	208.06	0	0	0	0
1.4	0.018	0.018	0	0	1.037	1.037	193.85	193.85	0	0	0	0
1.5	0.030	0.021	0	0	1.110	1.010	177.92	168.63	0	0	0	0
1.6	0	0	0.116	0.089	0.787	1.273	145.99	120.30	0	0	0	0
1.7	0	0	0.116	0.092	1.030	1.033	159.02	185.26	0	0	0	0
2.1	0.023	0.011	0	0	0.870	1.192	204.24	148.36	0	0	0	0
2.2	0.024	0.013	0	0	0.791	1.282	241.28	138.59	0	0	0	0
2.3	0.022	0.022	0	0	0.930	0.930	215.54	215.54	0	0	0	0
2.4	0	0	0.089	0.057	0.842	1.179	195.35	147.98	0	0	0	0
2.5	0.023	0.019	0	0	0.856	1.003	216.64	189.91	0	0	0	0
3.1	0.023	0.023	0	0	1.017	1.017	201.04	201.04	0	0	0	0
3.2	0.014	0.018	0	0	1.205	1.207	138.15	120.36	0	0	0	0
3.3	0	0	0.056	0.056	0.998	0.998	181.26	181.26	0	0	0	0
4.1	0.018	0.018	0	0	0.968	0.968	198.11	198.11	0	0	0	0
5.1	0.026	0.026	0	0	0.798	0.798	236	236.00	0	0	0	0
5.2	0	0	0.139	0.139	0.771	0.771	224.96	224.96	0	0	0	0
5.3	0	0	0.087	0.087	0	0	0	0.00	329.63	329.63	186.59	186.59
5.4	0	0	0.127	0.127	0	0	0	0.00	354.74	354.74	117.38	117.38
5.5	0.040	0.040	0	0	0	0	0	0.00	367.25	367.25	208.67	208.67
6.1	0.039	0.039	0	0	0.668	0.668	248.37	248.37	0	0	0	0

3.3.3 Process of spreading on the sea surface

Spreading of an oil spill on the sea surface is calculated based on the effects of gravity and viscosity in the first hours of a spill. Afterwards the hydraulic and oceanographic conditions determine the spreading process through differences in the surface currents.

The initial spreading due to gravity and viscosity is determined based on the analytical methods, usually applied in the spill models. The applied formulae are also applied in SINTEF's oil weathering manual (Reed, 2004). The formulae assume that the oil spill is circular, which is a simplification, particularly for spills that are followed over longer periods. Changing current and wind conditions will stretch the spill. However, the ratio between the length and the width of a spill will within the first days of a spill most often be the same order of magnitude. The radius of the spill is determined as

$$\frac{d}{dt}X^{\frac{4}{3}} = 1.75(h^2\rho g')^{\frac{2}{3}}(\rho_w\mu_w)^{-\frac{1}{3}} \quad (3.6)$$

with

X : Radius (m)
t : Time (s)
h : Thickness (m)
ρ : Density of oil (kg/m^3)
g' : Reduced and normalised gravity ($(\rho_w-\rho)/\rho_w$)
ρ_w : Density of water (kg/m^3)
μ_w : dynamic viscosity of water (kg/(ms)

The kinematic viscosity V equals the dynamic viscosity μ divided by the density ρ.

The oil volume is included indirectly in the formula above as it operates with both the radius (X) and the spill thickness (h).

The development over time of the spill radius is illustrated for a 3,000-tonne spill of crude oil ($\mu = 1.8 \cdot 10^{-3}$ kg/(ms)). The development is in principle depending on several processes, such as vertical dispersion. This process has been included in the Seatrack Web simulations, and it was found that this process only plays a significant role in severe and therefore rare storm situations. Therefore, the effect of vertical dispersion is omitted in the present analysis. An example of the radius development is shown in Figure 3-9 below.

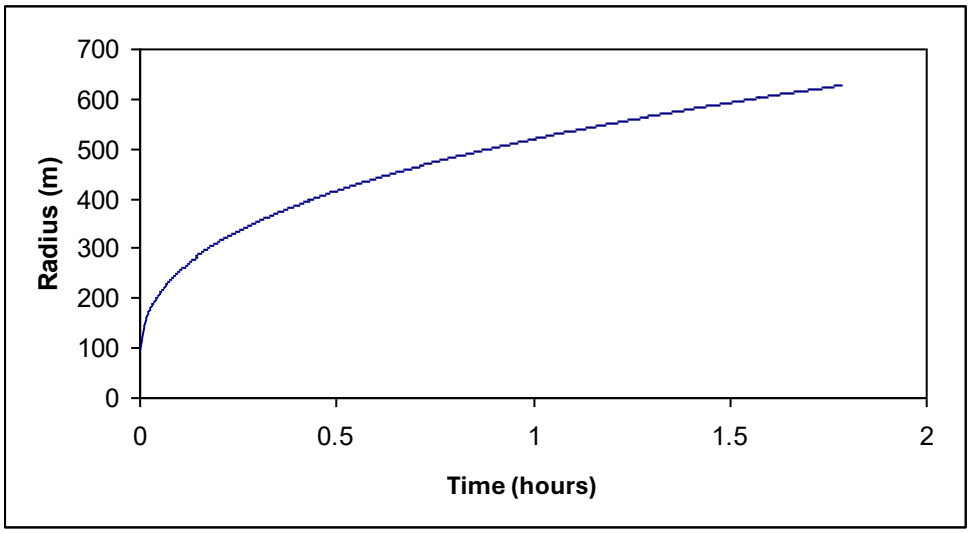

Figure 3-9 *Example of the initial phase of the development of the spill radius for a 3,000 t crude oil spill, calculated after (Reed, 2004).*

It is seen from the graph above that the radius in the initial phase increases logarithmically and becomes almost linear in the later phase. The linear development of the spill radius is analysed based on several simulations of different spill sizes and results in a final assumption as illustrated in Figure 3-10 below

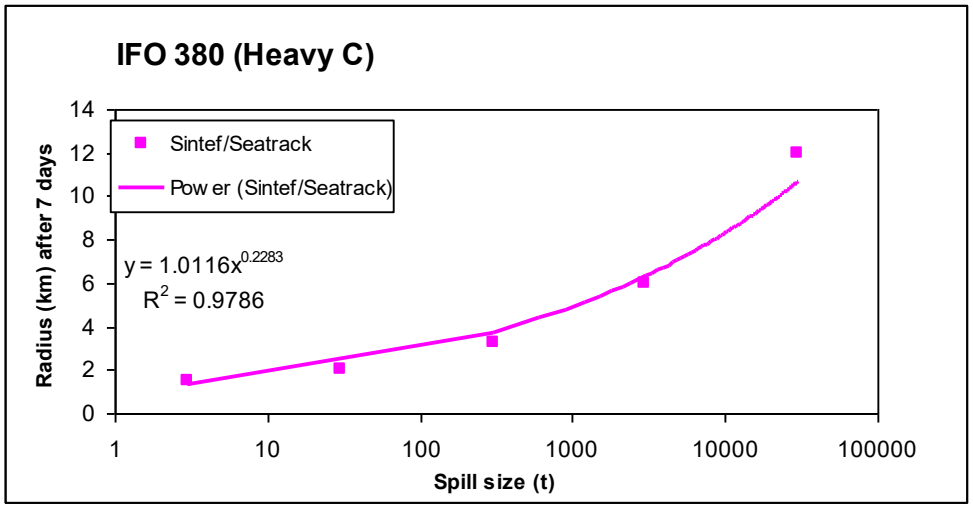

Figure 3-10 *Example of the effect on the spill radius of a heavy oil spill after 7 days*

The effect of different viscosities (oil types) on the radial spreading of the spill is illustrated in Figure 3-11 below, where the increase of spill radius for a heavy high-sulphur fuel oil (kinematic viscosity v = 50,000 cSt) is shown together with the increase of the spill radius of a light oil (v = 50 cSt).

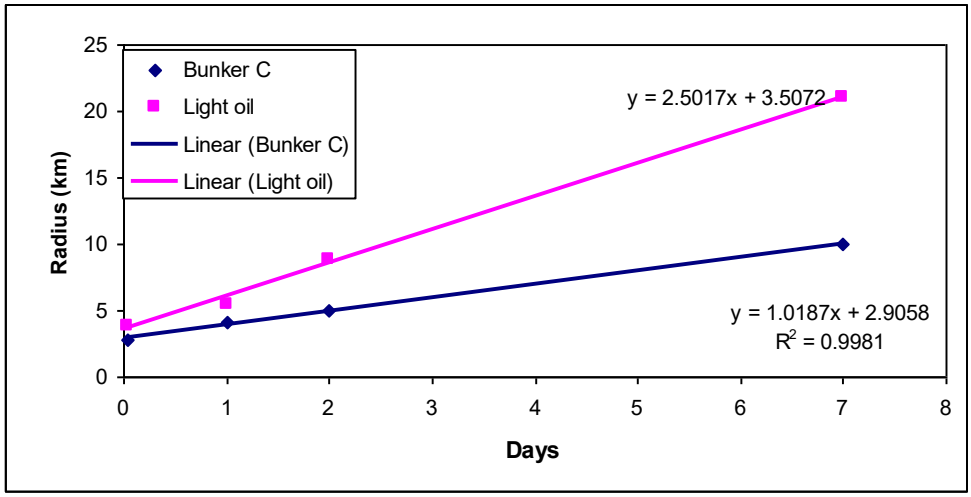

Figure 3-11 *Development of spill radius as function of oil type (viscosity) for a 30,000-tonne spill*

The linear relation between time and spill radius is described with the below expression. In order to describe the large range of the viscosities (three decades), a logarithmic expression is chosen. This also has the advantage (compared to Reeds expression) of resulting in an explicit description, avoiding time consuming solutions of differential equations. The resulting expression for spill radius is hence:

$$R(t, M, v) = 0.113 \cdot M^{0.22} \cdot [(0.13 - 0.02 \log v)t + (3.8 - 0.2 \log v)] \quad (3.7)$$

R : Radius of oil spill (km)
t : Time (hours)
M : Mass of spilt oil (tonnes)
v : Kinematic viscosity (cSt) at the given temperature

The viscosity in the above expression is given by the user based on the specific oil type and the specific temperature.

3.3.4 Density and viscosity

Four different oil type are investigated in the present study. Their respective densities and viscosities at different temperatures are given below.

Diesel

Table 3-2 *Density and viscosity for diesel at four temperatures. For water temperatures close to freezing point the relations are extrapolated (Environment Canada, 2006)*

	4 °C	7 °C	11 °C	16 °C
Density (kg/m^3)	837	834	828	827
Viscosity (cSt)	3	3	3	2

Crude

Table 3-3 *Density and viscosity for Komineft crude at four temperatures. For water temperatures close to freezing point the relations are extrapolated (Environment Canada, 2006)*

	4 ºC	7 ºC	11 ºC	16 ºC
Density (kg/m^3)	852	849	845	840
Viscosity (cSt)	46	37	25	10

High-sulphur fuel oil (HSFO)

Table 3-4 *Density and viscosity for HSFO at four temperatures. For water temperatures close to freezing point the relations are extrapolated (Environment Canada, 2006)*

	4 ºC	7 ºC	11 ºC	16 ºC
Density (kg/m^3)	998	996	992	988
Viscosity (cSt)	54,000	34,000	18,500	8,600

Vegetable oil

Table 3-5 *Density and viscosity for vegetable oil at four temperatures. For water temperatures close to freezing point the relations are extrapolated (Environment Canada, 2006)*

	4 ºC	7 ºC	11 ºC	16 ºC
Density(kg/m^3)	926	923	920	915
Viscosity (cSt)	159	139	112	78

Apart from the oil types, selected soluble hazardous chemicals are investigated. The densities and viscosities for the selected chemicals are given below.

Gasoline

Table 3-6 *Density and viscosity for gasoline (Casinghead, Leaded) at four temperatures. For water temperatures close to freezing point the relations are extrapolated (Environment Canada, 2006)*

	4 ºC	7 ºC	11 ºC	16 ºC
Density (kg/m^3)	712	709	705	700
Viscosity (cSt)	0.61	0.58	0.54	0.49

Benzene

Table 3-7 *Density and viscosity for benzen at four temperatures. For water temperatures close to freezing point the relations are extrapolated (Chevron Phillip, 2005)*

	4 ºC	7 ºC	11 ºC	16 ºC
Density (kg/m^3)	895	892	888	883
Viscosity (cSt)	0.92	0.89	0.84	0.78

Toluene

Table 3-8 *Density and viscosity for toluen at four temperatures. For water temperatures close to freezing point the relations are extrapolated (Chevron Phillip, 2005)*

	4 ºC	7 ºC	11 ºC	16 ºC
Density (kg/m^3)	882	879	875	870
Viscosity (cSt)	0.81	0.79	0.75	0.71

Low-sulphur fuel oil

Low-sulphur fuel oil (LSFO) is inherently difficult to model due to the large degree of variation associated with its behaviour when spilt.

The IMAROS 1 and IMAROS 2 projects analysed samples of LSFO with respect to their viscosity at different temperatures (IMAROS 1, 2022 and IMAROS 2, 2025).

IMAROS 1 analysed different samples of very low-sulphur fuel oil (VLSFO) at 5 and 15° C, whereas IMAROS 2 analysed some new samples of both very low-sulphur fuel oil (VLSFO) and ultra low-sulphur fuel oil ULSFO, this time at 15 and 50° C.

Figure 3-12 displays the temperature-viscosity results of VLSFO samples from both projects as red dots. It is seen that the samples collected and analysed by the IMAROS 2 project are on average far more viscous than those from the IMAROS 2 project. When connecting the average values, it is seen that the relationship is linear in a logarithmic scale, i.e. the trend lines from IMAROS 1 and IMAROS 2 are almost parallel. This allows extrapolating the IMAROS 2 data (covering 15 and 50° C) to the lower temperature ranges to prevailing in the Baltic Sea during the cold season.

Figure 3-13 displays the same relationship for the ULSFO samples collected and analysed by the IMAROS 2 project. Here, it is seen that the trendline is much steeper than for VLSFO, i.e. viscosity increases significantly more strongly at lower temperatures.

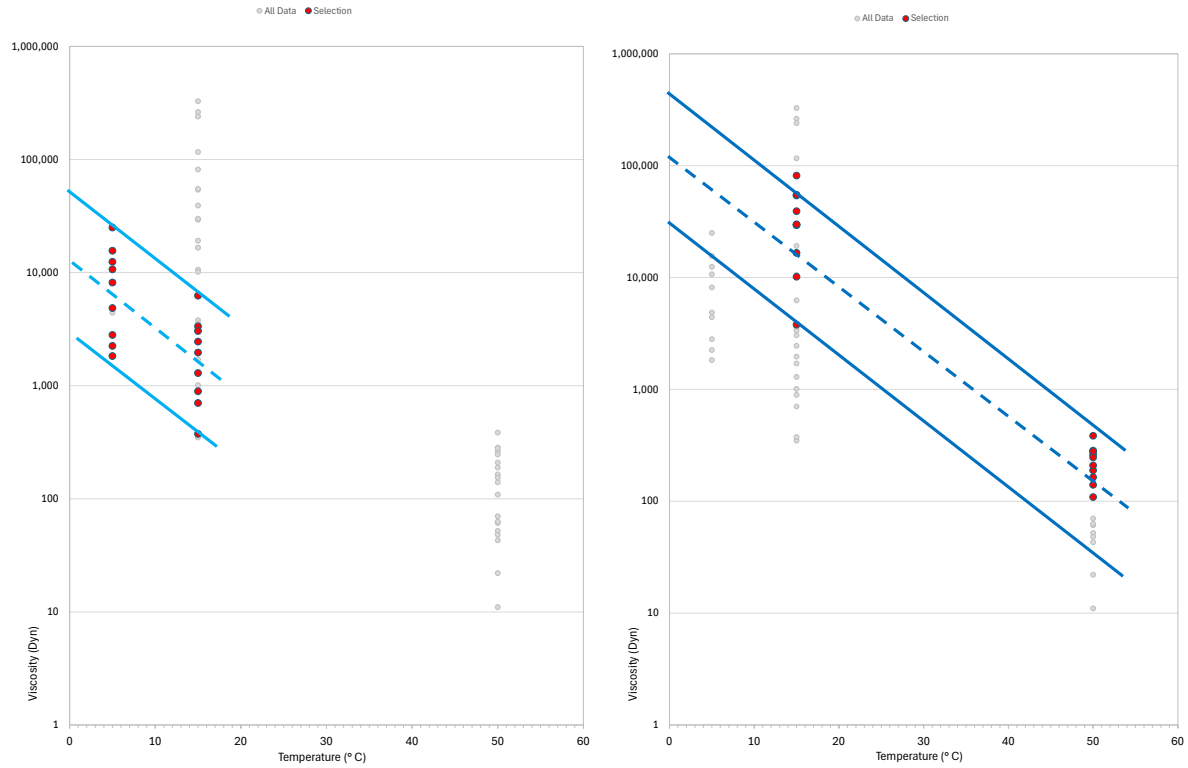

Figure 3-12 *Temperature-viscosity relationship of VLSFO samples from IMAROS 1 (left) and IMAROS 2 (right)*

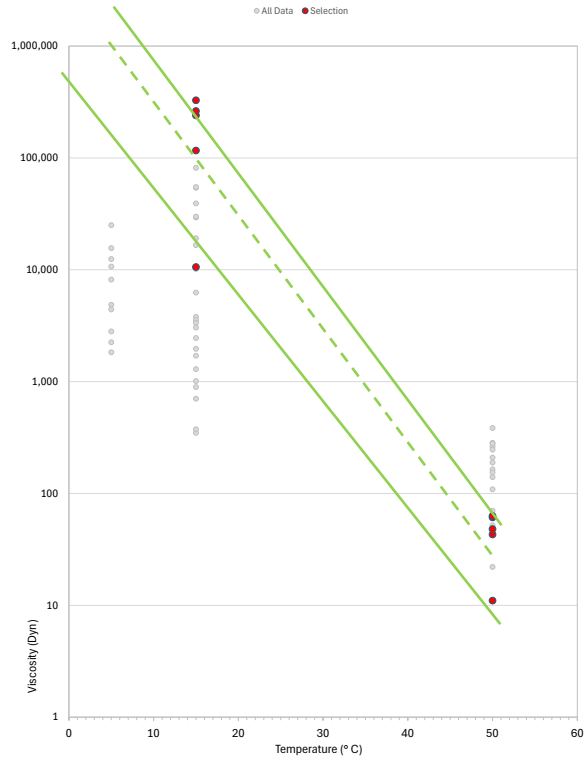

Figure 3-13 *Temperature-viscosity relationship of ULSFO samples from IMAROS 2*

For the BRISK II project, it is assumed that VLSFO behaves according to the IMAROS 1 samples in half of the cases and according to the IMAROS 2 samples in the other half of the cases. In this way, the model takes the large variation in possible behaviours into account:

$$v(T) = \begin{cases} 1.32 \cdot 10^4 \cdot \exp(-0{,}130 \cdot T) \ldots 50\ \% \text{ of the cases} \\ 6.88 \cdot 10^4 \cdot \exp(-0{,}123 \cdot T) \ldots 50\ \% \text{ of the cases} \end{cases} \quad (3.8)$$

For ULSFO, a single relationship is applied:

$$v(T) = 3.78 \cdot 10^6 \cdot \exp(-0{,}230 \cdot T) \quad (3.9)$$

In Eqs. 3.8 and 3.9,

v : Dynamic viscosity (cSt)
T : Temperature (° C)

3.3.5 Weathering and decay

Weathering and decay processes are highly complex and subject to very comprehensive research and modelling work. In order to keep the present model effort within limits the explicit and simplified description by ITOPF (ITOPF, 2006) below is applied.

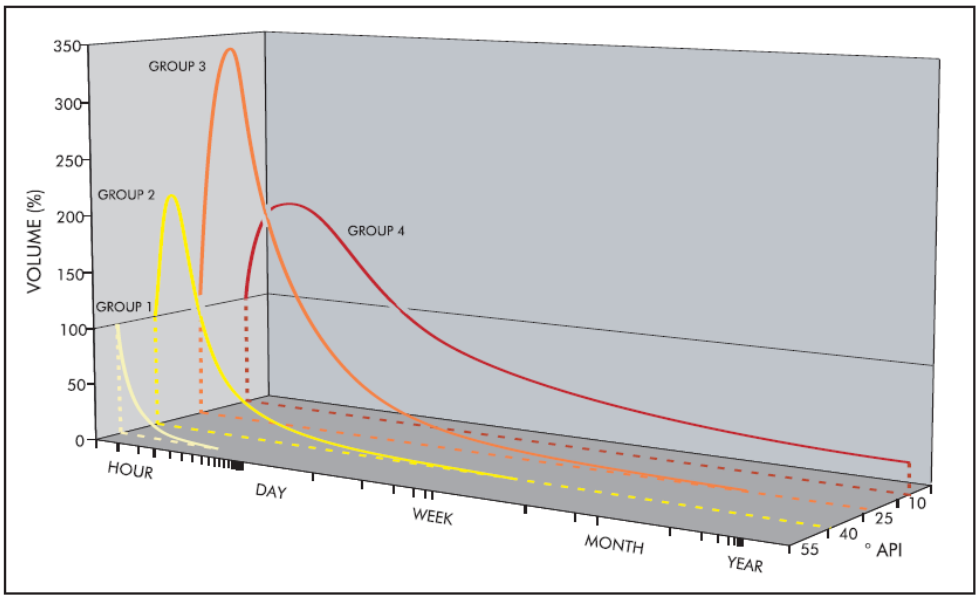

Figure 3-14 *Volume of oil and water in oil emulsion on the sea surface. The curves represent average decay of different oil types (ITOPF, 2006). Group 4 represents high-sulphur fuel oil, group 2 and 3 light and heave crude oil, resp. Group 1 represents diesel.*

The above volumes of oil and oil-in-water emulsions are expressed in simplified terms and illustrated below. The processes of evaporation as well as emulsification are integrated in the description.

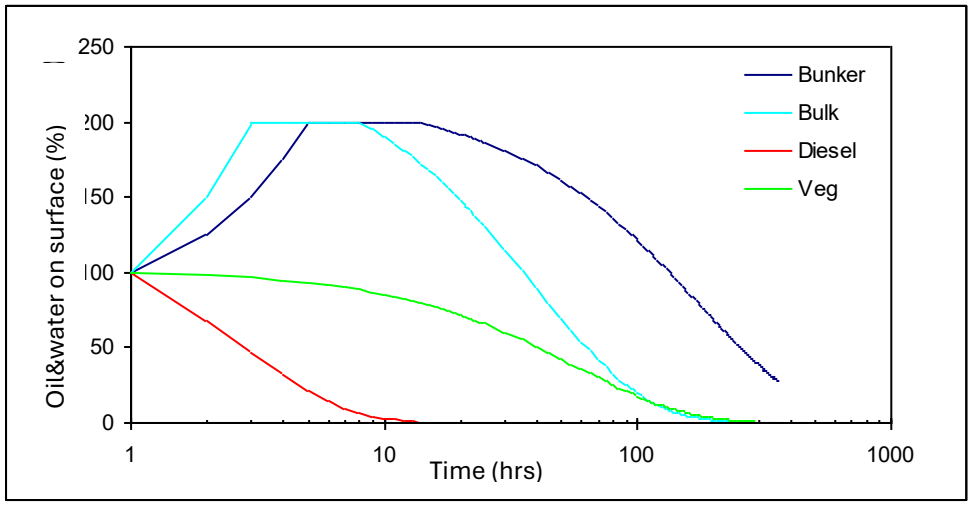

Figure 3-15 Simplified remaining mass of oil and oil- water emulsion on the sea surface, after ITOPF 2006.

Light oils and chemicals

Light oils and chemicals (diesel and vegetable oils) do not emulsify. Floating HNS are fugitive and will evaporate with similar time scales as for diesel. The mass of light oil and floating HNS M_{light} on the sea surface in percent of the initial spill is determined using the following approximation:

$$M_{\text{light}}(t) = 100 \cdot \exp\left(-\frac{t}{3.3 \cdot v^{0.4}}\right) \tag{3.10}$$

With

t : time (hours), (≥0)
v : Viscosity (cSt) given for the respective season (function of temperature)

Heavy oils (crude and fuel oil) do emulsify. This complicated process is described in simple terms as a function of viscosity. The algorithms for the percentage of the spilt mass of heavy oils M_{heavy} on the surface are given below:

$$\begin{cases} M_{\text{heavy}}(t) = 100 \cdot \exp\left(\frac{t}{\ln v}\right) + 100 & \text{... for } 0 < \frac{t}{\ln v} < 1 \\ M_{\text{heavy}}(t) = 200 & \text{... for } 1 < \frac{t}{\ln v} < 3 \\ M_{\text{heavy}}(t) = 200 \cdot \exp\left(-\frac{t - 3\ln v}{17\ln v - 32}\right) & \text{... for } 3 < \frac{t}{\ln v} \end{cases} \tag{3.11}$$

The terms are explained above for the light oils.

3.3.6 Simulation stop criteria

In order to limit the simulation time, it is necessary to specify criteria when the modelling of a single spill has to be stopped. In general, it is decided to stop the simulation when 5% of the oil is left on the sea surface.

The rest of the oil is either

- Decayed

- Floated ashore
- Floated towards the open boundary towards the North Sea
- Removed by response actions

4 Modelling of spreading of HNS

4.1 Evaporating HNS

Substances evaporating within minutes are not covered by the impact model. Substances evaporating after more time are modelled as floating or soluble HNS depending on their behaviour.

4.2 Floating HNS

Floating HNS are modelled according to the same principles as oil, see Chapter 3.

With respect to weathering and decay, the following applies: Floating HNS are fugitive and will evaporate with similar time scales as for diesel. They are thus modelled in the same way by applying Eqs. (3.10) and (3.11), see Section 3.3.5.

4.3 Soluble HNS

4.3.1 Applied model

The effect of soluble chemicals in the marine waters is based on mixing processes described in traditional environmental hydraulics. The mixing is based on a diffusion principle, in which the mixing at different scales is characterised by diffusion coefficients. These coefficients are a function of current velocity, water depth and a general classification of the water bodies. A detailed description of the model is given in Appendix A and Appendix B.

The mixing processes for dissolved chemicals are described by a stationary model which calculates the distance L from the discharge point where the concentration levels have reached a limit below which there is no effect on marine organisms. This detection limit has been derived for a number of chemicals, on basis of eco-toxicological experiments with marine organisms such as plankton.

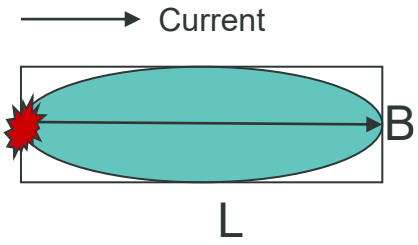

Figure 4-1 *Principle of a spill of soluble chemicals. The discharge point is shown with a red star. The plume is shown with green colour and has a width B and a length L.*

The expected dilution concentration is termed "Predicted Effect Concentration (PEC)", and the detection limit for no effect is termed "Predicted No Effect Concentration (PNEC)". The model calculates the distance from the discharge point to the location where the two concentrations are equal, i.e. PEC/PNEC = 1. The model is developed and applied for evaluation of the effect of spills from offshore oil and gas installations.

It is assumed that the width B is a fixed fraction of the plume length L. Typically, the width amounts to 1:10 on either side of the centre line of the oval shown in Figure 4-1. Therefore, it is assumed that the affected area can be described by a rectangle where the width is 20 % of the length.

The orientation of the rectangle is determined by the drift direction (a result from the oil spill modelling).

The model is especially suitable for the present purpose. The reason is that the model calculates the maximum affected area over the entire spill event, and it is therefore not necessary to calculate the spill event dynamically. Further, the concentration of the substance is directly related to the toxicological effect, wherefore it is easily determined whether an area is affected or not.

4.3.2 Modelled soluble chemicals

The reasoning behind the selection of the soluble chemicals is the following:

The primary selection criterion is a conservative selection of eco-toxicologically thoroughly investigated compounds. Based on a general knowledge of the eco-toxicological effects, compounds are selected which are at the high end of the general toxicity level within their specific compound group. It is further ensured that the selected compounds are thoroughly investigated and that their eco-toxicological characteristics are empirically based. The selected compounds are shown in the table below. The PNEC values shown are calculated as described in the appendices and based on data from (Ecotox, 2006).

Table 4-1 Selected soluble chemicals

Compound	Acetonecyanhydrin	Acrylonitrile	MTBE
Toxicity class	"very " red	Red	Yellow
Density (kg/l)	0.93	0.8	0.741
PNEC aquatic (mg/l)	0.010	0.200	0.672

4.3.3 Processes

The distance of effect for the mentioned compounds is calculated for each hydrographical area, for different depth and for different spill amounts. The results of the PEC/PNEC calculations are made linear, so that they can be included in a fast calculation algorithm. It is shown in Appendix B how the PEC/PNEC results are linearised.

The detailed PEC/PNEC model results shows that the distance L in which an effect is calculated, can approximately be described as a log distribution of the spilled amount. The entire upper water body is considered. It is defined as follows:

- Kattegat: 30 m
- Entrances to the Baltic Sea, Gulf of Bothnia, Gulf of Finland, Gulf of Riga: 15 m
- Baltic Proper: 60 m

The effect of wind and current velocity is without importance. The distribution into water body (Kattegat, Entrances to the Baltic Sea etc.) has a small effect, but the most important parameter is the toxicity of the compounds expressed as its toxicity class.

It has been chosen to disregard effects which are larger than 30 km in length or 180 km^2, as the assumptions for the calculations under such circumstances will fail. Especially the assumption of stationary flows and homogeneous mixing in the affected water volume will fail.

The following linear expression has been developed for the areas, which are affected by soluble chemicals: For each toxicity class and for each hydrographical area the linear expression becomes

$$L(\text{hydrographical area, toxicity class}) = a \cdot M^e$$

Where L is expressed in metres. The factor a and the exponent e are determined on basis of a number of PEC/PNEC model results. M is the spilt amount in tonnes.

The width of the affected area is assumed to be $0.2 \cdot L$, see Section 4.3.1.

An example of the calculated affected areas at the entrances to the Baltic Sea is seen in the table below.

Table 4-2 Example of the effect of soluble chemicals of danger class 'red' at the entrances to the Baltic Sea

Spill amount (t)	0.3	3	30	300	3,000	30,000
Affected length *L* (km)	0.4	1.7	6.9	27	>30	>30
Affected area (km^2)	0.04	0.6	9.6	150	>180	>180

The results of the factors and exponents are given in the table below.

Tabel 4.1 Values for inserting into the formula above for modelling of the impact distances at spill of soluble chemical substances.

Water body (hydrographical area ID)	Danger class	Factor (*a*)	Exponent (*e*)
Kattegat (6.1)	Very red	7,360	0.62
	Red	1,350	0.53
	Yellow	752	0.51
Entrances to the Baltic Sea, Gulf of Bothnia, Gulf of Finland, Gulf of Riga (1.1, 1.2, 1.3, 1.4, 1.5, 1.6, 1.7, 2.1, 2.2, 2.3, 2.4, 2.5, 5.1, 5.2, 5.3, 5.4, 5.5)	Very red	5,390	0.52
	Red	907	0.60
	Yellow	729	0.46
Baltic Proper (3.1, 3.2, 3.3, 4.1)	Very red	14,500	0.49
	Red	2,880	0.59
	Yellow	1,320	0.54

4.4 Sinking HNS

Sinking HNS is assumed to sink to the sea bottom underneath the spill location, where it will create a continuous layer. As the effect of gravity is lower than at the sea surface due to buoyancy, the layer will be thicker than at the sea surface.

For the analysis of spill of oil and HNS in Danish waters (Oil spill DK, 2006), a layer thickness of 20 cm on the sea bottom was assumed. With this layer thickness, even spills of several 10,000 tonnes will cover a relatively small area, i.e. less than one of the 2 × 2 km grid cells used by the impact model.

5 Modelling of emergency response

5.1 Response modelling

The emergency response applies a wide range of different equipment including vessels, barges, pumps, skimmers, booms and barriers as well as different hardware such as radar etc. For oil spills in ice, it is assumed that special equipment is used. In order to describe the effect of the emergency response to the oil spills (and spills of floating HNS) in a practical manner in the model complex, the response methods are reduced to include only the capacity of pumps and skimmers, as well as the equipment applied to convey the spill to the skimmers, e.g. booms attached to tow boats. The time lag for mobilising and transport from home port to spill position is included in the model.

The effect of the emergency response is modelled as a reduction of the amount of oil in the circular oil slick. The diameter hereof is unchanged, while the thickness reduces.

The presence of ice is represented by an ice coefficient. The recovery rate for open water condition is multiplied by the ice coefficient in case of ice coverage.

In order to calculate the effect of the emergency response it is chosen to define an artificial model response which replicates a possible and realistic emergency response, without simulating the actual emergency response. It is assumed that the response is carried out in three isolated actions at times T1, T2 and T3, so that the total response capacity increases with time, as more vessels will reach the scene.

The capacity for oil removal is calculated on basis of the total number of vessels on scene, oil skimmers and pumps, as well as the total length of booms that is available.

In addition, the modelling contains a number of conditions which may reduce the effectiveness of the emergency response, such as visibility, darkness, limiting significant wave height etc.

5.2 Applied response capacity for each sub-region

The regional response to oil spills is based on the response capacities as they have been reported by the countries. A condensed version of the database in provided in Appendix C. This information represents an update of the existing database stored at HELCOM.

The database includes the names of each vessel, its dimensions, speed, home port, alarm time, and its equipment in terms of pumps, skimmers and storage. Further, additional equipment that is store on barges and in depots is included in the database.

The sub-regions of the Baltic Sea (incl. the Swedish North Sea) are illustrated in Figure 5-1

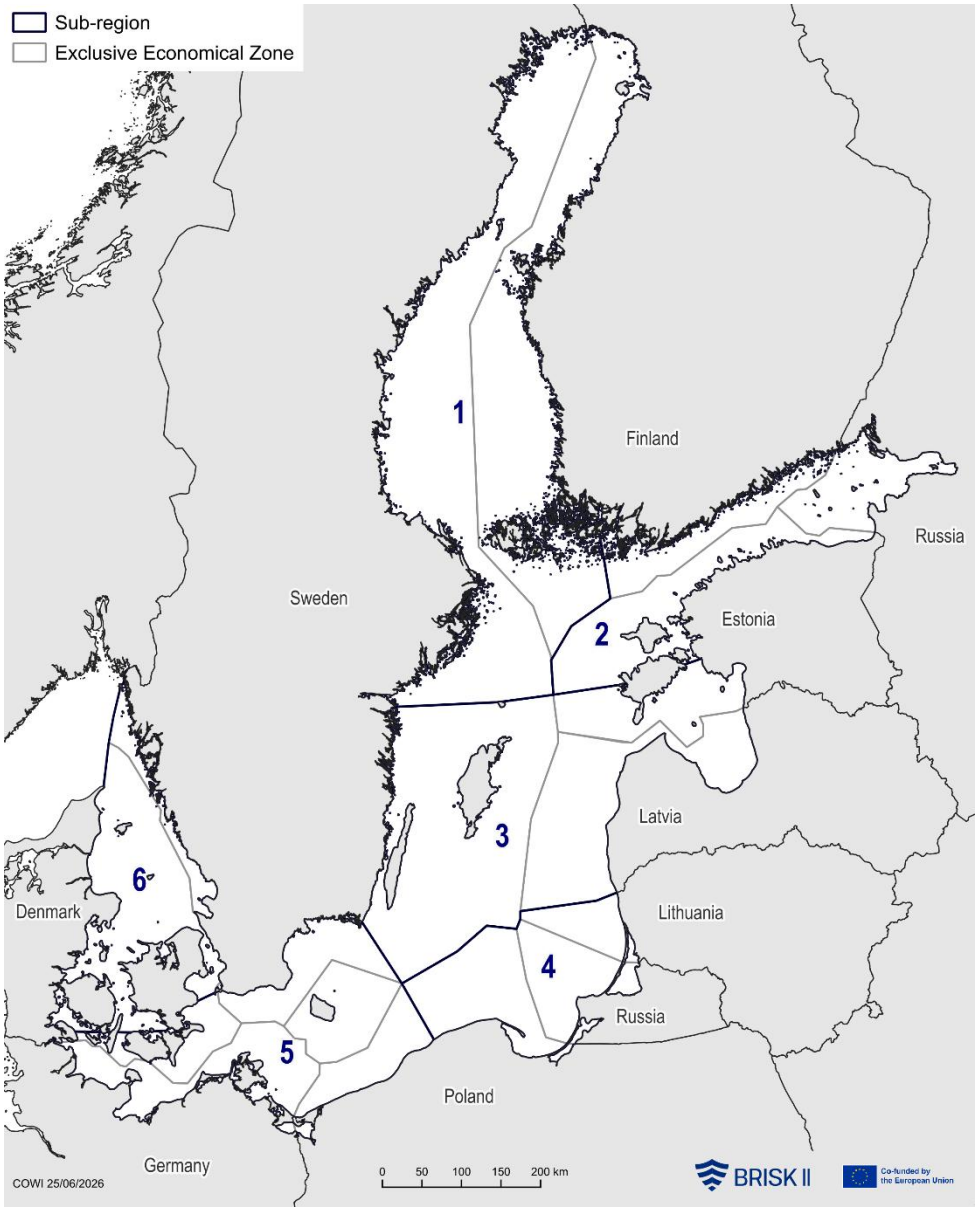

Figure 5-1 Illustration of the sub-regions for emergency response

The response capacity is aggregated for each sub-region in order to provide an integrated value for applicable booms and skimmers. For three fixed periods, the radii are determined for each vessel, indicating how far the vessel can be expected to reach within the given three periods, i.e. within what distance from the home port the vessel is expected to be operational. The calculations of the operation radii take account of the cruise speed of the vessel and the remaining time after the vessel is mobilised and leaves the port. The circle defined by the respective radius is weighted by the vessel's nominal recovery rate in m^3/h.

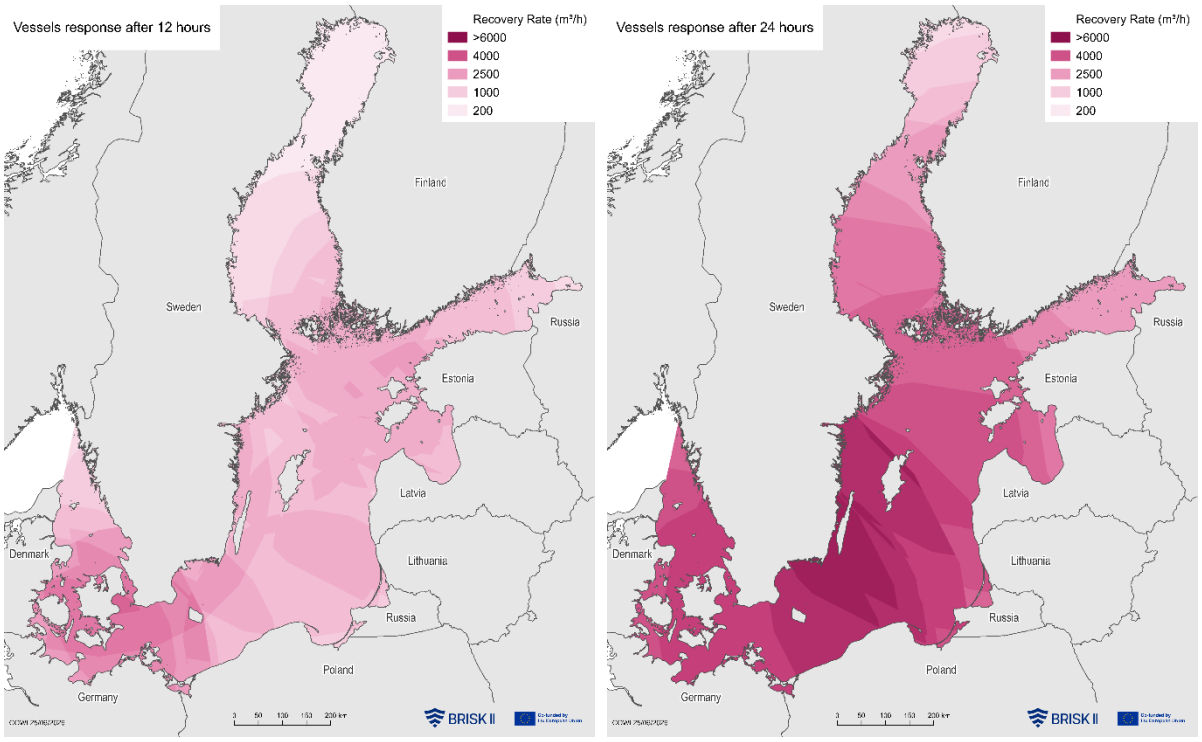

Figure 5-2 Nominal recovery rate 12 hours (left) and 24 hours (right) after alarm, based on existing response capacities (2024). For illustration purposes only, i.e. not corrected for various reduction factors or for boom capacity.

It is seen in Figure 5-2 that almost all areas of the Baltic Sea can be reached by some vessel within 12 hours after alarming. However, the model is simplified in the sense that it ignores the barrier effect of coasts and islands that will prevent vessels from sailing in a direct line from home port to spill scene.

The mobilised booms and skimmers can only collect oil and reduce environmental damage if they can be applied in the areas where spills will occur. If they are placed close to the hot spots, they will be able to collect a larger amount of oil compared to a situation where they are placed far away from the hot spots. Therefore, values for "effective capacities" have to be determined. The capacities in terms of mobilised booms and skimmers are therefore weighed with respect to how well they are placed relative to the likely locations of the risk for pollution.

This weighing is conducted by multiplying the capacity of each vessel with the risk for releases that lies within the operational radius. The risk-weighed capacities are integrated for the entire sub-region and then divided with the integrated risk of the sub region. This way, "efficient capacities" can be found for pump capacities and for boom lengths. Further, different efficiencies are determined for three different periods from the time of alarm to operation and for open water condition and for ice condition. For illustration see Table 5-1.

Table 5-1 Illustration of the cases for which effective capacities

Parameter	Number of scenarios	Description
Period	3	8, 16, 60 hours
Sub-region	6	See Figure 5-1
Capacities	2	Pumps/skimmers, booms
Water condition	2	Open water, ice
Total	72	-

As it is seen from the table above a total of 72 effective capacities have been determined based on the specifics of the regional responses. These have been recalculated for two different responses, i.e. existing response (2024), planned future response (2036) (144 effective capacities).

The selection of response times for BRISK II is based on the model decisions made for BRISK I: Three response times were selected for the BRISK I (BRISK I, Spreading, 2012). Vessels arrive at different times so there should be more than one response time. On the other hand, the calculation effort needs to be limited to keep the calculation model operational. Three response times was considered an adequate solution to this. The first time has to represent the quick response of small vessels that can be at location in fairly short time and start response activities. Therefore, 8 hours was chosen. The longest response time was chosen as 60 hours, i.e. 2½ days. With this long response time, almost all vessels in the Baltic Sea will be able to contribute to a major oil spill. Therefore, the total recovery capacity of the entire Baltic Fleet can come to affect at this time of the spill. In between 8 and 60 hours a period of 16 hours is chosen to illustrate the effect when the vessels of the entire sub-region can come into action. The three response times therefore represent the effect of local, sub-regional and regional sea-wide response capacity.

Maps of spill locations together with information on mean annual spill risk expressed as annually expected tonnes were prepared in the analysis of accidents and spill, (BRISK II, Prob. of release, 2026).

For each response time *t* (8, 16 and 60 hours), for each sub-region *k* an 'applied capacity' is calculated as a weighted quantity on basis of all individual spill locations *i* and response vessels *j* as

$$\text{Applied capacity}(t,k) = \frac{\sum_i \left(\text{spill risk}_{k,i} \cdot \sum_j \text{capacity}_{t,i,j}\right)}{\sum_i \text{spill risk}_{k,i}}$$

The resulting model is shown in Table 5-2 and Table 5-3. Table 5-2 shows the existing response capacities in 2024, whereas Table 5-3 shows the currently planned capacities in 2036. Both models are referred to as ‘baseline’ models as they provide the basis of comparison to the alternative response scenarios defined in report D3.2 Risk-reduction scenario selection (BRISK II, RRM scenarios, 2026). The values in the table show the total response capacity (i.e. from several vessels) that can be mobilised at a representative spill location in a given sub-region.

Table 5-2 Applied response capacity (existing situation in 2024)

Response time (hours)	Sub-region	Applied pump capacity [m^3/h]		Applied boom length [m]	
		Ice season	Ice-free season	Ice season	Ice-free season
8	1	117	615	1,560	1,634
8	2	185	1,166	1,807	2,513
8	3	934	934	1,637	1,637
8	4	744	744	1,929	1,929
8	5	1,859	1,859	1,161	1,161
8	6	1,126	1,126	1,223	1,223
16	1	375	1,999	4,876	5,212
16	2	377	2,191	4,659	5,644
16	3	3,062	3,062	7,241	7,241
16	4	2,515	2,515	5,287	5,287
16	5	3,923	3,923	4,439	4,439
16	6	3,504	3,504	3,722	3,722
60	1	729	6,594	8,900	12,284
60	2	728	6,478	8,900	12,271
60	3	6,798	6,798	12,350	12,350
60	4	6,796	6,796	12,350	12,350
60	5	6,755	6,755	12,350	12,350
60	6	6,775	6,775	12,350	12,350

Table 5-3 Applied response capacity (currently planned situation for 2036)

Response time (hours)	Sub-region	Applied pump capacity [m^3/h]		Applied boom length [m]	
		Ice season	Ice-free season	Ice season	Ice-free season
8	1	151	795	2,420	2,531
8	2	257	1,692	3,271	4,836
8	3	1,392	1,392	2,382	2,382
8	4	1,304	1,304	2,573	2,573
8	5	2,160	2,160	2,522	2,522
8	6	1,559	1,559	3,455	3,455
16	1	489	2,781	7,519	8,110
16	2	539	3,185	8,146	9,178
16	3	4,510	4,510	11,285	11,285
16	4	3,630	3,630	7,454	7,454
16	5	4,754	4,754	7,929	7,929
16	6	4,142	4,142	6,890	6,890
60	1	896	8,590	12,500	19,647
60	2	895	8,519	12,500	19,634
60	3	8,734	8,734	19,713	19,713
60	4	8,732	8,732	19,713	19,713
60	5	8,691	8,691	19,713	19,713
60	6	8,711	8,711	19,713	19,713

It is seen from the above table that the response capacity increases with time (from 8 to 16 and 60 hours) and that the response in ice conditions is significantly reduced compared with open water condition (for sub-regions that are prone to ice). Under ice conditions, two effects come together: First, vessels that can operate under ice conditions are operating at a reduced recovery rate. Second, vessels that cannot operate under ice conditions (typically from more southern sub-regions) do not contribute at all.

5.3 Viscosity

The relationship between type of spill, temperature and viscosity is described in Section 3.3.4. Especially fuel oil (HSFO and LSFO) can become very viscous at low temperatures. High viscosity can make recovery of oil much more cumbersome. This is reflected by the following modelling assumption:

- Response vessels that are equipped to handle highly viscous oil (>50,000 cSt) will recover oil at a reduced rate corresponding to 25 % of that for normal (less viscous) spills (factor 0.25).

- Response vessels that are not equipped in such a way will not be able to recover any highly viscous oil at all, i.e. their recovery rate will be 0 % of the rate for normal (less viscous) spills (factor 0).

It is assumed that 50 % of the vessels existing in 2024 are equipped to recover highly viscous oil. All vessels built after 2024 are assumed to be able to recover highly viscous oil.

5.4 Substance-specific reduction factors

Low-sulphur fuel oil

In many cases, it cannot be predicted which equipment will work for collecting an LSFO spill. In those cases, response vessel crews may have to change between different types of equipment (brushes, belts, disks) to find out which of them actually works.

This is modelled by an average delay of 1 hour before the actual response can begin.

These assumptions were adopted by the BRISK II core project team authoring this report.

Floating HNS

Recovery of floating HNS is modelled as being 50 % as efficient as recovery of oil (factor 0.5). This factor was adopted by the BRISK I project partners (BRISK I, Spreading, 2012).

Fire hazard class “red”

In the D2.4 Cargo analysis (BRISK II, Cargo analysis, 2025), all substances were allocated to a white, yellow and red hazard class, where “red” means “very hazardous”.

Recovery of substances with red fire hazard class is modelled as being 70 % as efficient as recovery of substances with yellow or white fire hazard class (factor 0.7). This factor was adopted by the BRISK I project partners (BRISK I, Spreading, 2012).

Health hazard class “red”

In the D2.4 Cargo analysis (BRISK II, Cargo analysis, 2025), all substances were allocated to a white, yellow and red health class, where “red” means “very hazardous”.

Recovery of substances with red health hazard class is modelled as being 70 % as efficient as recovery of substances with yellow or white health hazard class (factor 0.7). This factor was adopted by the BRISK I project partners (BRISK I, Spreading, 2012).

5.5 Visibility

The visibility coefficient is defined as the ratio of the time where response to oil spill is not possible due to fog, haze and snow. The estimations of the coefficient are based on description of the visibility in the Baltic Pilot (Baltic Pilot, 2009).

Based on the indications in Baltic Pilot the following ratios for bad visibility are prepared:

Table 5-4 *Visibility coefficient for the sub-regions and seasons. The coefficient describes the quotient of time where response operation is not possible due to bad visibility.*

Sub-region		Season					
		1	2	3	4	5	6
		Jan, Feb	Mar	Apr, May	Jun, Jul, Aug	Sep, Oct, Nov	Dec
Nr.	Description	Winter, ice	Spring, ice	Spring, no ice	Summer	Autumn	Winter, no ice
1	Bay of Bothnia	0.03	0.01	0.03	0.02	0.01	0.02
2	Golf of Finland	0.03	0.01	0.03	0.02	0.01	0.02
3	Central Baltic Proper	0.03	0.03	0.05	0.04	0.02	0.02
4	SE Baltic Proper	0.03	0.03	0.05	0.04	0.02	0.02
5	SW Baltic Proper	0.08	0.06	0.04	0.02	0.04	0.06
6	Entrances to the B.S.	0.08	0.06	0.04	0.02	0.04	0.06

An illustration of seasonal variability of the above coefficients is provided in Figure 5-3 below.

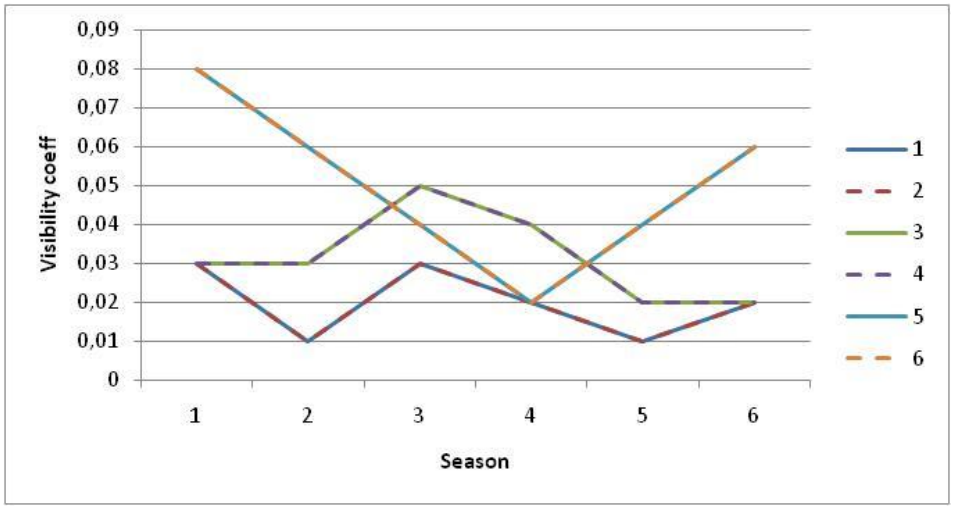

Figure 5-3 *Seasonal variability of visibility coefficient for the sub-regions 1 to 6. The coefficient describes the quotient of time where response operation is not possible due to bad visibility.*

5.6 Darkness

The darkness coefficient is defined as ratio of the time where response to oil spill is not possible due to too little daylight. The theory for calculating the length of the day is given by (Glamer, 2011).

The following image shows the tilted and shifted solar circle for the winter solstice at 45° N. It is only the part b out of the whole circle in which the sun is visible; when continuing its path on the blue line it is night.

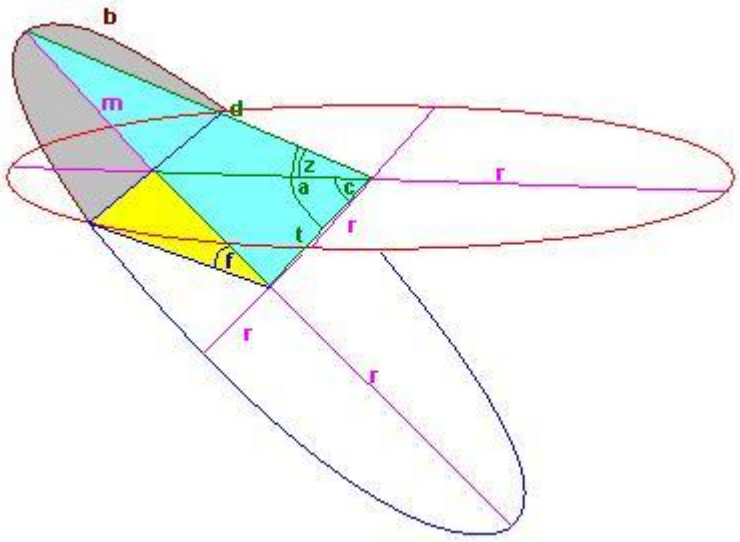

Figure 5-4 Solar circle for the winter solstice at 45° N (Glamer, 2011).

The period of darkness is defined as the full day period (24h) minus the length of the day and minus the time of the twilight.

In this theory the length of the day is determined based on

- the latitude (lat) of the observer (0° at the equator, 90° at the poles)
- the obliquity (ε) of the ecliptic as the rotation of the earth is not perpendicular to its orbital plane, the equatorial plane is not parallel to the ecliptic plane, but makes an angle of 23.439°)
- the day of the year (day) (starting with the day of winter solstice)

In (Glamer, 2011) the theory can by simplified to the formula

$$\text{Darkness} = \frac{1 - \cos^{-1}(1 - n)}{\pi}$$

where

$$n = 1 - \tan(\text{lat}) \cdot \tan(\varepsilon \cdot \cos(j \cdot \text{day})) + \frac{h}{\cos(\text{lat})}$$

with j = 0.0172 and h = tan(12°).

The results for the different sub-regions and the different seasons are determined and given below:

Table 5-5 *Darkness coefficient for the sub-regions and seasons. The coefficient describes the quotient of time where it is dark and operation therefore not is possible.*

Sub-region		Lat	Season					
			1	2	3	4	5	6
			Jan, Feb	Mar	Apr, May	Jun, Jul, Aug	Sep, Oct, Nov	Dec
Nr.	Description	(° N)	Winter, ice	Spring, ice	Spring, no ice	Summer	Autumn	Winter, no ice
1	Bay of Bothnia	63.0	0.549	0.464	0.160	0.000	0.536	0.718
2	Golf of Finland	60.0	0.540	0.461	0.206	0.093	0.524	0.679
3	Central Baltic Proper	57.5	0.532	0.458	0.233	0.152	0.515	0.653
4	SE Baltic Proper	56.0	0.529	0.456	0.247	0.176	0.511	0.640
5	SW Baltic Proper	55.0	0.526	0.456	0.255	0.190	0.508	0.632
6	Entrances to the B.S.	56.5	0.530	0.457	0.242	0.169	0.512	0.644

The darkness coefficient also can be illustrated graphically as in Figure 5-5 below:

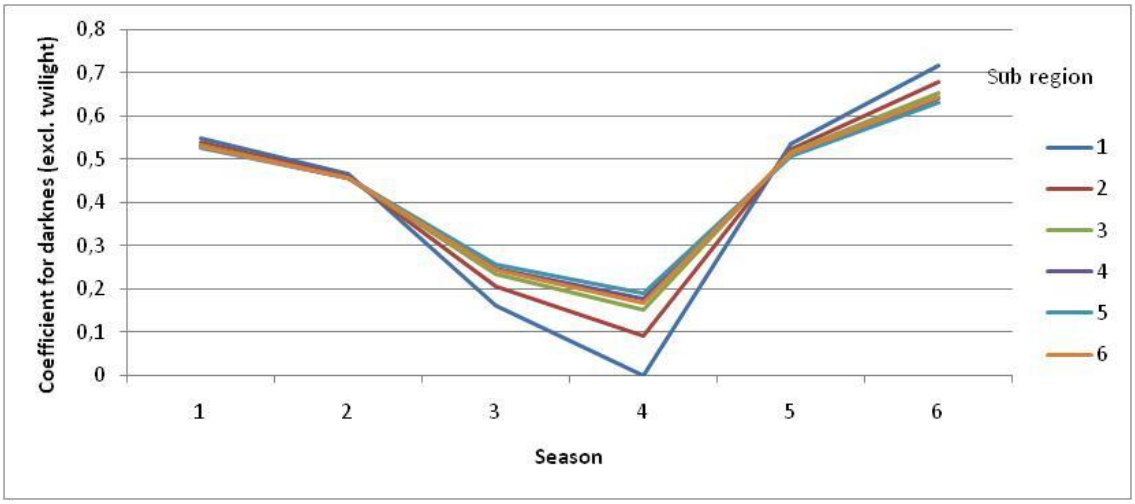

Figure 5-5 *Illustration of darkness coefficient for each sub-region and each season*

As shown above the darkness indicator is fairly equal across sub-regions 3, 4 and 5, whereas some difference is found for sub-regions 1 and 2. In agreement with expectations, sub-regions 1 and 2 have a lower darkness coefficient during summer (seasons 3 and 4) and a higher darkness coefficient during winter (season 6).

5.7 Wave height

The wave height has a dominant effect on the recovery efficiency. This is included in the model via the introduction of a maximum significant wave height. As long as the wave height is smaller than this threshold, recovery can continue without limitations. If the waves are larger, recovery stops.

The wave height is determined by the wind speed. Free fetch is estimated as one value for each sub-region. Water depth and duration of wind play minor roles since the waters are mostly deep and the periods for oil spill response (few days) are long compared to the duration for establishment of a wave field (few hours). Steep wind generated waves will always cause the main limitations for the response action, whereas long swell waves do not limit the operation.

It was decided by the project partner experts of the BRISK I project that A wave height of 1.3 m represents the limit for effective response (BRISK I, Spreading, 2012). This assumption is carried forward to the BRISK II project.

The wind speeds required for given maximum wave height levels are determined for each sub-region as shown in Table 5-6 below.

Table 5-6 *Wind speeds (m/s) required to obtain different significant wave heights H_s in the different sub-regions. The shaded wave height was selected as the critical wave height H_{crit}.*

Cell values = wind speed [m/s]	Sub-region					
	1	2	3	4	5	6
Fetch [km]	100	150	200	250	150	50
H_s = 0.7m	4.8	4.7	4.6	4.6	4.7	5.5
H_s = 1.0m	6.6	6.4	6.2	6	6.4	7.7
H_s = 1.3m	8.0	7.5	7.3	7.2	7.5	9.5
H_s = 1.6m	10.2	9.5	9.0	8.7	9.5	12.5
H_s = 2.0m	14.0	13.0	12.4	12.0	13.0	17.2

It is seen that the critical wave height of 1.3 m is reached for wind speeds between 7.2 and 9.5 m/s.

Based on the wind statistics given in (Baltic Pilot, 2009), the probability for wind speeds larger than a given level is shown in Figure 5-6 for each sub-region.

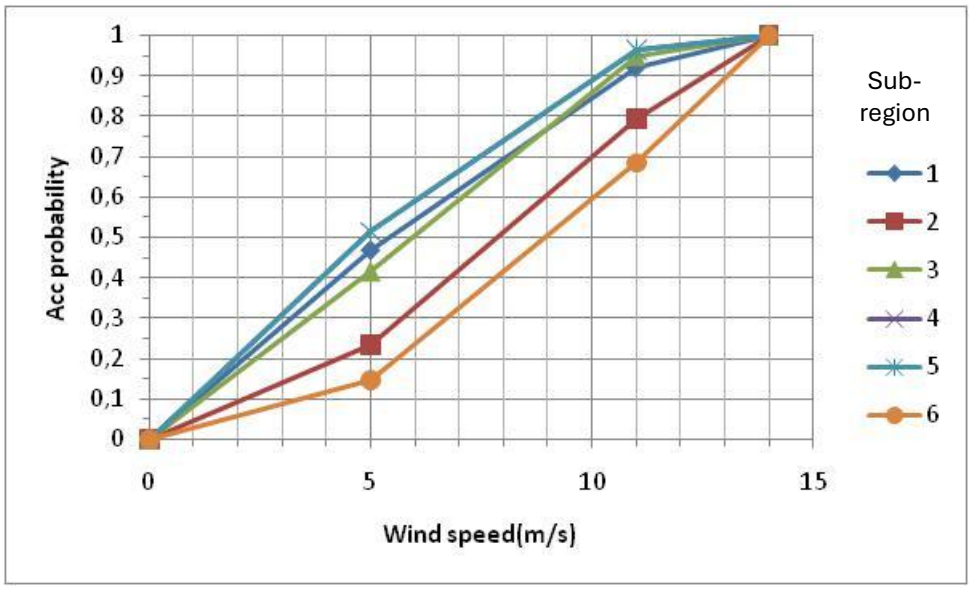

Figure 5-6 *Accumulated probability for wind speeds less than a given speed per sub-region.*

The corresponding probability for wave height H_s smaller than a critical level H_{crit} in each sub-region is given in Figure 5-7 below.

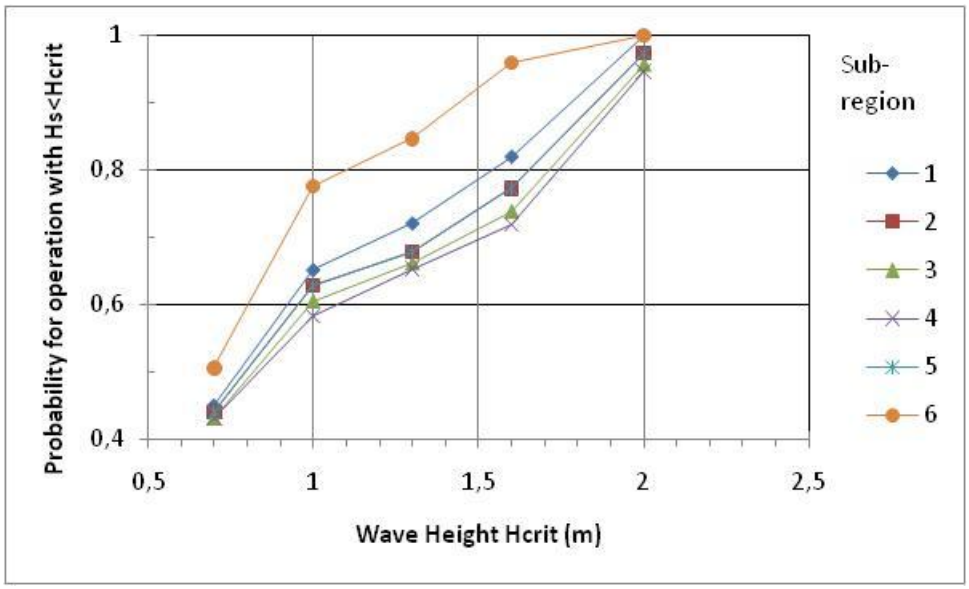

Figure 5-7 *Probability for wave height H_s smaller than a critical level H_{crit} for each sub-region.*

The probabilities for encountering $H_s \geq 1.3$ m are determined and applied in the model as cut-off values for response operation.

6 Risk of oil and HNS impact

6.1 Introduction

This chapter presents the risk of impact of oil and hazardous and noxious substances (HNS). Impact is about the presence of spilt substances in the biosphere. The unit of impact differs depending on the substance and situation:

- Impact of oil and floating HNS on the water is expressed as tonnes (average tonnage present at a given point in time, thus not "per year"): This definition takes into account that one tonne of oil floating around for ten days will have five times the impact of the same amount of oil floating around for two days.
- Impact of oil and floating HNS at the coast is expressed as tonnes per year.
- Impact of soluble HNS in the water body is expressed as events per year times the sea area affected by each of the events. The resulting unit is affected km^2 per year.
- Impact of sinking HNS on the seafloor is expressed as tonnes per year.

The impact risk is calculated for the following three scenarios:

Table 6-1 Scenarios analysed with respect to oil and HNS impact

Scenario	Traffic scenario	Prevention measures	Response capacities
0-0	2024	2024 (actual situation)	
1-0	2036 unchanged or worsened geopolitical situation	2036 (situation according to current planning)	
2-0	2036 improved geopolitical situation		

The results are mainly presented in tables. Figures are only shown for the 2024 case, as the visual differences between the three scenarios are too small to be easily distinguishable for the eye.

6.2 Oil and floating HNS

The impact of oil and HNS spills describes how much oil from accidental spills can be expected at different positions on the sea surface. It is based on the spills described in deliverable D2.6 *Probability of oil and HNS release* (BRISK II, Prob. of release, 2026) and includes the effect of drift and spreading of oil and floating HNS on the surface, the fate and weathering processes as well as the recovery by response vessels. Oil and HNS that drift on shore are considered as oil and HNS on coast and not on the sea surface anymore.

The oil on the sea surface from a specific spill will cover a specific area with a specific thickness for a certain period of time. The thickness of the specific spill is evenly distributed over the entire recurrency period of the specific spill volume. This gives the average thickness over time for this specific spill volume. The contributions for all spill volumes are integrated to an overall thickness. This theoretical thickness represents a statement on the geographical distribution of the general risk for oil and floating HNS.

The unit of impact risk is quantity on the water × time until the quantity disappear / duration of one year, i.e. tonnes × year / year or simply tonnes. In other words, the impact quantifies the amount of oil found on the water at any given point in time.

When plotting the impact risk on a map, the risk is converted into tonnes / km^2 (or for practical reasons into grams / km^2).

Oil reaching the coast is expressed as tonnes per year.

The results are mainly presented in tables. Figures are only shown for the 2024 case, as the visual differences between the three scenarios are too small to be easily distinguishable for the eye.

6.3 Oil and floating HNS

The impact of oil and HNS spills describes how much oil from accidental spills can be expected at different positions on the sea surface. It is based on the spills described in deliverable D2.6 *Probability of oil and HNS release* (BRISK II, Prob. of release, 2026) and includes the effect of drift and spreading of oil and floating HNS on the surface, the fate and weathering processes as well as the recovery by response vessels. Oil and HNS that drift on shore are considered as oil and HNS on coast and not on the sea surface anymore.

The oil on the sea surface from a specific spill will cover a specific area with a specific thickness for a certain period of time. The thickness of the specific spill is evenly distributed over the entire recurrency period of the specific spill volume. This gives the average thickness over time for this specific spill volume. The contributions for all spill volumes are integrated to an overall thickness. This theoretical thickness represents a statement on the geographical distribution of the general risk for oil and floating HNS.

The unit of impact risk is quantity on the water × time until the quantity disappear / duration of one year, i.e. tonnes × year / year or simply tonnes. In other words, the impact quantifies the amount of oil found on the water at any given point in time.

When plotting the impact risk on a map, the risk is converted into tonnes / km^2 (or for practical reasons into grams / km^2).

Oil reaching the coast is expressed as tonnes per year.

The results are mainly presented in diagrams. Figures are only shown for the 2024 case, as the visual differences between the three scenarios are too small to be easily distinguishable for the eye.

Scenario 0-0 (2024)

Figure 6-1 shows the risk of impact of oil and soluble HNS on the water for the year 2024. Naturally, the pattern follows that seen in the spill risk maps presented in D2.6 *Probability of oil and HNS release*

(BRISK II, Prob. of release, 2026). At the same time, it can be clearly seen how wind action spreads the spills from the modelled spill locations into all directions.

Figure 6-2 aggregates the same results for each of the six sub-regions (as defined in Figure 5-1). It also provides a break-down into spills up to 5,000 tonnes and spills above 5,000 tonnes. Moreover, the figure also shows the additional impact that would arise if there were no response capacities at all. A number of effects can be observed:

- Response has a clear effect on the risk of impact. Without response capacities, the risk of impact would be almost double.

- In most sub-regions, the impact from spills up to 5,000 tonnes (small-to-large spills) is larger than that of spills above 5,000 tonnes (very large spills). This may look surprising, as the opposite distribution is seen for the risk of oil release in D2.6. The reason is that spills under 5,000 tonnes contain a higher fraction of fuel oil (HFSO and LFSO), as bunkers spills typically fall within this size class. Fuel oil remains in the water for a longer time than other oil fractions, partly because it does not evaporate, partly because some of it floats beneath the sea surface, from where it cannot be recovered. As spill under 5,000 tonnes stay in the water for a longer time, they have a higher impact according to the definition provided above.

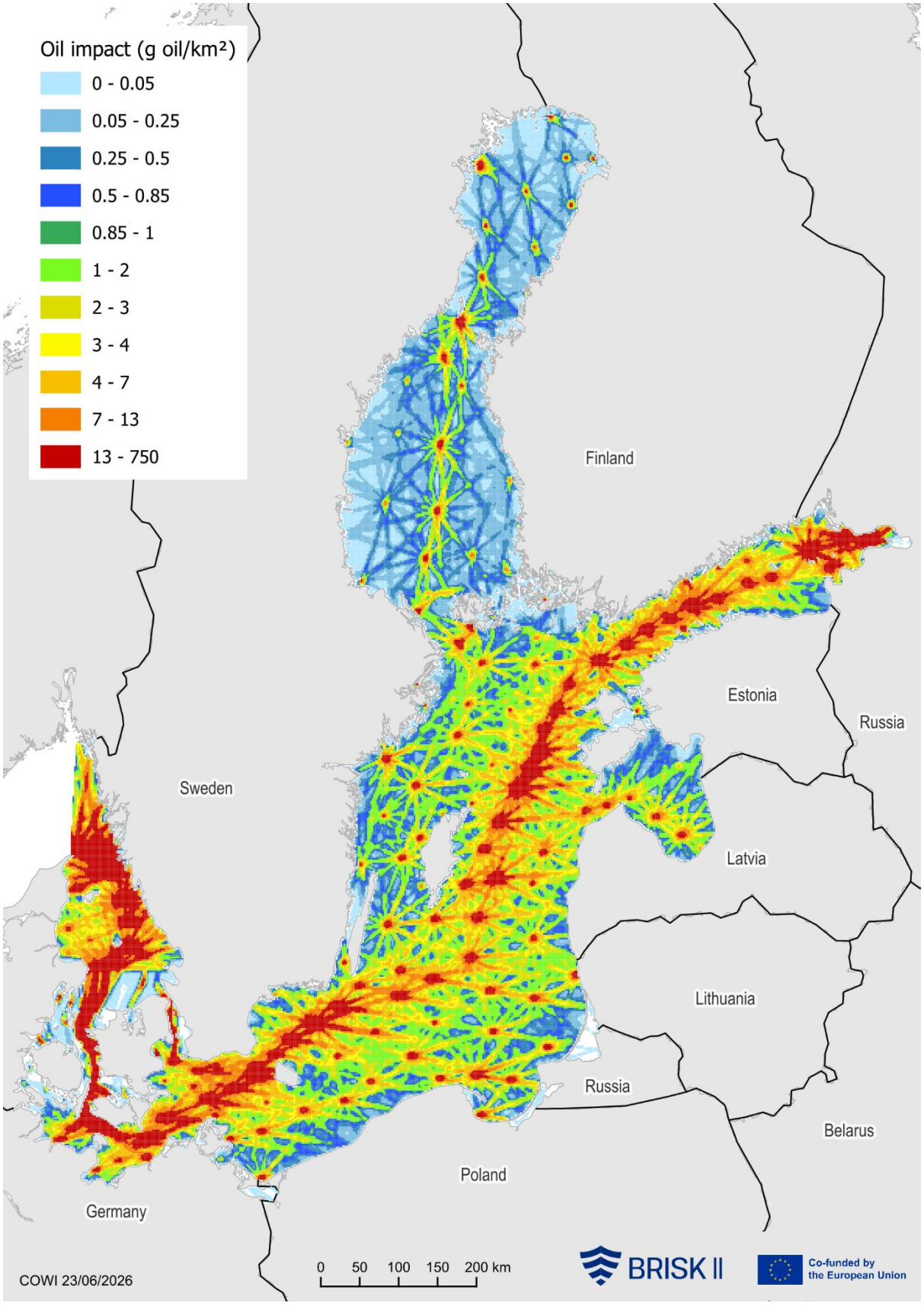

Figure 6-1 Impact of oil and floating HNS on the water in 2024

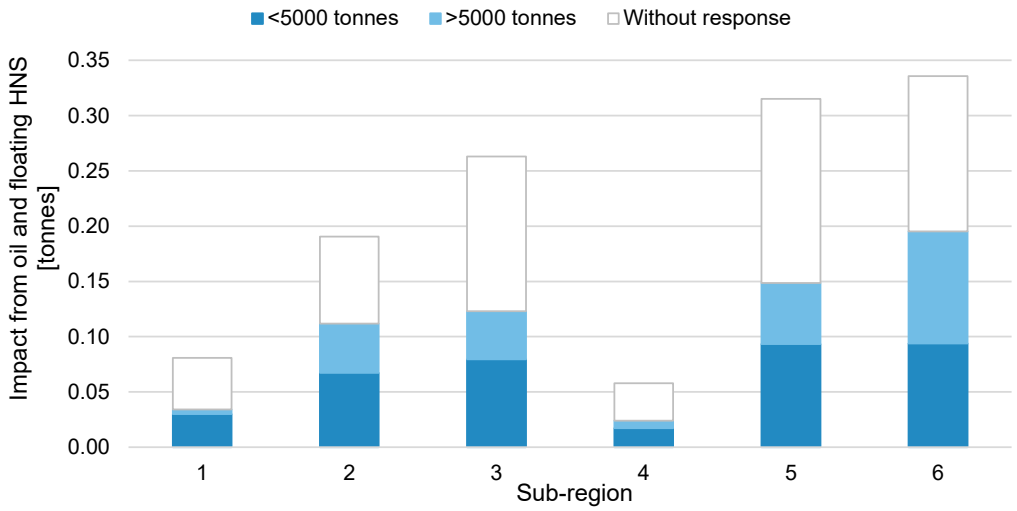

Figure 6-2 *Impact of oil and floating HNS on the water in 2024 (actual impact in blue, theoretical additional impact without response in white)*

Figure 6-3 shows the impact of oil and floating HNS on the coast, expressed as tonnes per year reaching the coast. Some of the main insights can be made by comparing to the impact on the water:

- Sub-region 2 (Gulf of Finland) features a similar impact on the water as sub-region 3 (Central Baltic Proper) but has a much higher impact at the coast. This illustrates the difference between a narrow sea area (sub-region 2), where the oil reaches the coast much faster, thus making it much more difficult to intervene in time as compared to the much wider sea area (sub-region 3).

- The same effect can be observed when comparing sub-region 6 (Kattegat incl. the very narrow Sound and Great Belt) vs. the more open sub-region 5 (Wester Baltic Proper).

- Also, it can be seen that the effect of response is smaller in narrow sub-regions (2 and 6) than in wide sub-regions (3 and 5) for the same reason.

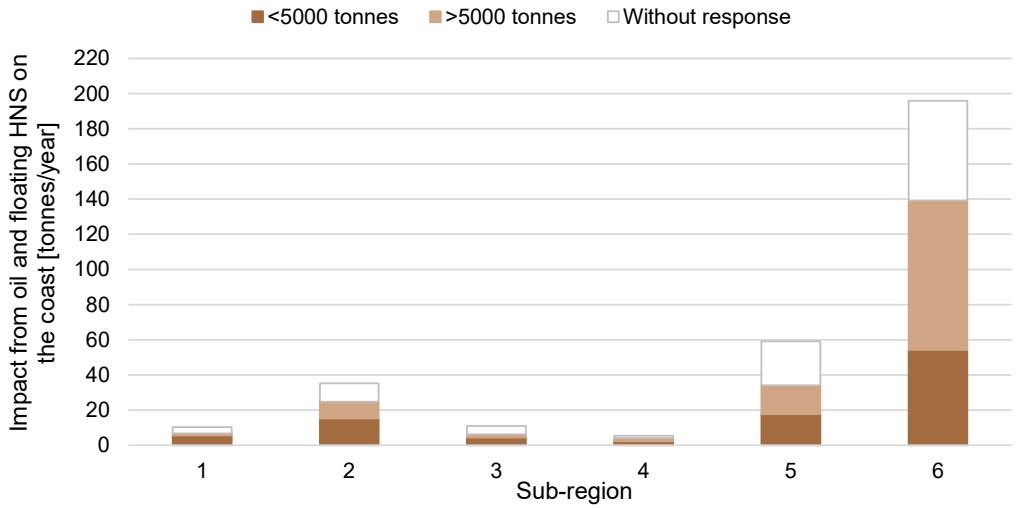

Figure 6-3 *Impact of oil and floating HNS on the coast in 2024 (actual impact in brown, theoretical additional impact without response in white)*

Scenario 1-0 (2036 unchanged/worsened)

Figure 6-4 and Figure 6-5 show the impact on the water and at the coast for Scenario 1-0. The pattern is essentially the same as for Scenario 0-0, albeit with lower absolute impact values. The lower impact is a direct consequence of the lower probability of release described in D2.6 (BRISK II, Prob. of release, 2026) for the same scenario.

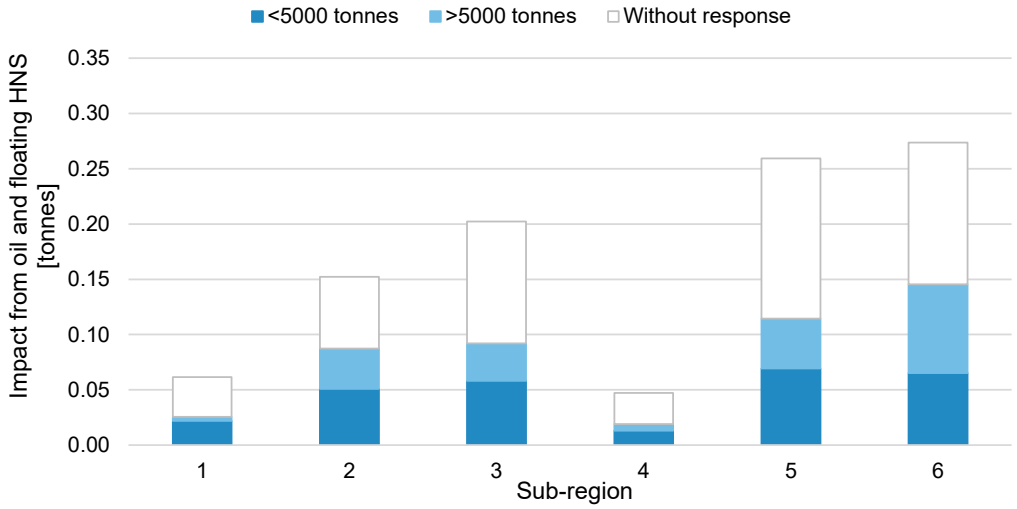

Figure 6-4 *Impact of oil and floating HNS on the water in 2036, unchanged or worsened geopolitical situation (actual impact in blue, theoretical additional impact without response in white)*

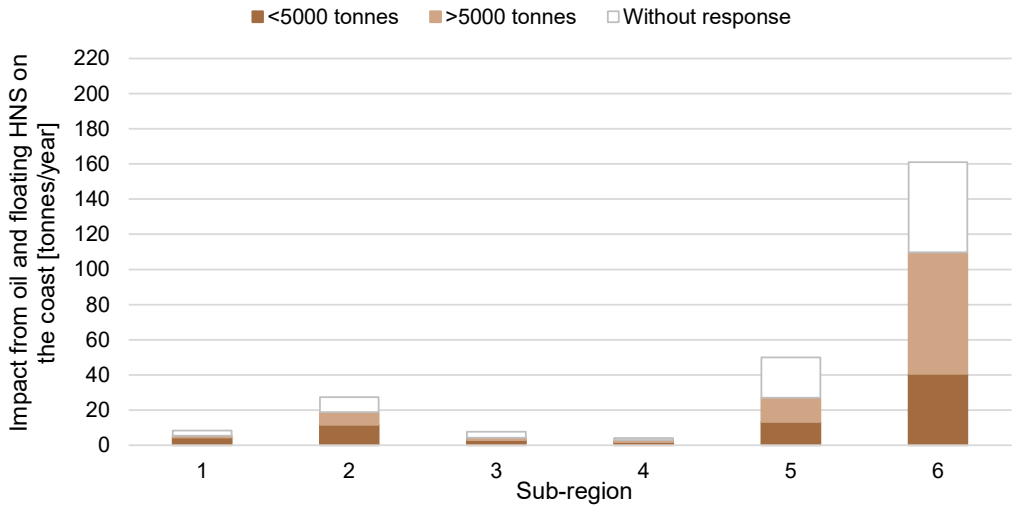

Figure 6-5 *Impact of oil and floating HNS on the coast in 2036, unchanged or worsened geopolitical situation (actual impact in brown, theoretical additional impact without response in white)*

Scenario 2-0 (2036 improved)

Figure 6-6 and Figure 6-7 show the impact on the water and at the coast for Scenario 2-0. Again, the same overall pattern as in Scenario 0-0 and 1-0 is seen. The absolute risk values resemble those in Scenario 0-0, which reflects the similar probabilities of oil and HNS release for the two scenarios.

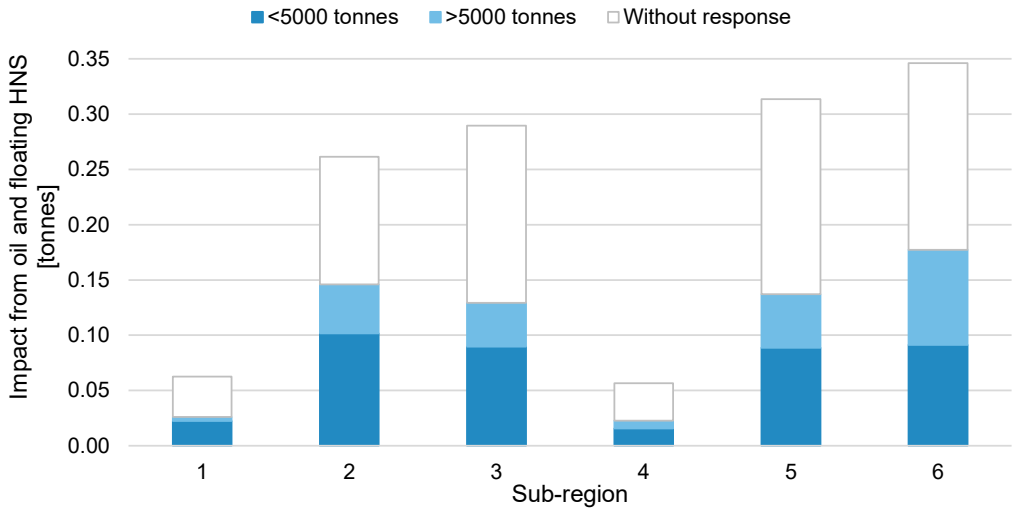

Figure 6-6 *Impact of oil and floating HNS on the water in 2036, improved geopolitical situation (actual impact in blue, theoretical additional impact without response in white)*

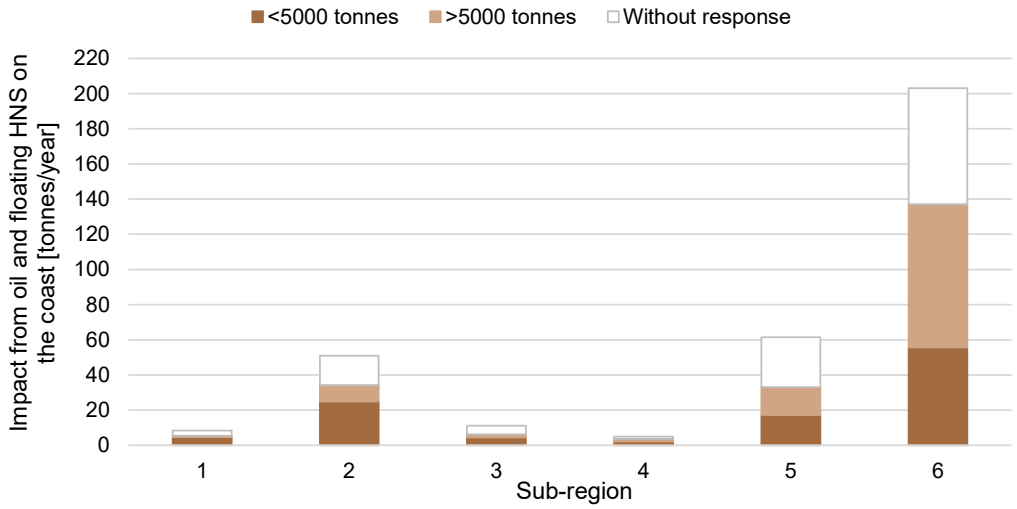

Figure 6-7 *Impact of oil and floating HNS on the coast in 2036, improved geopolitical situation (actual impact in brown, theoretical additional impact without response in white)*

Overview

When comparing the overall impact results for the three scenarios (Figure 6-8 and Figure 6-9), the following can be observed:

- The general trend follows that observed for the probability of release in report D2.6 (BRISK II, Prob. of release, 2026), i.e. a reduced risk 2036 compared to 2024 in case of an unchanged or worsened geopolitical situation (Scenario 1-0) .

- Also, an almost unchanged risk in 2036 compared to 2024 in case of an improved geopolitical situation is seen (blue and brown parts of the diagrams) (Scenario 2-0).

- However, the risk-reducing effect of the response units (white part of the diagrams) is significantly higher in Scenario 2-0 than 0-0. The root to this difference lies within the split between spills under and above 5,000 tonnes. As Scenario 2-0 features more of the smaller spills, the fraction of fuel oil becomes higher. Frequent smaller events are easier to handle for the response forces than rare very large events.

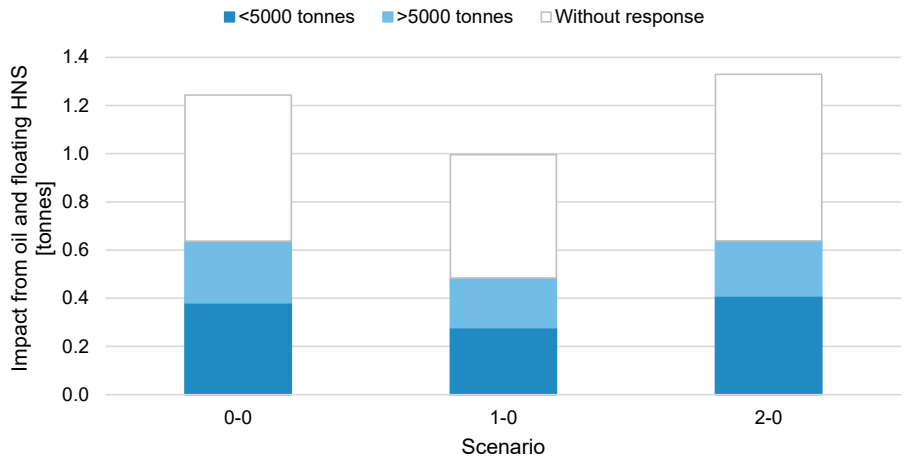

Figure 6-8 *Comparison of the Impact of oil and floating HNS on the water for all three scenarios*

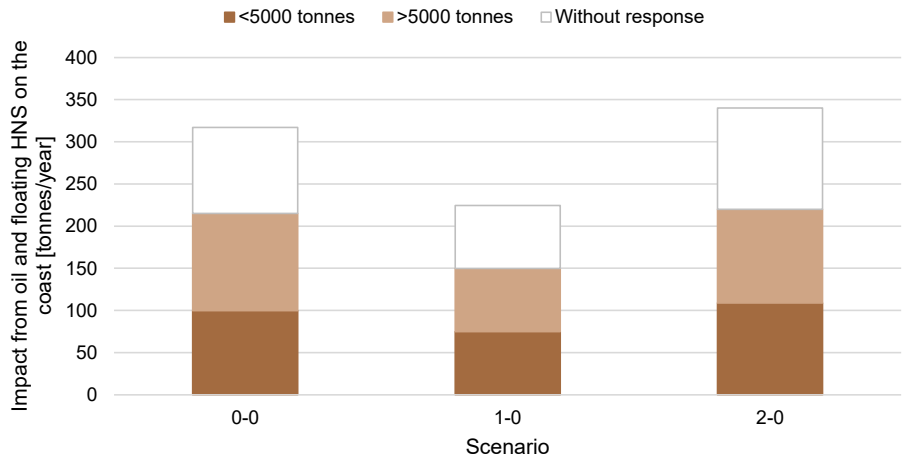

Figure 6-9 *Comparison of the Impact of oil and floating HNS on the coast for all three scenarios*

6.4 Soluble HNS

In section **Error! Reference source not found.**, the PEC/PNEC model was introduced. In essence, it says that there is a critical concentration of soluble HNS in the sea water. If the concentration falls under this value, there will not be any significant impact.

Based on this modelling principle, it makes sense to distinguish between (completely) affected and (completely) unaffected parts of the sea in case of a release. The sea is sub-divided into many small grid cells measuring 2× 2 km. For each grid cell, it can be determined whether there is an impact or not.

As a consequence, the unit of impact from soluble HNS can be defined as events per grid cell and year. This is how it is shown in a map. When expressing the impact for an entire sea area, the number of affected km^2 per year is used.

Scenario 0-0 (2024)

Figure 6-11 shows the risk of impact of soluble HNS for the year 2024. Also here, the pattern follows that seen in the spill risk maps presented in D2.6 *Probability of oil and HNS release* (BRISK II, Prob. of release, 2026). At the same time, it can be clearly seen how dilution spreads the spills into all directions from the modelled spill locations.

Figure 6-10 aggregates the same results for each of the six sub-regions (as defined in Figure 5-1). It also provides a break-down into spills up to 5,000 tonnes and spills above 5,000 tonnes. Also here, the risk of impact is closely linked to the probability of release shown in report D2.6.

When comparing to the impact of oil and floating HNS in section 6.3, a number of interesting observations can be made:

- The relative contribution from spills under 5,000 tonnes is much higher. This is maybe not surprising given that chemicals are normally transported in smaller ships than mineral oil and that most spills only involve one or two cargo compartments.

- The distribution between the sub-regions is different than for oil and floating HNS. Most notably, sub-region 1 (Gulf of Bothnia) and 3 (Central Baltic Proper) show elevated values when using sub-region 2 (Gulf of Finland) in Figure 6-2 as benchmark.

- Also, sub-region 5 (Western Baltic Proper) shows higher impact values than sub-region 6 (Kattegat and entrances to the Baltic Sea) as opposed to oil and floating HNS in Figure 6-2.

These differences show that transport of chemicals is following a different logic than transport of oil; while the oil transport pattern is dominated by the main transport corridor from Russia to the North Sea, transport of chemicals follows the needs of the industry along the coast of the Baltic Sea countries.

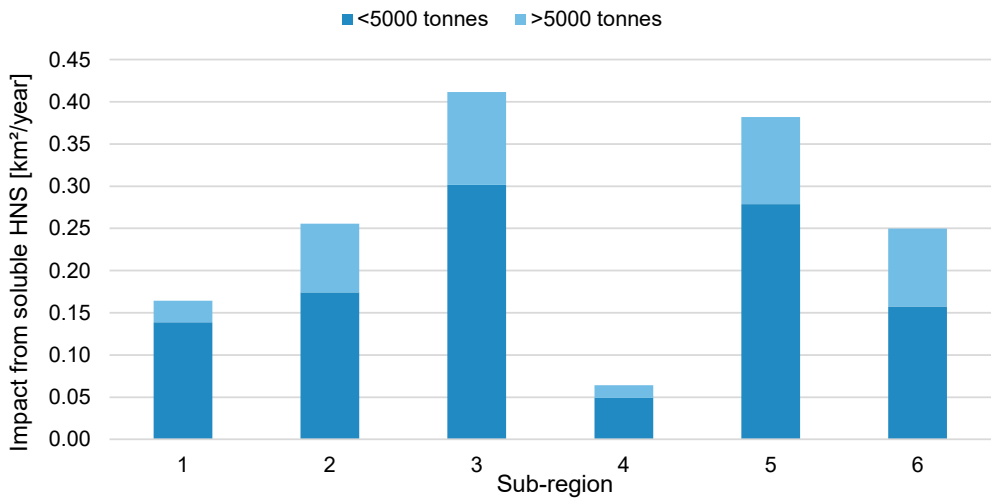

Figure 6-10 Impact of soluble HNS in 2024

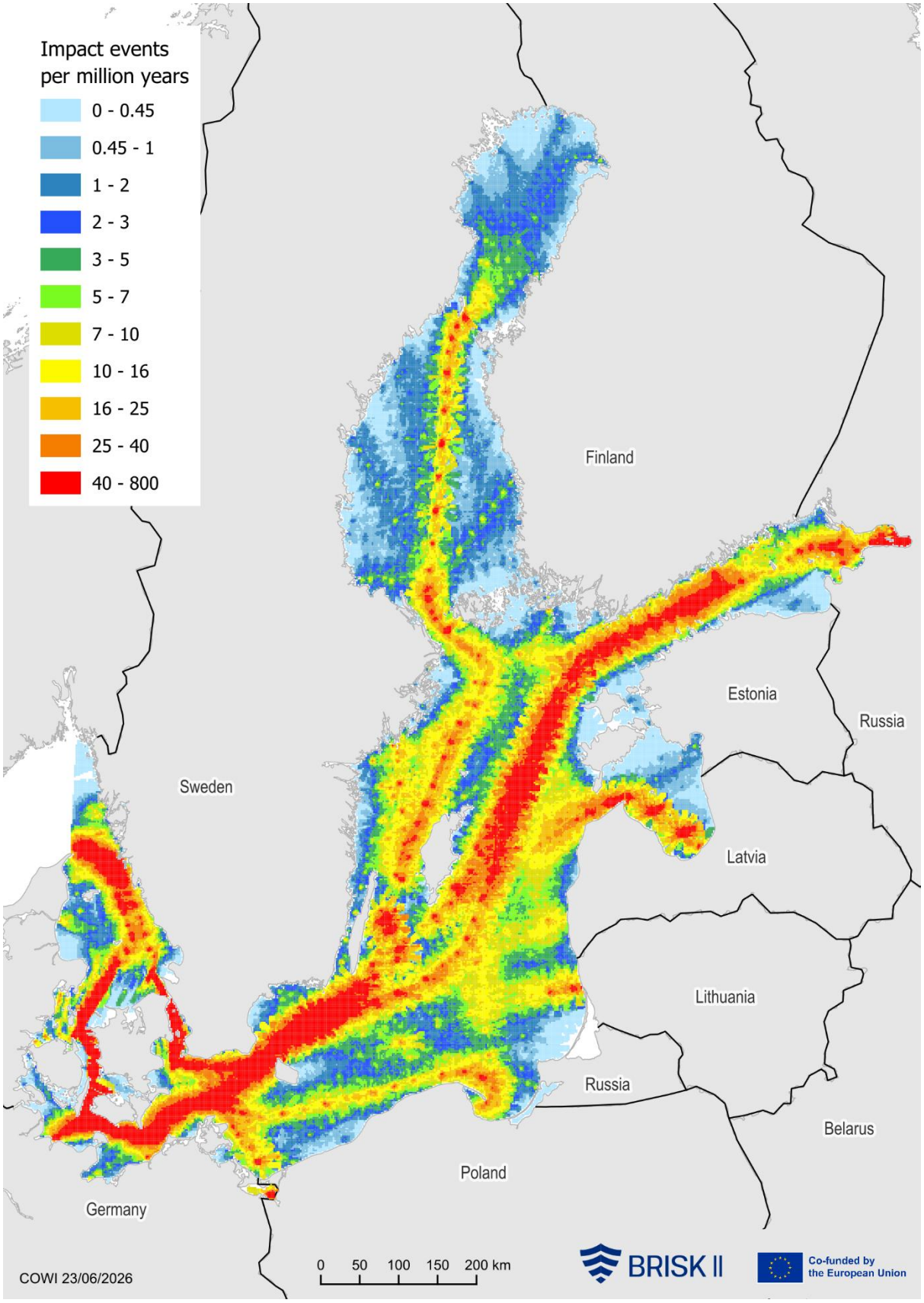

Figure 6-11 Impact of soluble HNS in 2024 (probability of impact expressed for each 2 × 2 km grid cell)

Scenario 1-0 (2036 unchanged/worsened)

Figure 6-12 shows the impact for Scenario 1-0. The pattern is essentially the same as for Scenario 0-0, albeit with lower absolute impact values. The lower impact is a direct consequence of the lower probability of release described in D2.6 (BRISK II, Prob. of release, 2026) for the same scenario.

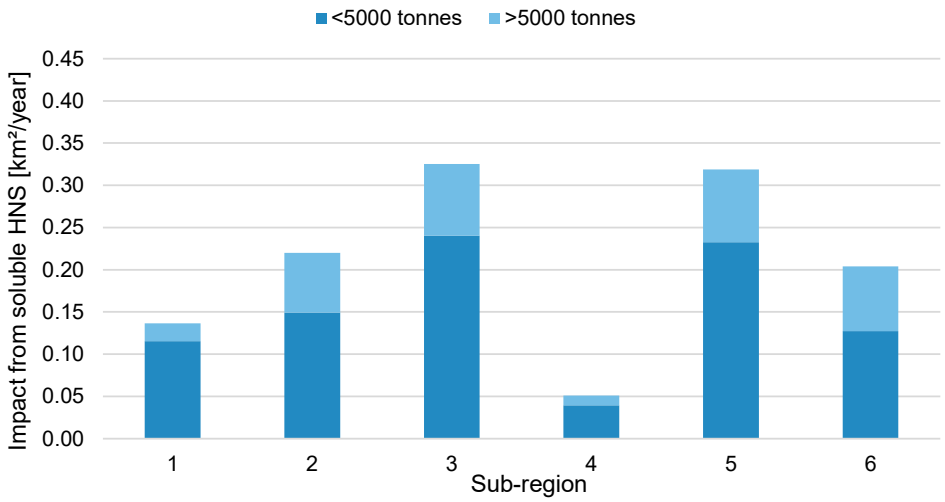

Figure 6-12 *Impact of soluble HNS in 2036, unchanged or worsened geopolitical situation*

Scenario 2-0 (2036 improved)

Figure 6-13 shows the impact on the water and at the coast for Scenario 2-0. Again, the same overall pattern as in Scenario 0-0 and 1-0 is seen. The absolute risk values are lower than in Scenario 0-0 but higher than in Scenario 1-0, which reflects the corresponding trend for release of soluble HNS described in report D2.6 (BRISK II, Prob. of release, 2026).

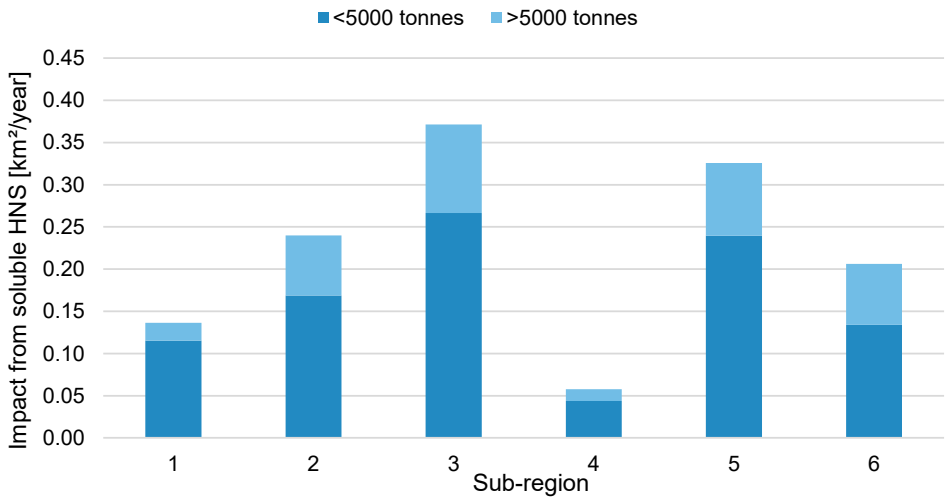

Figure 6-13 *Impact of soluble HNS in 2036, improved geopolitical situation*

Overview

Figure 6-14 provides an overview of the overall impact values for soluble HNS for the three scenarios.

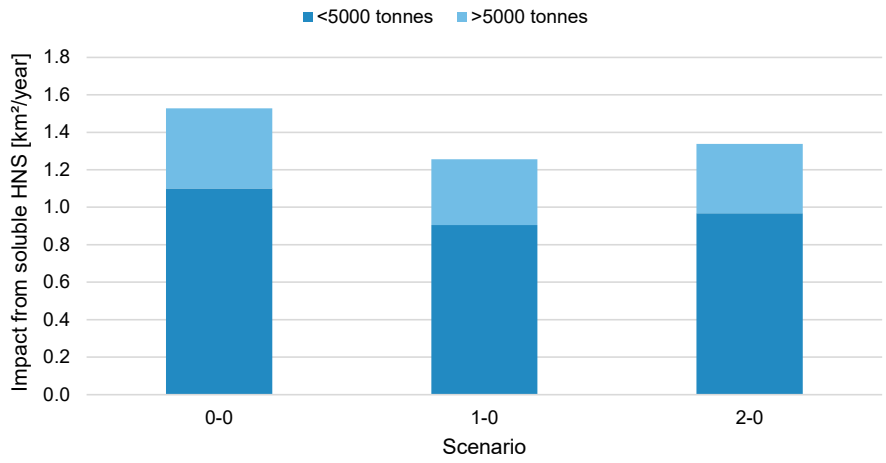

Figure 6-14 *Comparison of the impact of soluble HNS for all three scenarios*

6.5 Sinking HNS

The impact of sinking HNS is identical to the probability of release of sinking HNS described in report D2.6 (BRISK II, Prob. of release, 2026). Figure 6-15 provides and overview over those numbers.

The distribution between the six sub areas resembles that of oil and floating HNS (section 6.3) more than that of soluble HNS (section 6.4). On the other hand, the trend for Scenario 1-0 and 2-0 relative to the "current situation" case 0-0 has its own pattern that is distinct from either of that seen in the previous cases.

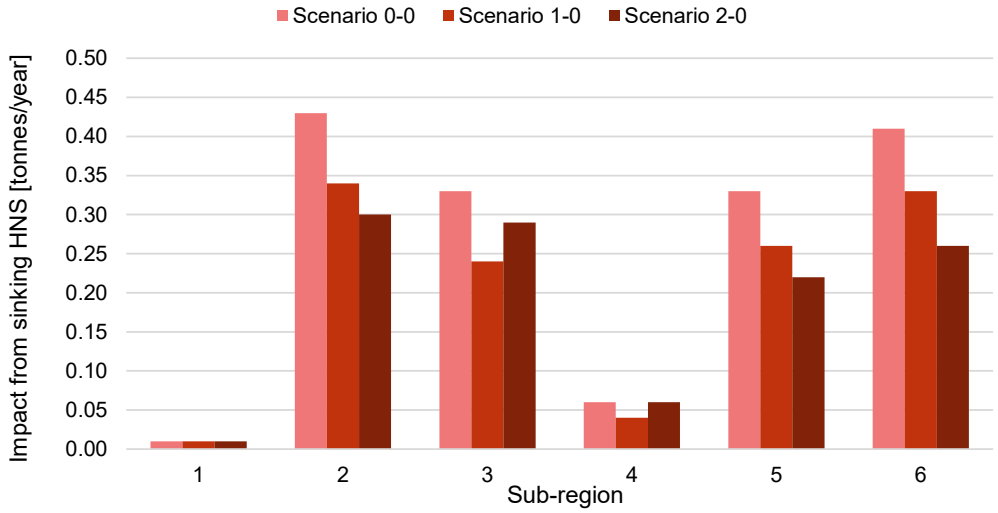

Figure 6-15 *Comparison of the impact of soluble HNS for all three scenarios*

7 Abbreviations

DAMSA	Danish Maritime Safety Administration (former entity, succeeded by FCOO, see below)
FCOO	Forvarets Center for Operativ Oceanografi (Danish Defence's Centre for Operative Oceanography)
HNS	Hazardous and noxious substances
HSFO	High-sulphur fuel oil
LSFO	Low-sulphur fuel oil
VLSFO	Very low-sulphur fuel oil (sub-set of LSFO)
ULSFO	Ultra low-sulphur fuel oil (sub-set of LSFO)
SMHI	Swedish Meteorological and Hydrological Institute

8 References

Baltic Pilot, 2009	Admiralty Sailing Directions, "Baltic Pilot, volume I, II and III, (NP 18, NP 19, NP 20). United Kingdom Hydrographic Office, 2006-2009.
BRISK I, Spreading, 2012	BRISK, Model report: Part 5 - Spreading and containment of spilt oil and hazardous substances, 2012
BRISK II, Method note, 2025	BRISK II, Method note, deliverable D2.1, 2025
BRISK II, Traffic analysis, 2025	BRISK II, Traffic analysis, deliverable D2.3, 2025
BRISK II, Cargo analysis, 2025	BRISK II, Cargo analysis, deliverable D2.4, 2025
BRISK II, Spill model, 2026	BRISK II, Accident and spill model, deliverable D2.5, 2026
BRISK II, Prob. of release, 2026	BRISK II, Probability of oil and HNS release, deliverable D2.6, 2026
BRISK II, RRM scenarios, 2026	BRISK II, Risk reduction scenario selection, deliverable D3.2, 2026
Chevron Phillip, 2005	Chevron Phillip Chemical Company LP, Safe Handling and Storage of Benzene, Rev 1. 2005
Ecotox, 2006	U.S. Environmental Protection Agency. ECOTOX Database, viewed in 2006, http://cfpub.epa.gov/ecotox/
Environment Canada, 2006	Environment Canada, Extract from database: http://www.etc-cte.ec.gc.ca/database/OilProperties/, 2006
Glamer, H., 2011	Glamer, H., Length of day, http://herbert.gandraxa.com/length_of_day.xml, viewed 2011
IMAROS 1, 2022	IMAROS, Deliverable 3.2: Summary of WP3, 2022, https://www.kystverket.no/globalassets/oljevern-og-miljoberedskap/forskning-og-utvikling/imaros/deliverable-d3-2-summary-of-wp3.pdf/download
IMAROS 2, 2025	IMAROS, Deliverable D3.1: Summary report of WP 3. Characterisation and impacts, 2025, https://civil-protection-knowledge-network.europa.eu/system/files/2025-12/report-from-work-package-3.pdf

ITOPF, 2006	ITOPF, technical information papers: "Fate of marine oil spills", http://www.itopf.com/tip2.pdf, 2006
Oil spill DK, 2007	Risikoanalyse: Olie- og kemikalieforurening i danske farvande (Risk analysis: Oil and chemicals pollution in Danish waters), delrapport Spredning og bekæmpelse af udslip (sub-report Spreading and combat of spills), prepared for Danish Ministry of Defence by COWI, COWI report 63743-1-09, January 2007
SMHI, 2008a	Swedish Meteorological and Hydrological Institute, Technical documentation Sea Track Web, Physical Processes, numerics, algorithms and references, Version 2.2.0., 2008.
SMHI, 2008b	Swedish Meteorological and Hydrological Institute, SeaTrack Web Scientific documentation http://seatrack.smhi.se/seatrack/STW_manual_Technical_documentation.pdf, 2008

Appendix A PEC/PNEC model results

The values from the detailed modelling are shown in the figures below as a function of water body and danger class. Simulations are carried out with drift velocities of 0.05 m/s, 0.08 m/s and 0.2 m/s, corresponding to wind velocities of approximately 1.2 m/s, 2 m/s og 5 m/s.

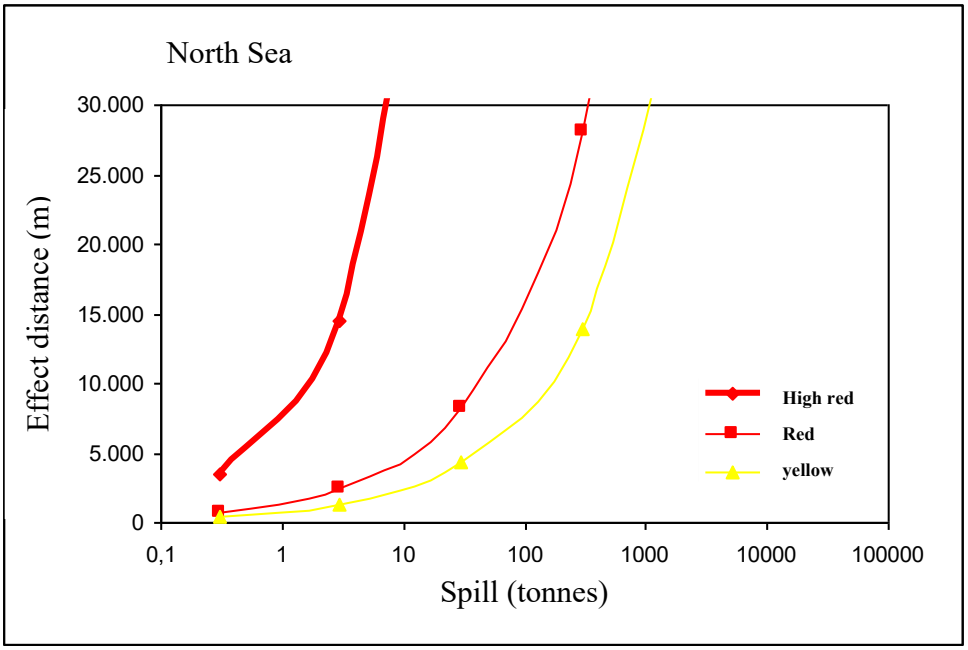

Figure A-1 *Length (L) of effect calculated for the North Sea. The effect length of up to 30 m is calculated as a function of the spilled amount for different danger classes*

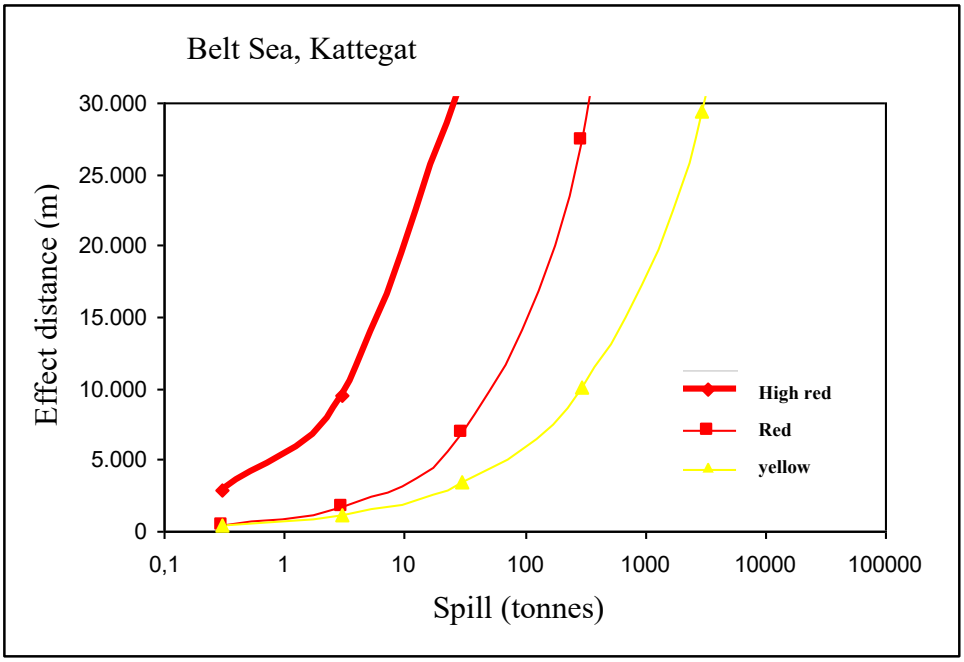

Figure A-2 *Length (L) of effect calculated for the Danish straits and Kattegat. The effect length of up to 30 m is calculated as a function of the spilled amount for different danger classes.*

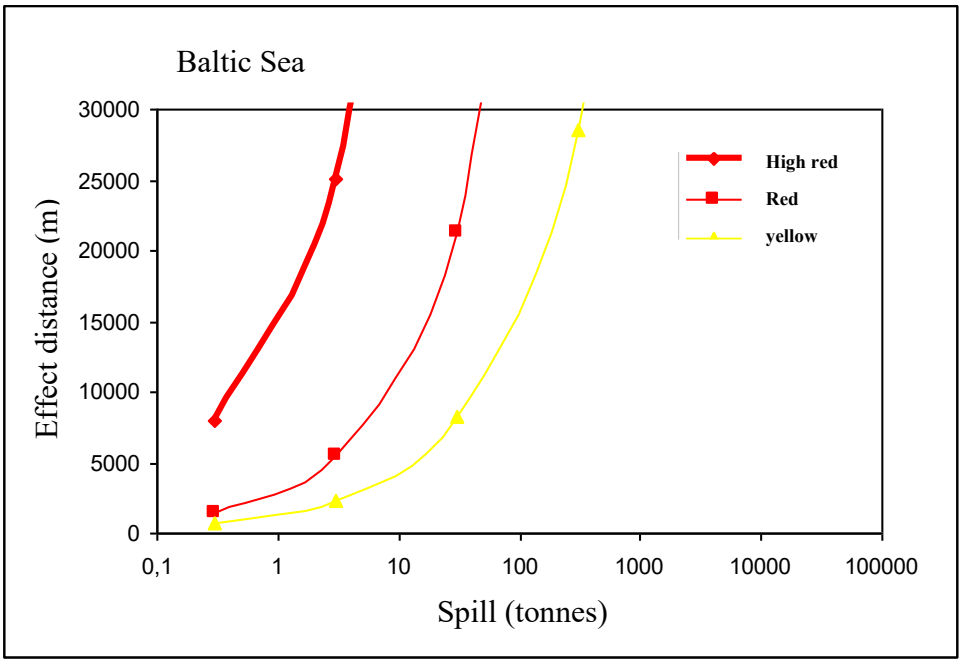

Figure A-3 *Length (L) of effect calculated for the Baltic Sea. The effect length of up to 30 m is calculated as a function of the spilled amount for different danger classes.*

Appendix B Documentation for dilution calculations of soluble chemicals (PEC/PNEC)

B.1 Methodology for calculations of PEC/PNEC ratios

The environmental impact assessment of chemicals and aqueous discharges or spills is based on the comparison of calculated Predicted Environmental Concentration (PEC) and Predicted No Effect Concentration (PNEC). When PEC is larger than PNEC, the concentration in the environment exceeds the concentration at which the chemical is considered not to exert any toxic effects. The model corresponds with CHARM project (Karman et al., 1996 and Thatcher et al., 2001). Discharge specific chemical concentrations (C_w) are used in the model, which is more precise than using the generic calculation of C_w in CHARM.

The discharged chemicals may either stay in the water column or drop to the sediment on the seabed with settling particles. PEC and PNEC are, therefore, calculated for both water and sediment. Staying in the water column, the concentration of the chemical will decrease with time due to dilution, sedimentation and biodegradation. Once in the sediment, the concentration will depend on the partitioning of the chemical between sediment and water, and the chemical's potential for biodegradation.

By the use of the dilution model, the distance at which the chemical will impact the pelagic environment may be calculated. Due to the rapid dilution of the discharges, biodegradation in the water column is ignored.

The distance at which the chemical will impact the benthic environment is calculated under the assumption that the sedimenting particles settle evenly around the platform under the influence of a standard refreshment rate of the seawater. Biodegradation in the sediment is assumed to occur only approx. 10% of the time due to bioturbation of anaerobic marine sediments and resulting oxygen depletion.

The potential for bioaccumulation of discharged chemicals is assessed on the basis of information on bioconcentration factors (BCF) or octanol-water partition coefficients (P_{ow}). The potential for bioaccumulation is not quantified.

B.2 Calculation of PEC and PNEC

B.2.1 Calculation of PEC_{water} and $PNEC_{pelagic}$

PEC_{water} designates the predicted environmental concentration at a given distance from the point of discharge. In this assessment PEC_{water} is calculated for distances of 100 m; 250 m; 500 m; 1,000 m; 1,780 m and 5,000 m (1,780 m being the radius of a circle with the area of 10 km^2). Based on the maximum concentrations at these distances, a graph showing the concentration as a function of the distance is produced and the distance at which PEC_{water} equals $PNEC_{pelagic}$ is deducted.

PEC_{water} is calculated using the dilution model described in Section B.3. This model is validated through field work carried out by scientific workers and is recognised through the last 30 years where COWI has used the model. The dilution model is more advanced than for instance the dilution model of CHARM.

$PNEC_{pelagic}$ is deducted from reported results of ecotoxicological tests and the application of assessment factors. The endpoint of the ecotoxicological tests is most commonly LC50 and EC50 values. LC50 values designate the concentration at which 50% of the tested organisms die, whereas EC50 values designate the concentration at which the tested parameter (e.g. growth rate, immobilisation) is inhibited by 50%. In order to predict the concentration, at which the chemical is not anticipated to cause adverse effects to the ecosystems, the ecotoxicological endpoint value is divided with an assessment factor. The size of the assessment factor depends on the amount and character of the data available for the assessment. Table B-1 indicates the assessment factors applied. The assessment factor is applied to the lowest value available among the set of endpoints for the chemical.

Effect assessment of discharged products has been carried out under the assumption that the product can be defined by the properties of each of its compounds and the total toxicity of the product. Effect assessment of discharged products has been carried out for each non-PLONOR compound. The concentration of the compound in the product is often given as an interval. In these cases, the assessments are made conservative: the lowest concentration is used for calculating toxicity (EC) and the highest concentration is used for calculating the water concentration (C_w).

Table B-1: Assessment factors for converting ecotoxicological endpoint data into PNEC

Assessment Factors		EC_{50} and LC_{50} values		
		At least data for algae, crustaceans **and** fish	Data but not for algae, crustaceans **and** fish	No data
NOEC values	At least data for algae, crustacean **and** fish	NOEC/10	NOEC/10	NOEC/10
	Data but not for algae, crustaceans **and** fish	NOEC/10 or EC_{50}/100	NOEC/10 or EC_{50}/1000	Not relevant
	No data	EC_{50}/100	EC_{50}/1000	No result

B.2.2 Calculation of $PEC_{sediment}$ and $PNEC_{benthic}$

$PEC_{sediment}$ is calculated using the following formulas:

$$PEC_{sediment} = C_w * D_{regional} * P_{sw} * (1-d_{sediment}) \quad \text{(B.1)}$$

$$D_{regional} = \frac{\frac{F_w}{V_p}}{r + d_1} \quad \text{(B.2)}$$

$$P_{sw} = f_{oc} * P_{ow} \quad \text{(B.3)}$$

$$d_{sediment} = 1 - (1-d_1)^{36.5} \quad \text{(B.4)}$$

$$d_1 = 1 - 10^{\frac{\log(1-d_{28})}{28}} \quad \text{(B.5)}$$

in which:

C_w =	Concentration of the chemical before discharge (mg/l)
$D_{regional}$ =	Regional dilution factor
P_{sw} =	Partition coefficient between sediment and water
$d_{sediment}$ =	Degradation of a substance in the sediment after 1 year (fraction)
F_w =	Volume of produced water discharged (m^3/day)
V_p =	Volume of water per platform (m^3); standard platform area (10 km^2) * the depth at the satellite fields (60 m)
r =	Refreshment of the seawater in the area around the platform; standard value: 0.24 day^{-1}
d_1 =	1 day biodegradation (fraction)
d_{28} =	28 day biodegradation (fraction)
f_{oc} =	Fraction organic carbon in sediment (fraction of wet weight); standard value: 0.04
P_{ow} =	Partition coefficient between octanol and water.

$PNEC_{benthic}$ may be calculated using ecotoxicological endpoint values for sediment reworking animals and applying the assessment factors presented in Table B-1, or by converting $PNEC_{pelagic}$ to $PNEC_{benthic}$ by the following formula:

$$PNEC_{benthic} = P_{sw} * PNEC_{pelagic}. \quad (B.6)$$

B.3 Dilution model

B.3.1 Introduction

This report describes the formulas used by COWI for calculating the dilution of wastewater discharged to the sea from platforms in the North Sea. This model has not been validated scientifically by COWI in the North Sea, but it is based on field work carried out by scientific workers and is recognised through the last 30 years where COWI has used this model in projects for municipalities and the industry in Denmark and abroad.

The formulas are valid for the case with no or only weak stratification in the sea. This means no or only small density differences between the surface water and the bottom water which is the normal situation at water depths up to about 40 m in the North Sea. Around the satellite fields, situated at 60 m depth, stratification may occur occasionally, and the dilution model will not be able to model transport across the stratification layer. However, this layer will act as a boundary for the plume to pass on to the section below the layer. Therefore, as a "worst case" description, the model is used with a standard depth of 40 m, assuming that a stratification layer will limit the mixing of the plume below 40 m.

The dilution of wastewater depends on many physical processes. Near to the outlet, i.e. in the so-called near field, the dilution is governed by the characteristics of the discharge: Outlet velocity, density, diameter, etc. Farther from the outlet, i.e. in the far field, the dilution is governed by the characteristics of the receiving water: Depth, current velocity, wind and waves, etc.

In sections B.3.2 and B.3.3, the dilution in the near field and in the far field are described.

In B.4 the uncertainty in the dilution calculations is described.

B.3.2 The near field

In the near field momentum from the outlet and buoyancy phenomena dominate the dilution.

If the density of the wastewater equals that of the seawater there will be no buoyancy. In this case the discharge will form a pure jet governed by the outlet momentum.

With no outlet momentum, but a density difference between the wastewater and the seawater the discharge will form a pure plume. If the density of the waste water is lower or higher than the density of the sea water, the waste water will rise to the sea surface or fall down to the bottom of the sea.

If both momentum and buoyancy are present the discharge may be called either a jet or a plume, depending on the size of the so-called densimetric Froude number:

$$F_\Delta = \frac{V_o}{\sqrt{\Delta_o g D_o}} \quad \text{(B.7)}$$

$$\Delta_O = \frac{\rho_a - \rho_0}{\rho_a} \quad \text{(B.8)}$$

in which:

V_o: Outlet velocity (m/s)
Δ_o: Outlet density difference (no dimension)
g: Acceleration of gravity (= 9.81 m/sec^2)
D_o: Diameter of outlet (m)
ρ_a: Density of ambient water, i.e. seawater (kg/m^2)
ρ_o: Density of waste water (kg/m^3).

If F_Δ is greater than one, momentum dominates, and the discharge will act mostly as a jet. If F_Δ is less than one, the discharge will act mostly as a plume.

Normally, the initial dilution is interpreted as the dilution from the outlet to the sea surface or the sea bottom. If the outlet is a horizontal jet, the wastewater will spread horizontally. In this situation, an initial dilution cannot be defined.

The general equation describing the velocity and the dilution in the centre axis for vertical jets and plumes are (Abraham, 1963):

$$\frac{V_{\max}}{V_o} = 6.2 \frac{D_o}{s} \left(1 + 0.33 \left(\frac{s}{D_o F_\Delta} \right)^2 \right)^{1/3} \quad \text{(B.9)}$$

$$S_{\min} = 0.18 \frac{s}{D_o} \left(1 + 0.22 \left(\frac{s}{D_o F_\Delta} \right)^2 \right)^{1/3} \quad \text{(B.10)}$$

in which:

V_{max}: Maximum velocity, i.e. the centre axis velocity (m/s)
S_{min}: Minimum dilution, i.e. the centre axis dilution
s: Distance from outlet (m).

Equations similar to Eqs. B.9 and B.10 have been developed by others, e.g. (Cederwall, 1968).

For pure jets, i.e. $F_\Delta \to \infty$, the Eqs. B.9 and B.10 reads:

$$\frac{V_{\max}}{V_o} = 6.2 \frac{D_o}{s} \tag{B.11}$$

$$S_{\min} = 0.18 \frac{s}{D_o} \tag{B.12}$$

These equations are valid for all directions of jets, i.e. including horizontal and vertical jets. Instead of the constant 0.18 (Fisher, 1979) proposes 0.20.

With no outlet momentum, i.e. $F_\Delta \to 0$, the Eqs. B.9 and B.10 describe the pure plume situation:

$$\frac{V_{\max}}{V_o} = 4.3 F_\Delta^{-2/3} \left(\frac{s}{D_o}\right)^{-1/3} \tag{B.13}$$

$$S_{\min} = 0.109 F_\Delta^{-2/3} \left(\frac{s}{D_o}\right)^{5/3} \tag{B.14}$$

Instead of the constant 0.109, (Fisher, 1979) proposes 0.129.

If the outlet is horizontal, Eqs. B.11 and B.12 may be used for jets as explained above. For plumes, the following simple equation may be used (Liseth, 1977):

$$S_{\min} = \frac{2}{3} \frac{s}{D_o} \tag{B.15}$$

This equation is valid for s/D_oF_Δ greater than one and less than 20. Outside this range, graphical solutions may be used, see e.g. (Liseth, 1977).

For jets the mean dilution will be between 1.4 and 2.0 times the minimum dilution. This range may also be used for plumes as a reasonable approximation.

The maximum concentration in the centre axis is the reciprocal of the minimum dilution. If the wastewater is diluted before it is discharged to the sea, the maximum concentration is:

$$C_{\max} = \frac{C_o}{S_{\min}} \tag{B.16}$$

in which C_o : Concentration of matter in outlet water.

B.3.3 The far field

By an analogy to molecular diffusion, see e.g. (Fisher, 1979), the dispersion of wastewater in the far field it is assumed to follow Fick's Law. This law states that the mass of waste crossing a unit area per unit time in a given direction is proportional to the gradient of waste concentration in that direction.

Using Fick's Law the one-dimensional equation describing the dispersion in case of no convection is:

$$\frac{\partial C}{\partial t} = D \frac{\partial^2 C}{\partial x^2} \qquad \text{(B.17)}$$

in which

C: Concentration, i.e. volume wastewater to volume seawater (m^3/m^3)
t: Time (s)
x: Coordinate (m)
D: Dispersion coefficient (m^2/s)

The term dispersion describes the combined dispersal owing to turbulent diffusion and spatial velocity variations. In the ocean there will often be a velocity variation between top and bottom, leading to different velocities of wastewater between top and bottom. The result will be a larger mixing than in the case of no spatial velocity variations.

In the one-dimensional case, if all waste to time t = 0 is placed in the plane x = 0, the solution to Eq. B.17 is, see e.g. (Engelund, 1968):

$$C = \frac{1}{2\sqrt{\pi D t}} \exp\left(-\frac{x^2}{4Dt}\right) \qquad \text{(B.18)}$$

This equation equals the well-known Gaussian equation, if

$$\sigma^2 = 2Dt \qquad \text{(B.19)}$$

in which σ^2: Variance (m^2)

In the far field the wastewater follows the mean current in the sea. Calling the horizontal coordinate in the current direction x_1, the mean velocity of the sea current is:

$$U = \frac{x_1}{t} \qquad \text{(B.20)}$$

In the two-dimensional case (plume), in case of a steady outflow of waste to the sea the transport of waste is:

$$Q_o = U \int_{\infty}^{\infty} \int_{\infty}^{\infty} C(x_1, x_2, x_3,) \, dx_2 dx_3 \quad \text{(B.21)}$$

in which:

Q_o: Wastewater transport (m^3/s)
x_1: Horizontal coordinate in the flow direction (m)
x_2: Horizontal coordinate lateral to the flow direction (m)
x_3: Vertical coordinate lateral to the flow direction (m).

Assuming Gaussian concentration profiles, i.e. using Fick's Law we have:

$$C(x_1, x_2, x_3) = C(x_1, 0, 0) \exp \left\{ - \frac{x_2^2}{2\sigma_2^2} - \frac{x_2^3}{2\sigma_2^3} \right\} \quad \text{(B.22)}$$

For the Gaussian distribution the following equation is valid:

$$\int_{\infty}^{\infty} \frac{1}{\sqrt{2\pi}} \exp \left(- \frac{x^2}{2} \right) dx = 1 \quad \text{(B.23)}$$

Inserting Eq. B.23 in Eqs. B.22 and B.21 yields:

$$Q_o = UC(x_1, 0, 0) \, 2\pi \sigma_2 \sigma_3 \quad \text{(B.24)}$$

C (x_1, 0, 0) is the concentration at the centre line of the plume, i.e. the maximum concentration. The reciprocal of this value is the minimum dilution:

$$S_{\min} = \frac{2\pi U \sigma_2 \sigma_3}{Q_0} \quad \text{(B.25)}$$

If the wastewater is discharged at the surface or near the bottom, mixing from the top or the bottom of the plume is impossible. In this case, the dilution is only 50%:

$$S_{\min} = \frac{\pi U \sigma_2 \sigma_3}{Q_o} \quad \text{(B.26)}$$

Using Eqs. B.19 and B.20 in Eq. B.26 we get:

$$S_{\min} = \frac{\pi U}{Q_o} \sqrt{2 D_2 \frac{x_1}{U}} \bullet \sqrt{2 D_3 \frac{x_1}{U}} \quad \text{(B.23)}$$

or:

$$S_{\min} = K \frac{U x_1 y}{Q_o} \quad \text{(B.24)}$$

in which y: Depth of water (m) and K: Constant defined by:

$$K = \frac{2\pi\sqrt{D_2 D_3}}{yU} \quad \text{(B.25)}$$

The length scale of the vertical fluctuations is considerably smaller than for the horizontal fluctuations. For this reason, the vertical dispersion coefficient, D_3, is much smaller than the horizontal coefficient, D_2.

Field experiments have shown, see e.g. (Koh and Fan, 1970), that D_3 depends on the vertical density gradient. In relatively shallow waters, i.e. depths less than about 40 m, the density gradient is normally small. This means that in the Danish sector of the North Sea, the influence of density gradients may be neglected.

In coastal waters, the following dispersion coefficients may be applied (Odgaard, 1976):

$$D_2 = Uy \quad \text{(B.26)}$$

$$D_3 = 0.004\,Uy \quad \text{(B.27)}$$

In the ocean, D_2 and D_3 will be smaller than in coastal waters, especially due to smaller spatial velocity variations. To take care of this, a reduction constant, k, is introduced:

$$D_2 = k\,Uy \quad \text{(B.28)}$$

$$D_3 = k\,0.004\,Uy \quad \text{(B.29)}$$

The following values of k are used:

Coastal waters:	k = 1.0
Ocean, surface layer:	k = 0.07
Ocean, medium layer:	k = 0.035
Ocean, bottom layer:	k = 0.0175

If, as an example, the water depth is 40 m and the velocity of the ocean current is 0.1 m/s, the dispersion coefficients in the surface layer are:

$D_2 = 0.28\ m^2/s$
$D_3 = 0.001\ m^2/s$

In (Schroeder, 1976) the following ranges are given:

$D_2 = 0.01 - 1\ m^2/s$
$D_3 = 0.0001 - 0.01\ m^2/s$

It is seen that the values based on Eqs. B.28 and B.29 are in the middle of the range.

Inserting the constants k in Eqs. B.25, B.28 and B.29 gives the following results:

Coastal waters: K = 0.40
Ocean, surface layer: K = 0.028
Ocean, medium layer: K = 0.028
Ocean, bottom layer: K = 0.007

For the medium layer, k = 0.035 has been used, and mixing from both top and bottom of the plume. For this reason, there is no difference between the surface and the medium layers.

The corresponding plume dilution equations may be established using the above given values for K and Eq. B.24:

Coastal waters: $$S_{\min} = 0.4 \frac{Ux_1 y}{Q_o} \quad \text{(B.30)}$$

Ocean, surface layer and medium layer: $$S_{\min} = 0.028 \frac{Ux_1 y}{Q_o} \quad \text{(B.31)}$$

Ocean, bottom layer: $$S_{\min} = 0.007 \frac{Ux_1 y}{Q_o} \quad \text{(B.32)}$$

In case of a single puff-discharge, i.e. a momentary outlet, there will be mixing in the direction of the current as well. The dispersion coefficient in this direction, D_1 is an order of magnitude larger than D_2, i.e.:

$$D_1 = k\,10\,Uy \quad \text{(B.33)}$$

The dilution equation corresponding to Eq. B.22 reads:

$$S_{\min} = \frac{\pi\sqrt{2\pi}\,\sigma_1\sigma_2\sigma_3}{V_o} \quad \text{(B.34)}$$

in which

V_o = Total volume of waste discharge (m^3).

Using the same principles as for the plume we get:

Coastal waters: $$S_{\min} = 4.45 \frac{(yx_1)^{3/2}}{V_o}$$

Ocean, surface layer: $$S_{\min} = 0.082 \frac{(yx_1)^{3/2}}{V_o} \quad \text{(B.35)}$$

Ocean, medium layer: $$S_{\min} = 0.058 \frac{(yx_1)^{3/2}}{V_o} \quad \text{(B.36)}$$

Ocean, bottom layer: $$S_{\min} = 0.010 \frac{(yx_1)^{3/2}}{V_o}$$ (B.37)

The constant K for the surface layer differs from the constant K for the medium layer. The reason is that K in the puff case depends non-linearly on k, while in the plume case there is a linear dependence.

The PUFF model: If the discharge is neither a plume nor a jet, COWI's PUFF model may be used. This model uses a series of puffs, simulating a discharge limited in time. Each puff is treated as a single puff and the resulting concentration is obtained by superposing these single puffs.

The sea current in the Danish sector has been measured by DHI (DHI, 1982-85).

The typical velocity in the bottom layer is 0.1-0.2 m/s and in the surface layer 0.1-0.3 m/s.

As conservative values the following velocities normally have been used by COWI:

Surface and medium layer:	0.08 m/s
Bottom layer:	0.05 m/s

Other velocities may be used, for instance an actual distribution of velocities at a given site (e.g. a current rose). This may be used to establish several dilution lines, each representing a given fraction of the time in which the dilution will be greater (or smaller) than indicated by the line.

B.4 Uncertainty

The concentrations in the sea estimated by the formulas presented in sections B.2 and B.3 are encumbered by uncertainties, e.g. due to fluctuations in the discharge and variations in the sea current.

To take care of such uncertainties, either conservative parameters or uncertainty factors (UF) may be used.

In the calculations performed by COWI, both concepts are used as will be explained in this chapter.

Furthermore, reference will be made to the methods used for onshore industries, illustrated by the considerations carried out in connection with the discharge of wastewater from Junckers Industrier (VKI, 1991) and (Miljøstyrelsen, 1992).

The concept of uncertainty factors is described in these three references.

The basic idea is that the concentration of a given toxic matter in the environment (the sea) shall be less than the concentration with no effects on the environment:

$$\frac{NEC}{C} > 1$$ (B.38)

in which:

NEC: No effect concentration (theoretic)
C: Concentration in the environment (theoretic)

If NEC and C are assessed using a limited or an uncertain knowledge - which is the normal situation - uncertainty factors (UF) may be introduced. By definition, these factors are greater than one, and we have:

$$\frac{NEC}{C} = \frac{NOEC / UF_{NOEC}}{PEC \bullet UF_{PEC}} > 1 \qquad \text{(B.39)}$$

or

$$\frac{NOEC}{PEC} > 1 \bullet UF_{NOEC} \bullet UF_{PEC} \qquad \text{(B.40)}$$

in which:

NOEC: No observed effect concentration
PEC: Predicted environmental concentration, e.g. based on the formulas in chapters 2 and 3
UF_{NOEC}: Uncertainty factor, NOEC
UF_{PEC}: Uncertainty factor, PEC.

The greater the uncertainty is, the greater the UF should be.

In this report dealing with dilution, only UF_{PEC} will be treated. The analysis is based on the formulas described in sections B.2 and B.3.

Referring to (VKI, 1991) the uncertainty factor UF_{PEC} mainly depends on:

- Variation in the wastewater discharge
- Uncertainty in the data and in the calculation of the dilution in the sea.

The variation in the discharge rate of toxic matter, m_o, is included in the uncertainty factor UF_{NEC}, see (VKI, 1991).

This means that m_o may be understood as a fixed parameter when dealing with UF_{PEC}, while the discharge rate of wastewater may fluctuate.

Normally, the discharge rate of toxic matter is small compared to the discharge rate of wastewater. For this reason, the concentration in the outlet is:

$$C_o = \frac{m_o}{Q_o} \qquad \text{(B.41)}$$

in which:

m_o: Discharge rate of toxic matter (m^3/s)
Q_o: Discharge rate of wastewater (m^3/s).

In case of a continuous discharge, combination of Eqs. B.41, B.12, B.21, B.31 and B.32 yields:

$$Near\ field:\ PEC = \frac{C_o}{S_{\min}} = \frac{m_o D_o}{Q_o k_n s} \quad \text{(B.42)}$$

$$Far\ field:\ PEC = \frac{C_o}{S_{\min}} = \frac{m_o}{K_F U x_1 y} \quad \text{(B.43)}$$

The constant k_N is 0.18 or 2/3 and the constant K_F is 0.028 or 0.007, as described in sections B.2 and B.3.

In case of a momentary discharge, an analysis similar to the following analysis for the continuous discharge may be carried out.

The discharge rate of toxic matter, m_o, may with regard to PEC be understood as a fixed value as explained above. Furthermore, the outlet diameter, D_o, and the distance from the outlet, s or x_1, may be regarded as well-known parameters without uncertainties.

Therefore, dealing with the near field dilution, the only parameters encumbered by uncertainties are Q_o and k_N.

Near field

In the near field, e.g. just after the termination of the initial dilution, acute effects are most important. This means that the concentration considered should correspond to peak values modified due to equalization before the outlet, e.g. in the tanks of the treatment plant.

From Eq. B.42 it is seen that a low Q_o results in a high concentration. (VKI, 1991) proposes the use of the 95% fractile of the discharge flow (in the "low" end).

This concept of using conservative (i.e. small) wastewater flows has been used by COWI too.

The constant k_N is well documented and with only a small uncertainty.

Far field

The PEC in the far field used for the discharge from Junckers Industrier is the mean concentration from top to bottom, i.e. corresponding to full mixing in the entire water column.

The dilution equation used by COWI, Eq. B.43, does not describe the mean, but the maximum concentration. For this reason no UF_{PEC} is needed.

The influence of currents etc. has for the discharge from Junckers Industrier been treated by using data yielding the maximum concentration in a four-day-period, i.e. the concept of conservative parameters. This is in accordance with COWI's use of a small sea current, 0.05-0.08 m/s.

In the far field, i.e. hundreds of metres from the outlet, chronic effects are most important. This is the reason why a relatively long period of four days has been used for the discharge from Junckers Industrier.

In the far field formula, Eq. B.43, the size of K_F, y and U influence the result. U has been discussed above.

The depth of sea, y, should in principle be without uncertainty. However, in case of a stratified sea (density differences between surface and bottom layers), the depth y is only the depth of the layer in which the spreading occurs. The estimation of this depth may in some cases be uncertain. Normally, there will be no stratification, and here y is the depth of the sea, i.e. without uncertainty.

The constant K_F may be encumbered by a considerable uncertainty. However, the transformation of dispersion coefficients from coastal waters to the open sea, see Eqs. B.28 and B.29, using the constant k is rather conservative: A factor greater than 10 for the surface layer and a factor greater than 50 for the bottom layer.

The use of these conservative transformations shows that there is no need for uncertainty factors.

Thus, the formulas used by COWI and the way they are used does not rise a need for the introduction neither of additional uncertainty factors, UF_{PEC}, nor more conservative parameters.

The principles and concepts used are in accordance with the principles and concepts used for onshore industries, e.g. for the discharge from Junckers Industrier.

B.5 References

Abraham, 1963	Abraham, G., "Jet Diffusion in Stagnant Ambient Fluid", Delft Hydraulics Laboratory. Publication No. 29, 1963
Cederwall, 1969	Cederwall, K., "Hydraulics of Marine Waste Water Disposal", Report No. 42, Hydraulic Division, Chalmers Institute of Technology, Göteborg, 1968
DHI, 1982-85	Gorm Field Environmental and Structural Monitoring System, DHI for Mærsk Olie og Gas A/S, 1982, 1984 and 1985
Engelund, 1968	Engelund, F.A. "Hydrodynamik", Den private Ingeniørfond, DTH, 1968
Fisher, 1979	Fisher, H.B. et al, "Mixing in Inland and Coastal Waters", Academic Press, 1979
Karman et al., 1996	Karman C.C. et al, "CHARM III Main Report", TNO-MEP-R96/355, TNO Institute of Environmental Sciences, The Netherlands
Koh and Fan, 1970	Koh, R.C.I, and Fan, L.N., "Mathematical Models for the Prediction of Temperature Distributions Resulting from the Discharge of Heated Water in large Bodies of Water", EPA Water Pollution Control Research Series 16140 DWO, 1970
Liseth, 1977	Liseth, P. "Dykket utslipp i resipient", PRA-rapport nr. 14, Oslo, 1977
Miljøstyrelsen, 1992	"Økotoksikologisk vurdering af industrispildevand", Miljøprojekt nr. 188, Miljøstyrelsen, 1992
Odgaard, 1976	Odgaard, J., "Analytical Dilution Models", Lectures in Environmental Hydraulics, WHO, 1976

Schroeder, 1976	Schroeder, H., "Coastal Hydraulics", Lectures in Environmental Hydraulics, WHO, 1976
Thatcher et al, 2001	Thatcher et al. "A CIN revised CHARM III Report 2001. User guide for the evaluation of chemicals used and discharged offshore", Version 1.2. 12 July 2001
VKI, 1991	"Kravfastsættelse til industrispildevand, Junckers Industriers cellulosefabrik", Vandkvalitetsinstituttet, juni 1991

Appendix C Response capacity in the Baltic Sea

Table C-1 Simplified overview of the response capacity in the Baltic Sea (assumptions are shown with italics)

Country	In service?		Vessel name	Location	Sub-region	Recovery rate, nominal [m^3/h]	Storage capacity [m^3]	Boom length [m]
	2024	2036						
SE	Yes	Yes	KBV 181	Umeå	1	30	150	300
SE	Yes	Yes	KBV 078	Luleå	1	2	2	
SE	Yes	Yes	KBV 074	Härnösand	1	2	2	
SE	Yes	Yes	KBV 201	Härnösand	1	50	104	300
SE	Yes	Yes	KBV 076	Malmö	6	2	2	
SE	Yes	Yes	KBV 034	Malmö	6	80	255	300
SE	Yes	Yes	KBV 081	Karlskrona	5	2	2	
SE	Yes	Yes	KBV 003	Karlskrona	5	400	1100	500
SE	Yes	Yes	KBV 073	Oskarshamn	3	2	2	
SE	Yes	Yes	KBV 033	Oskarshamn	3	80	255	300
SE	Yes	Yes	KBV 080	Göteborg	6	2	2	
SE	Yes	Yes	KBV 010	Göteborg	6	50	212	300
SE	Yes	Yes	KBV 072	Göteborg	6	2	2	
SE	Yes	Yes	KBV 001	Göteborg	6	400	1050	500
SE	Yes	Yes	KBV 082	Slite	3	2	2	
SE	Yes	Yes	KBV 050	Södertalje	1	50	190	300
SE	Yes	Yes	KBV 071	Djurö	1	2	2	
SE	Yes	Yes	KBV 031	Djurö	1	80	255	300
SE	Yes	Yes	KBV 075	Gävle	1	2	2	
SE	Yes	Yes	KBV 202	Gävle	1	50	104	300
SE	Yes	Yes	KBV 081	Karlskrona	5	2	2	
SE	Yes	Yes	KBV 002	Slite	3	400	1050	500
SE	Yes	Yes	KBV 077	Västervik	3	2	2	
SE	Yes	Yes	KBV 032	Lysekil	6	80	255	300
PL	Yes	Yes	Kapitan Poinc	Gdynia	4	260	512	600
PL	Yes	Yes	Czesław II	Świnoujście	5	40	20	250
PL	Yes	Yes	Zodiak II	Gdańsk	4	15	200	500
PL	Yes	Yes	Planeta I	Świnoujście	5	15	200	500
PL	Yes	Yes	SG-301	Gdańsk	4	20	20	150
PL	No	Yes	New Vessel 1	Gdynia	4	260	500	600
LV	Yes	Yes	SEA BARGE JL-1	Liepaja	3	80	100	200
LV	Yes	Yes	AGE	Riga	3		1.5	
LV	Yes	Yes	ATE	Riga	3		1.5	
LV	Yes	Yes	A-90 VARONIS	Riga	3	100	120	800

Country	In service?		Vessel name	Location	Sub-region	Recovery rate, nominal [m^3/h]	Storage capacity [m^3]	Boom length [m]
	2024	2036						
LV	Yes	Yes	KA-14 ASTRA	Ventspils	3	100		100
LT	Yes	Yes	ŠAKIAI	Klaipėda	4	100	228	400
LT	Yes	Yes	SL TENGIZ	Baltic sea (Butinge oil terminal)	4	100	100	250
LT	Yes	Yes	RASA	Klaipėda	4	100	180	200
LT	No	Yes	New LT Navy vessel	Klaipėda	4	320	170	62.9
FI	Yes	Yes	Louhi	Kirkkonummi	2	180	1250	600
FI	Yes	Yes	Hylje	Kirkkonummi	2	96	900	600
FI	Yes	Yes	Turva	Hanko	2	180	1200	800
FI	Yes	No	Uisko	Hanko	2	72	100	0
FI	Yes	No	Tursas	Hanko	2	72	100	0
FI	Yes	Yes	Halli	Turku	1	108	1400	600
FI	Yes	Yes	Linja	Vaasa	1	67	500	0
FI	Yes	Yes	Aalto	Kalajoki	1	48	500	0
FI	Yes	Yes	Grisslan	Loviisa	2	108	500	0
FI	Yes	Yes	Otava	Kotka	2	48	100	0
FI	Yes	Yes	Jurmo	Kasnäs	2	48	100	0
FI	Yes	Yes	Svärtan	Marienhamn	1	50	52	0
FI	No	Yes	VL2025-A (Karhu)	Hanko	2	108	1180	800
FI	No	Yes	VL2025-B	Hanko	2	108	1180	800
EE	Yes	Yes	Kindral Kurvits	Tallinn	2	200	100	400
EE	Yes	Yes	Raju	Tallinn	2	200		200
EE	Yes	Yes	EVA-316	Tallinn	2	200	196	600
EE	Yes	Yes	Sektori	Tallinn	2	50	50	
EE	No	Yes	New Vessel 1	Tallinn	2	164		200
EE	No	Yes	Navy New 1 (Option A)	Saaremaa Süvasadam	2	200	200	600
EE	No	Yes	Navy New 1 (Option B)	Roomassaare	3	200	200	600
EE	No	Yes	Navy New 2	Tallinn	2	200	200	600
DK	No	Yes	OILREC 1	Kattegat	6	125	270	600
DK	No	Yes	OILREC 2	The Belt	6	125	270	600
DK	No	Yes	OILREC 3	Baltic West	5	125	271	600
DK	No	Yes	CHEMREC 1	Kattegat	6	125	850	900
DK	Yes	No	A563 MARIE MILJOE	Korsør	6	50	60	*200*
DK	Yes	No	A 562 METTE MILJOE	Frederikshavn	6	50	60	*200*
DK	Yes	No	A561 GUNNAR SEIDENFADEN	Korsør	6	60	311	*600*

Country	In service?		Vessel name	Location	Sub-region	Recovery rate, nominal [m^3/h]	Storage capacity [m^3]	Boom length [m]
	2024	2036						
DK	Yes	No	A 560 GUNNAR THORSEN	Frederikshavn	6	60	311	*600*
DE	Yes	No	ARKONA	Stralsund	5	640	430	
DE	Yes	No	BOTTSAND	Kiel	5	320	790	
DE	Yes	Yes	STRELASUND	Stralsund	5	160	200	
DE	Yes	Yes	HAITHABU	Kiel	5	160	200	
DE	Yes	Yes	VILM	Rostock	5	320	500	
DE	Yes	No	ORFE	Lubmin	5	20	14	
DE	Yes	Yes	KIEL	Kiel	5	160	325	
DE	Yes	Yes	LÜTT MATTEN	Sassnitz	5	60	16	*400*
DE	Yes	Yes	SCHARHÖRN	Kiel	5	640	1000	*400*
DE	No	Yes	(newbuilding)	Stralsund	5	1000	1000	400

Co-funded by
the European Union

BRISK II